# Scope of Presentations( I )

9th Meeting of the Liquid Metal Boiling Working Group
June 4 — 6 , 1980
Rome, Italy

Franco-Debene-PNC Specialists Meetings on FBR Subassembly Faults and Related Thermohydraulics
June 9 , 11, 1980
Karlsruhe, Federal Republic of Germany
Grenoble, France

July, 1 9 8 1



Power Reactor and Nuclear Fuel Development Corporation

動力炉・核燃料開発事業団（Power Reactor and Nuclear Fuel Development Corporation）

# SCOPE OF PRESENTATIONS (I)

9th Meeting of the Liquid Metal Boiling Working Group

June 4 - 6, 1980
Rome, Italy

Franco-Debene-PNC Specialists Meetings on
FBR Subassembly Faults and Related Thermohydraulics

June 9, 1980
Karlsruhe, Federal Republic of Germany

June 11, 1980
Grenoble, France

July, 1981

POWER REACTOR AND NUCLEAR FUEL DEVELOPMENT CORPORATION

SCOPE OF PRESENTATIONS (I)

9th Meeting of the Liquid Metal Boiling Working Group

June 4 - 6, 1980
Rome, Italy

Franco-Debene-PNC Specialists Meetings on
FBR Subassembly Faults and Related Thermohydraulics

June 9, 1980
Karlsruhe, Federal Republic of Germany

June 11, 1980
Grenoble, France

Edited by Katsuhisa YAMAGUCHI*

CONTENTS



* FBR Safety Section, Steam Generator Division, O-arai Engineering Center, Power Reactor and Nuclear Fuel Development Corporation (OEC/PNC).

# 1. 9TH MEETING OF THE LIQUID METAL BOILING WORKING GROUP

# 1 Temperature and Flow Fluctuations under Local Boiling in a Simulated Fuel Subassembly

by

H. Inujima, T. Ogino, M. Uotani and K. Yamaguchi

# 2 Local Temperature Rise and Boiling Behavior behind a Central Blockage in a Wire-Wrapped Pin Bundle

by

K. Yamaguchi, M. Uotani, K. Haga and M. Hori

# 3 Decay Heat Removal under Boiling Condition in a Pin-Bundle Geometry

by

K. Haga, M. Uotani, K. Yamaguchi and M. Hori

These papers are recorded as the PNC Reports of PNC N941 80-130 through 80-132 in the reversal order of those listed above. However, the manuscripts of the oral presentations and the used slides are not included in these PNC reports.

Liquid Metal Boiling Working Group

9th Meeting
June 4 - 6, 1980
Rome, Italy

# TEMPERATURE AND FLOW FLUCTUATIONS UNDER LOCAL BOILING IN A SIMULATED FUEL SUBASSEMBLY

H. Inujima and T. Ogino

Central Research Laboratory, Mitsubishi Electric Corporation, Japan

M. Uotani and K. Yamaguchi

O-arai Engineering Center, Power Reactor and Nuclear Fuel Development Corporation, Japan

## ABSTRACT

Out-of-pile experiments were carried out with the sodium test loop SIENA in O-arai Engineering Center of PNC, and the feasibility studies had been made on the local boiling detection by use of temperature and flow fluctuations. The studies showed that the temperature fluctuation transferred the information on local boiling toward the end of the bundle, but hardly to the outlet. In addition, it was proved that the anomaly detection method, which used the algorithm of whiteness test method to the residual time series data of autoregressive model, is an effective one for detecting anomaly such as local boiling.

## INTRODUCTION

For the safety operation of liquid metal fast breeder reactor, it is very important to detect a local boiling within a subassembly at its initial stage. Since flow blockage is one of the most typical causes of local boiling, many efforts have been concentrated on the study of detecting the flow blockage by use of temperature fluctuation at the outlet of subassembly[1],[2]. In-pile and out-of-pile experiments have been made on the local boiling detection by use of the same fluctuations[3],[4],[5]. The results showed that the utilization of temperature fluctuation was promising for the boiling detection of fast breeder reactor. However, further studies may be required for the application of the techniques to the actual anomaly detection system.

Out-of-pile experients were carried out with the sodium test loop SIENA in O-arai Engineering Center of PNC. One of the main purposes of the experiments

is to examine the feasibility of detecting local boiling accident by use of temperature and flow fluctuations. In order to make clear whether or not the detection is feasible, the following subjects are investigated in this paper through the interpretation of boiling experimental data:

(1) Statistical properties of temperature and flow fluctuations in the downstream of the blockage under local boiling conditions;
(2) Sensitivity of newly developed anomaly detection method which uses fluctuation signals.

## EXPERIMENTAL EQUIPMENT

Figure 1 shows the schematic representation of the electrically heated 61-pin bundle test section used in the present study. The diameter of each pin is 6.5 mm and the pin pitch is 7.9 mm. The clearance of neighboring pins is kept constant by wire spacers. The outer 24 pins of the test section are dummy pins. The 36 % central-type tight blockage is attached at the middle position of heated section.

Chromel-Alumel thermocouples represented by T-XXXX in Fig. 1 are located at various positions of the test section. The thermocouple T-004 is an ungrounded type sheathed thermocouple whose diameter is 4.8 mm, and the others are grounded type sheathed thermocouples whose diameters are 0.3 mm. The eddy current type flow-meter is installed at the outlet of the bundle.

The data acquisition system of fluctuation signals is shown in Fig. 2. The temperature and flow signals are transmitted to the control room using double shielded cables. The fluctuation signals are obtained from specially designed fluctuation measuring cicuits. The circuits consist of a low noise AC amplifier and a band pass filter. The specification of these components is as follows:

| | | | |
|---|---|---|---|
| AC amplifier | gain | : | 60 dB (max.) |
| | low cut off frequency | : | 0.01 Hz |
| Band pass filter | low cut off frequency | : | 0.01 Hz |
| | slope | : | 40 dB/dec |
| | high cut off freqeuncy | : | 15 Hz |
| | slope | : | 200 dB/dec |

## OPERATING PROCEDURE AND LOCAL BOILING EXPERIMENT

The flow velocity was initially maintained at the constant value of 1.5 m/sec, and the heat flux of each pin was adjusted to be 61 W/cm$^2$. When the steady state condition was attained, the flow velocity was decreased stepwise.

Figure 3 shows typical signals obtained in the local boiling experiment (Run No. 61WLB-101). FEC-1A is the flow fluctuation signal measured by the eddy current type flow-meter. T-024 and T-024A are the temperature and its fluctuation signals measured at the outlet, respectively. T-021G and T-021GA are the readings of the thermocouple whose location is 34 mm downstream of the blockage. P-111 is the pressure at the outlet. Inception of local boiling was monitored by this pressure signal. F-103 is the flow signal at the inlet of the test section.

The inlet sodium flow was decreased stepwise at 62, 86, 157 and 251 sec. The local boiling was initiated at about 95 sec, after the second reduction of flow rate. Three steady state local boiling tests were conducted under different conditions: "Local boiling I", "Local boiling II" and "Local boiling III". At the second and third reductions of flow rate, conspicious increases

were found in both the temperature and its fluctuation signals measured at the position immediately behind the blockage (T-021G and T-021GA). During the local boiling II and III tests, T-021G had reached the sodium saturation temperature. On the other hand, the temperature at the outlet, T-024, increased gradually by only 3 to 5 °C at each step of flow reduction. Conspicious changes were hardly found in the outlet temperature fluctuation, T-024A, during the flow decreases except the second one. The flow fluctuation, FEC-1A, did not show any visible changes not only during the flow reductions but also at the onset of local boiling.

## ANOMALY DETECTION METHOD

An anomaly detection method, which uses fluctuation signal, is generally based on the comparison of a typical statistical index of fluctuation signals at normal state with that at anomalous state. Power spectral density (PSD), RMS value, Skewness factor etc. are usually used for this purpose. It is desirable that the anomaly detection method take into account enough information from fluctuation signals to judge the operational status of a reactor, because the anomaly phenomena have not been thoroughly understood and the relation between anomaly status and temperature (or flow) fluctuation has not been fully clarified.

We have developed an anomaly detection method which uses the auto-regressive model (AR model). We called it Whiteness Test Method (WTM) in the present paper. Signal processing procedure of WTM is summarized as follows:

STEP 1 $$\varepsilon_n = \underline{x}_n - \sum_{i=1}^{M} a_i \, x_{n-i} \qquad \cdots\cdots\cdots (1)$$

$\varepsilon_n$ : residual time series data of the AR model fitting
$\underline{x}_n$ : fluctuation signal to be diagnosed
$a_i$ : preparatively determined AR model coefficients of fluctuation signal at normal state

STEP 2 $$\psi_{\varepsilon\varepsilon}(n,\tau) = \frac{1}{L} \sum_{j=1}^{N_o} \varepsilon_{n-j} * \varepsilon_{n+j-\tau} \quad , \tau = 1,2,\ldots,\tau_{max} \qquad \cdots\cdots (2)$$

$L$ : number of data used for computing $\phi_{\varepsilon\varepsilon}(n+N_o,\tau)$
$N_o$ : number of sampled data in the monitored interval
$\tau_{max}$ : maximum lag number of autocovariance function $\phi_{\varepsilon\varepsilon}(n,\tau)$

STEP 3 $$\phi_{\varepsilon\varepsilon}(n+N_o,\tau) = \phi_{\varepsilon\varepsilon}(n,\tau) + \psi_{\varepsilon\varepsilon}(n,\tau) - \psi_{\varepsilon\varepsilon}(n-L,\tau) \qquad \cdots\cdots\cdots (3)$$

The values of L and $N_o$ are so selected that $L/N_o$ shall be integer.

STEP 4 $$I(n+N_o,M,L,\tau_{max}) = \sum_{\tau=1}^{\tau_{max}} |\phi_{\varepsilon\varepsilon}(n+N_o,\tau)|^2 \qquad \cdots\cdots\cdots (4)$$

$I(n+N_o,M,L,\tau_{max})$ ; AR index

STEP 5 $$I_{mt}{}^{l} \leq I(n+N_o,M,L,\tau_{max}) \leq I_{mt}{}^{u} \quad : \text{Normal}$$

Otherwise : Anomary

where $I_{mt}{}^{l}$, $I_{mt}{}^{u}$ are lower and upper alarm levels.

The WTM algorithm has been developed for a mini-computer system. The computing time and the memory size of the WTM for each fluctuation signal are about 10 msec and about 150 words, respectively.

## TEMPERATURE AND FLOW FLUCTUATIONS UNDER LOCAL BOILING CONDITIONS

### RMS Value of Temperature Fluctuation

Figure 4 shows the RMS values of temperature fluctuations observed at several axial positions behind the blockage. The following items were made clear from these analyses:

(1) At the position immediately behind the blockage, the RMS values of temperature fluctuations under local boiling conditions were about 15 times larger than that under non-boiling condition.
(2) In the downstream beyond 144 mm from the blockage, noticeable changes were not found in the RMS values of temperature fluctuations between the two conditions.
(3) The RMS values of temperature fluctuations observed at the outlet were about 5 times larger than those at the end of the bundle.

### PSD of Temperature Fluctuation

Figures 5 and 6 show the PSDs of the same temperature fluctuations under non-boiling and local boiling III conditions. The temperature fluctuations in the bundle had spectral peaks around 4 Hz. The peaks were due to the repetitive cycle of bubble formation and collapse. On the other hand, the temperature fluctuation at the outlet had no spectral peak.

### PSD of Flow Fluctuation

As shown in Fig. 7, no conspicuous feature of local boiling was found in the PSDs of flow fluctuations measured at the outlet of the bundle.

### Transfer and Coherence Functions of Temperature Fluctuations

Figures 8 and 9 show the transfer and coherence functions between several couples of temperature fluctuations under the local boiling III condition: one is always fixed to that measured at immediately behind the blockage (T-021GA) and another is selected from those measured at various downstream locations.

Concerning the transfer functions, peaks appeared around 4 Hz only for the cases with the temperature fluctuations measured within the region less than 66 mm (T-021J) downstream of the blockage. Otherwise, the peak was attenuated remarkably. In the case of coherence functions, conspicuous peaks were found within the whole bundle section. However, it was hardly found at the outlet.

These analyses made clear the following items:

(1) The inconsistency between transfer and coherence functions, both calculated with the temperature fluctuation at the end of the bundle, was mainly due to the strong attenuation of fluctuation level during the axial motion of fluid (see Fig. 4). This fact proves that the information on local boiling is transferred almost linearly to the end of the bundle even though it is fairly small. Figure 4 shows the amount of information on local boiling transferred to the end of the bundle.
(2) At the outlet of the bundle, both transfer and coherence functions are small in whole frequency range. From this fact, it is deduced that the temperature fluctuation at the outlet is hardly correlated to that at the boiling position. The temperature fluctuation at the outlet may be

generated mainly by the turbulent mixing of the coolant flowing through the passage from the end of the bundle to the measured position, since the RMS value of temperature fluctuation at the outlet is about 5 times larger than that at the end of the bundle.

## FEASIBILITY OF LOCAL BOILING DETECTION

Figures 10 and 11 show the result of the anomaly detection by the RMS method and the WTM applied to the temperature and flow fluctuations, where the sampling interval and averaging time were selected to be 0.016 and 8.0 seconds, respectively. Concerning the RMS values of temperature and flow fluctuations, noticeable changes were not found during the run. In the AR index of temperature fluctuation, remarkable increases were found immediately after the reductions of flow rate. However, conspicuous increases were not always found in the AR index of flow fluctuation.

The RMS values of temperature and flow fluctuations under local boiling conditions were larger than those under non-boiling condition. The amount of the difference ($\leq$ 20 %) was, however, insufficient to detect local boiling.

Figure 12 shows the ratio of the average AR index under steady state local boiling conditions to that under non-boiling condition (averaging time is 32 sec). The ratio of the temperature fluctuations was from 1.5 to 1.8, and that of the flow fluctuations was from 2.0 to 2.5. This figure also shows that the ratio increases with boiling intensity.

As mentioned in the previous section, there was little correlation between temperature fluctuation at the boiling position and that (or the flow fluctuation) at the outlet of the bundle. Consequently, it is easy to infer that the local boiling may be detected only when the local boiling region is large enough to affect the temperature distribution at the outlet of the bundle or generate global flow oscillation due to void formation and collapse.

## CONCLUSIONS

Analyses of temperature and flow fluctuations under local boiling conditions yielded the following conclusions:

(1) The strong correlation was found for the temperature fluctuations observed at the boiling position and the end of the bundle, while the correlation has not been clarified with regard to the fluctuations at the subchannel outlet.
(2) It will be promising to detect local boiling accident when the boiling intensity becomes fairly large.
(3) The whiteness test method (WTM) of fluctuation signal was a sensitive and reliable method for detecting a local accident within a subassembly.

## ACKNOWLEDGMENT

The authers wish to acknowledge the technical contributions of Mr. T. Isozaki and Mr. T. Komaba at all stages of the experiments.

## REFERENCES

[1] D. N. Fry and W. H. Leavell, "TEMPERATURE NOISE ANALYSIS AT THE EXIT OF BLOCKED AND UNBLOCKED 19-PIN ELECTRICALLY HEATED LMFBR FUEL SUBASSEMBLY MOCKUPS", ORNL-TM-5464, Oak Ridge National Laboratory, Aug. (1976)

[2] E. Ohlmer and D. Schwalm, "THE USE OF THE AMPLITUDE DISTRIBUTION FUNCTION IN A SIMULATED REACTOR SUBASSEMBLY", Atomkernenergie, 25, 281 (1975)

[3] T. Ogino, H. Inujima et al., "FEASIBILITY STUDY OF LOCAL CORE ANOMALY DETECTION BY USE OF TEMPERATURE AND FLOW FLUCTUATIONS AT LMFBR FUEL SUBASSEMBLY OUTLET", International Meeting on Fast Reacter Safety Technology (1979)

[4] E. J. Burton, P. G. Bentley et al., "AN OVER VIEW OF THE DEVELOPMENT OF DIAGNOSTIC TECHNIQUES FOR FAST REACTOR", International Meeting on Fast Reactor Safety Technology (1979)

[5] D. Smith et al., "DFR SPECIAL EXPERIMENTS", International Symposium on Design, Construction and Operating Experiment of Demonstration LMFBR, International Atomic Energy Agency, Vologna (1978)

[6] H. Akaike, "FITTING AUTOREGRESSIVE MODELS FOR PREDICTION", Ann. Institute of Statistical Mathematics, 21, 243-247 (1969)

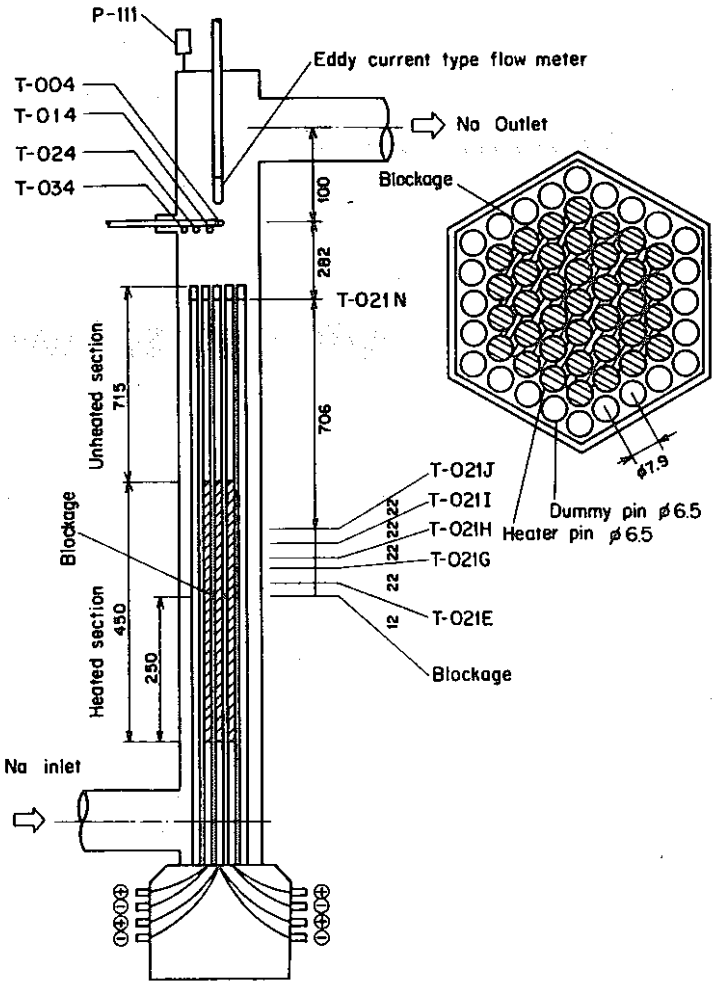


Fig. 1 Locally blocked 61-pin bundle test section

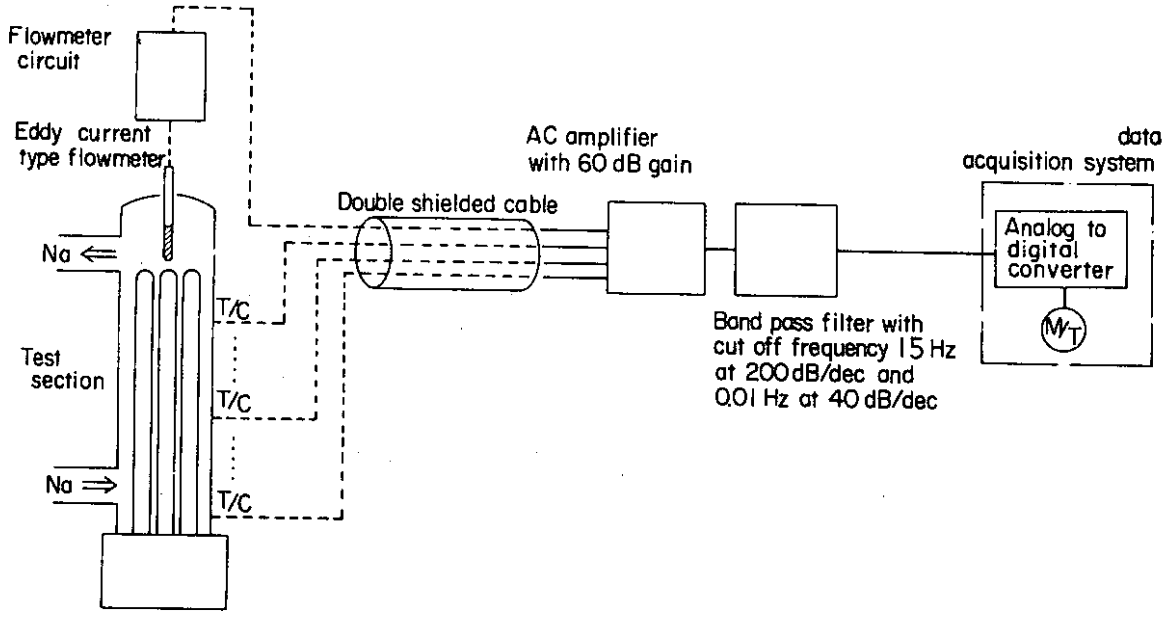


Fig. 2 Schematic diagram of the data acquisition system of fluctuation signals

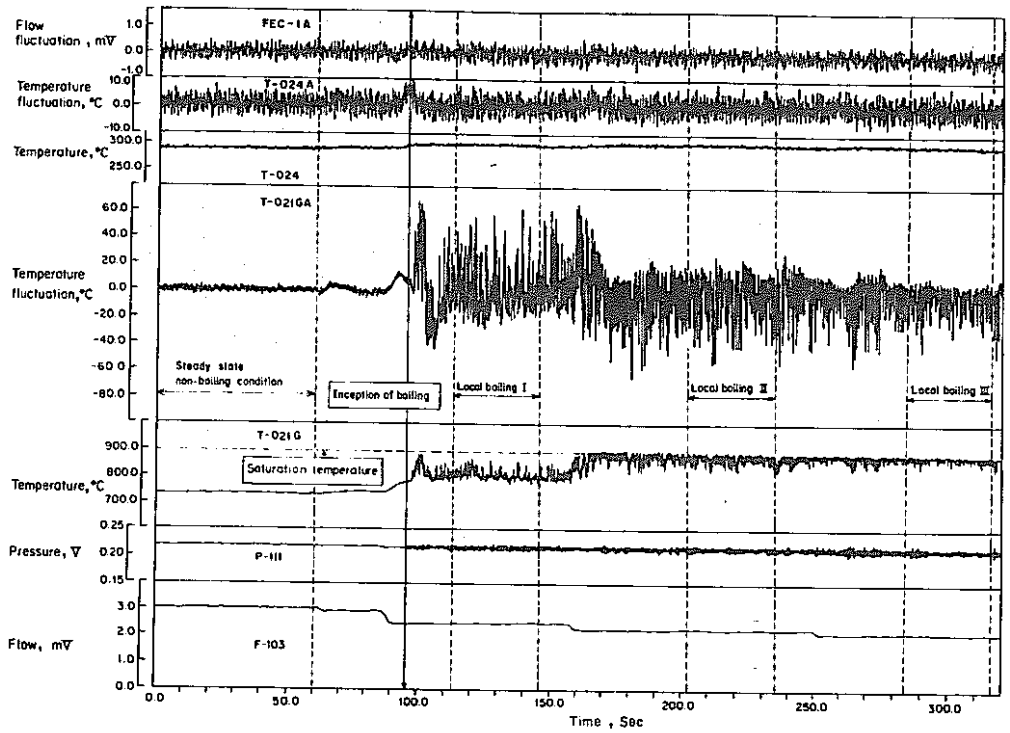


Fig. 3 Signals under local boiling condition (Run No. 61WLB-101)

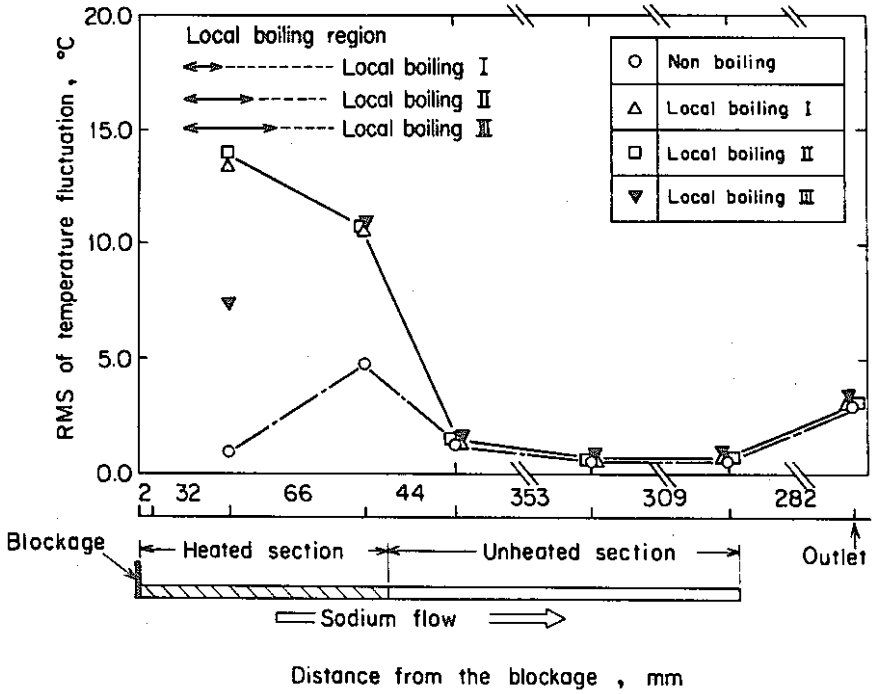


Fig. 4 RMS values of temperature fluctuations observed at several axial positions behind the blockage (Run No. 61WLB-101)

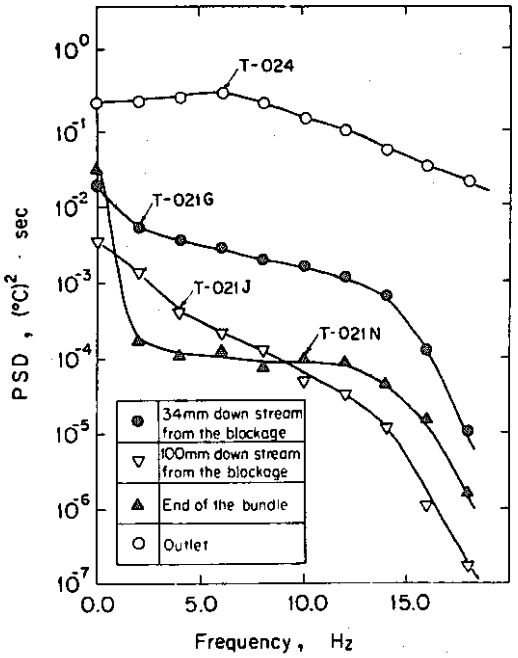


Fig. 5 Power spectral densities of temperature fluctuations observed at several axial positions,
-- Non-boiling condition
(Run No. 61WLB-101)

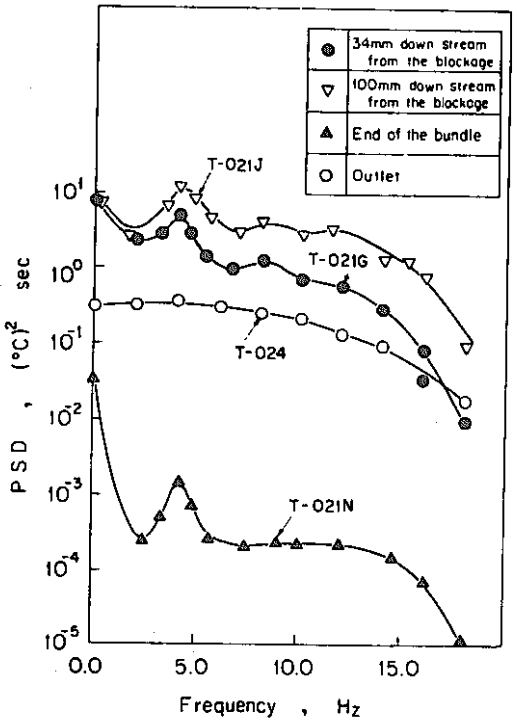


Fig. 6 Power spectral densities of temperature fluctuations observed at several axial positions,
-- Local boiling III condition
(Run No. 61WLB-101)

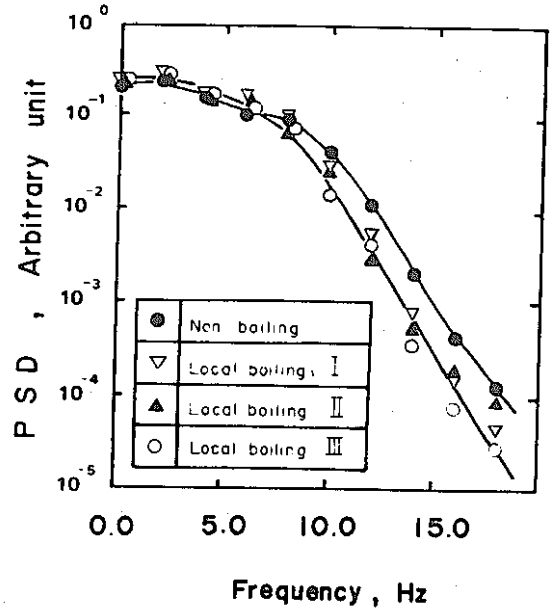


Fig. 7 Power spectral densities of flow fluctuation observed at the outlet of the bundle
(Run No. 61WLB-101)

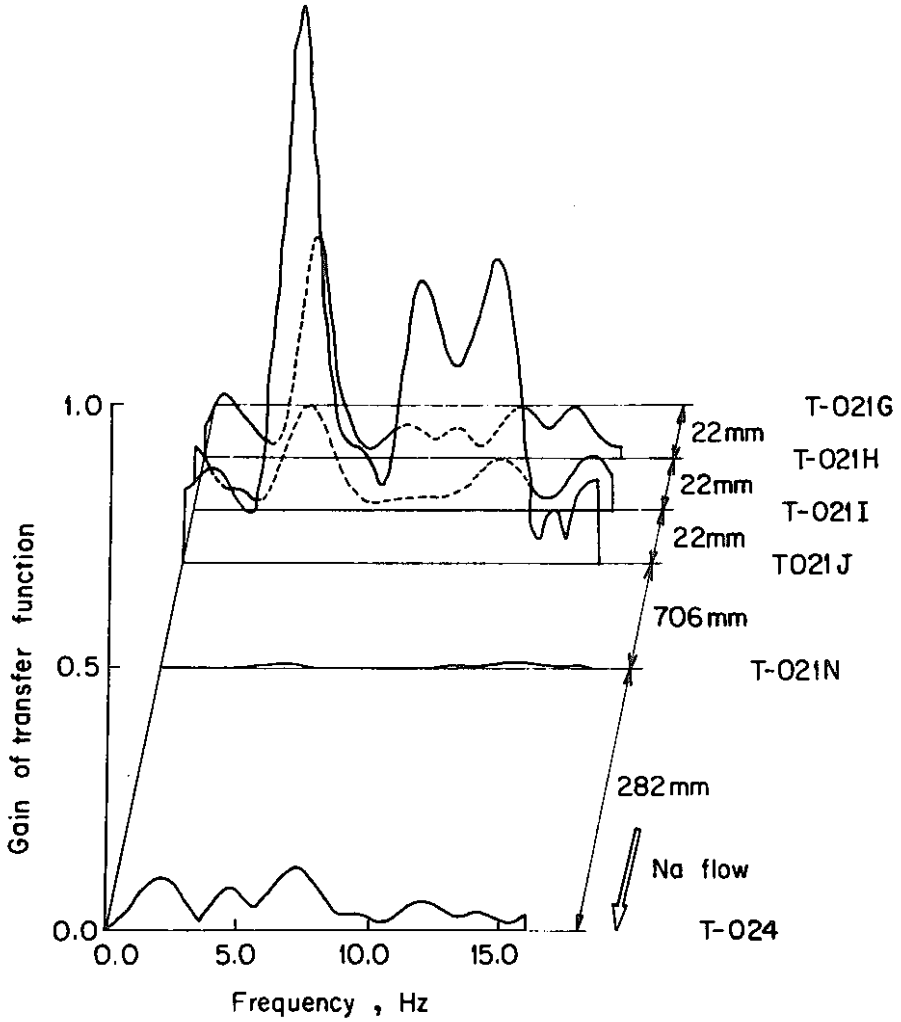


Fig. 8 Transfer functions between several couples of temperature fluctuations, one is T-021G and the opposite is one of the others (T-021H,..., T-024), -- Local boiling III condition
(Run No. 61WLB-101)

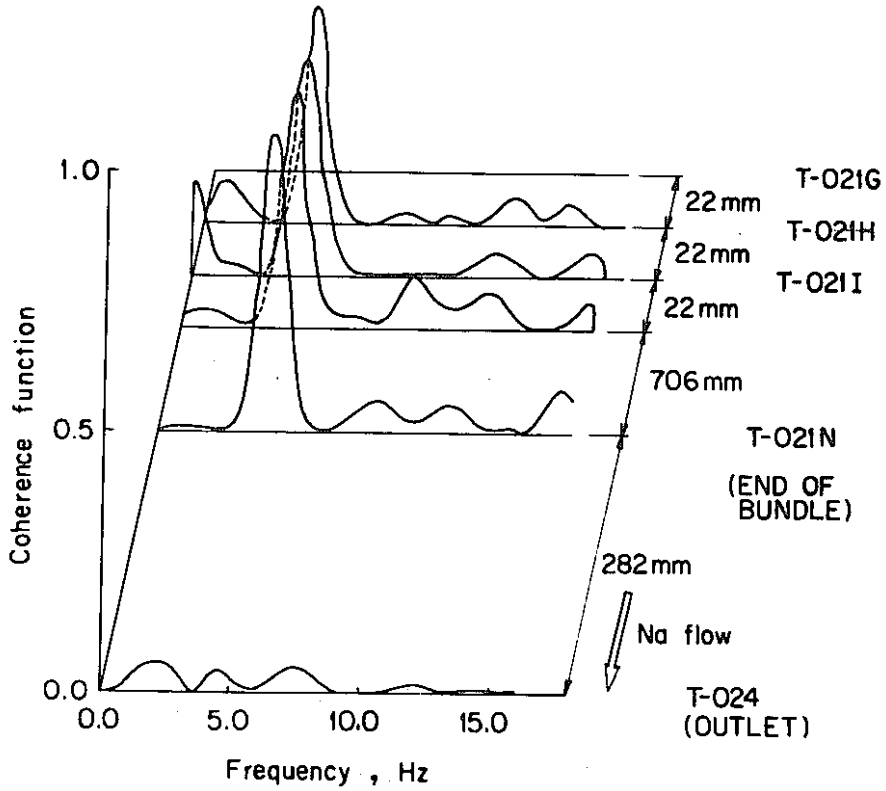


Fig. 9 Coherence functions between several couples of temperature fluctuations, one is T-021G and the opposite is one of the others (T-021H,..., T-024), -- Local boiling III condition
(Run No. 61WLB-101)

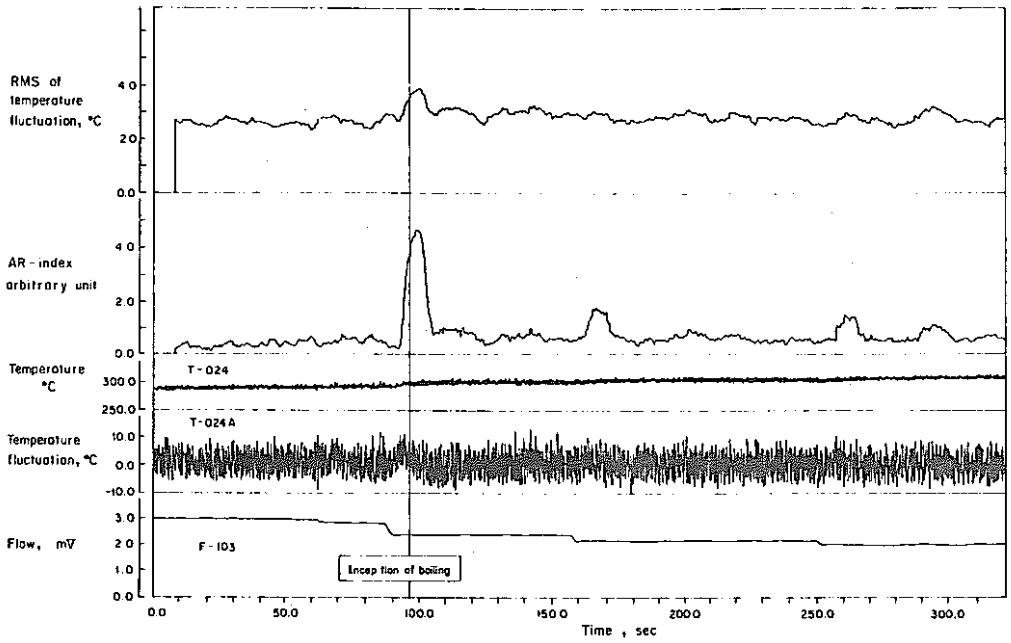


Fig. 10 RMS value and AR index of temperature fluctuation measured at the outlet of the bundle (T-024) (Run No. 61WLB-101)

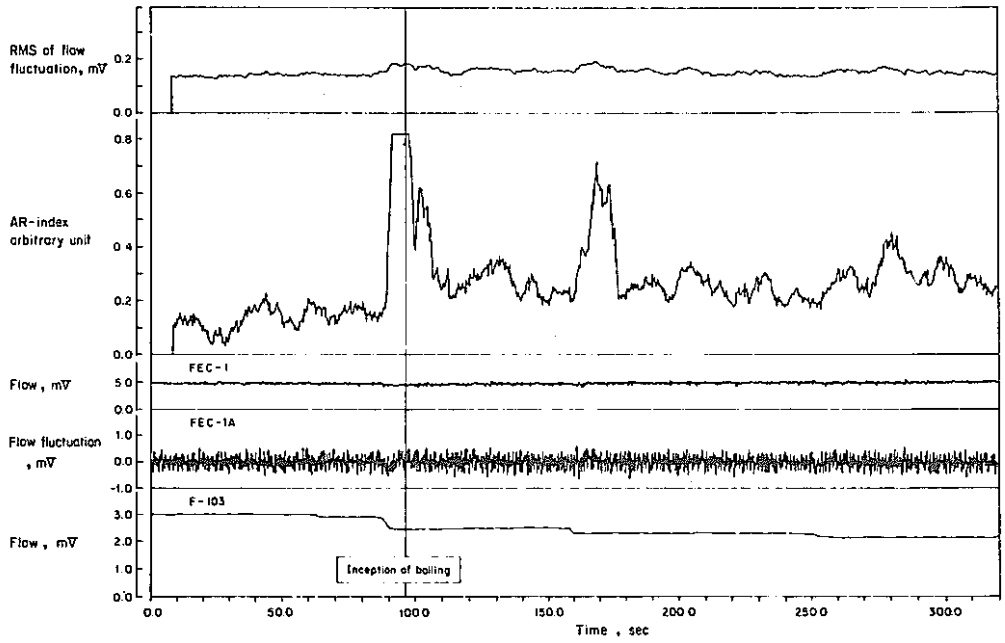


Fig. 11 RMS value and AR index of flow fluctuation measured at the outlet of the bundle (FEC-1) (Run No. 61WLB-101)

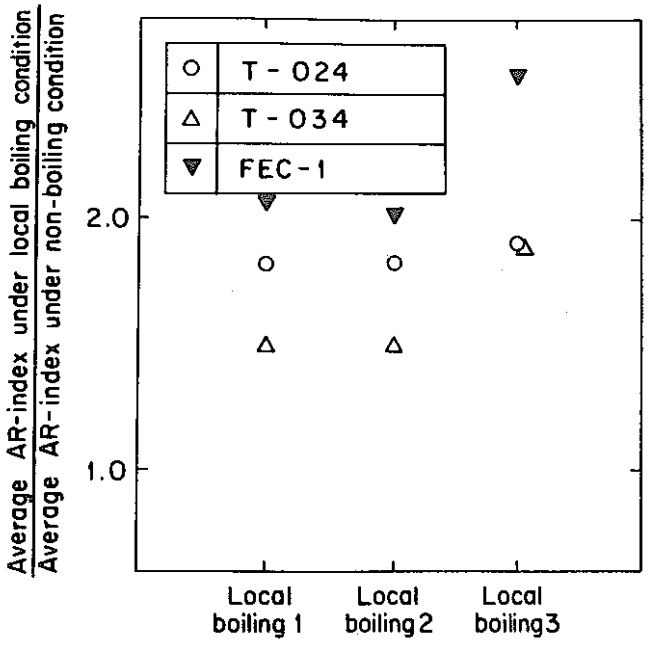


Fig. 12 Ratio of the average AR index under boiling condition to that under non-boiling condition
(Run No. 61WLB-101)

## APPENDIX: SCOPE OF PRESENTATION

Liquid Metal Boiling Working Group

9th Meeting
June 4 - 6, 1980
Rome, Italy

# TEMPERATURE AND FLOW FLUCTUATIONS UNDER LOCAL BOILING IN A SIMULATED FUEL SUBASSEMBLY

H. Inujima*, T. Ogino*, M. Uotani** and K. Yamaguchi**

* Central Research Laboratory, Mitsubishi Electric Co. Ltd., Japan
** FBR Safety Section, OEC/PNC, Japan

## INTRODUCTION

Thank you, chairman. My name is Katsuhisa Yamaguchi. I belong to the FBR Safety Section of PNC. Today, I would like to present our recent progress on the Anomaly Detection Test. This work has been conducted by the Joint Research between PNC and Mitsubishi Electric Cooperation, Japan.

9TH LIQUID METAL BOILING WORKING GROUP MEETING PNC-FS-017s
ROME, ITALY, JUNE 4-6, 1980

# TEMPERATURE AND FLOW FLUCTUATIONS UNDER LOCAL BOILING IN A SIMULATED FUEL SUBASSEMBLY

H.INUJIMA*, T.OGINO*, M.UOTANI** AND K.YAMAGUCHI**
* MISTUBISHI ELECTRIC CO. LTD., ** PNC, JAPAN

OBJECT

EXAMINE THE FEASIBILITY OF DETECTING A LOCAL BOILING ACCIDENT BY USE OF TEMPERATURE AND FLOW FLUCTUATIONS

APPROACHES

(1) INVESTIGATE STATISTICAL PROPERTIES OF TEMPERATURE AND FLOW FLUCTUATIONS BEHIND THE BLOCKAGE UNDER LOCAL BOILING CONDITIONS
(2) EXAMINE THE SENSITIVITY OF NEWLY DEVELOPED ANOMARY DETECTION METHOD WHICH USES FLUCTUATION SIGNALS

OBJECT ..... (First slide, please. SLIDE No. 1)

It is said that the local core accidents, such as a local boiling, may have sufficient potential to cause fuel failures in a subassembly. In worst cases, it may lead to a subassembly-to-subassembly failure propagation.

The development of the anomaly detection method will, therefore, contribute much to the safety operation of LMFBRs. In the case when the temperature or flow fluctuations are strongly transfered toward the downstream direction, we will be able to detect the local boiling at its early stages using the subassembly outlet instrumentations. However, it is not always the case. So, we must, first of all, check the transfer characteristics of boiling information. The performance of the detection scheme will be in question in the next step.

Our object is limited here to studying these two scopes using the temperature and flow fluctuations in a partially blocked subassembly. For this study, we have conducted out-of-pile experiments using the Sodium Boiling and Fuel Failure Propagation Test Facility, SIENA, in the O-arai Engineering Center of PNC.

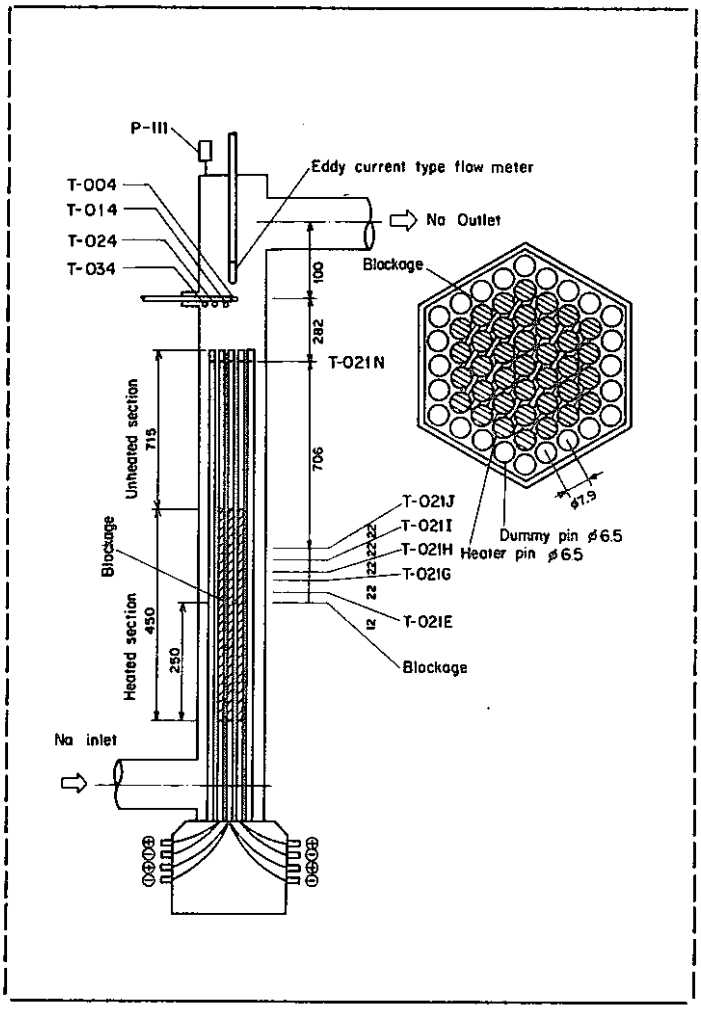


TEST SECTION ..... (Next slide, please. SLIDE No. 2, i.e. Fig. 1)

This is a schematic illustration of the 61-pin bundle test section used in the present study. The shaded part is a heated section and the other part is an unheated section. A 36 % central-type planar blockage is attached at the middle position of the heated section.

Here is a sketch of the blocked plane. Shaded circles mean heater pins, and blank circles mean dummy pins.

The thermocouple T-024 and the eddy-current-type flow-meter were used as the sensors for boiling detection. These sensors are situated at the subassembly outlet, apart from the uppor end of the pin bundle head by about 30 mm. Many C-A thermocouples are equipped at various positions in the test section. The output signals of these thermocouples were used to study the transfer characteristics of the temperature fluctuations.

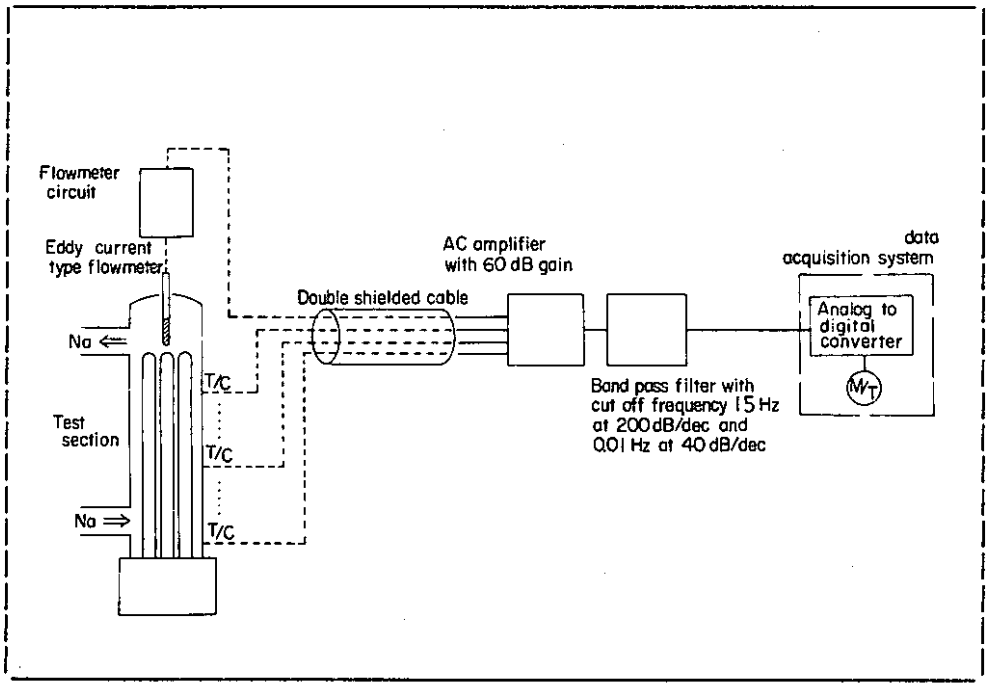


DATA LOGGER ..... (Next slide, please. SLIDE No. 3, i.e. Fig. 2)

This is a whole view of our data acquisition system.

Here is the test section. The pre-amplifier of the flow-meter is located near the test section to avoid the pick-up of foreign noise. From the same reason, double shielded cables are used for the signal transmission.

These are the signal conditioners. The circuits consist of a low noise AC amplifier and a band pass filter. The output signals of these circuits are recorded on a digital magnetic tape.

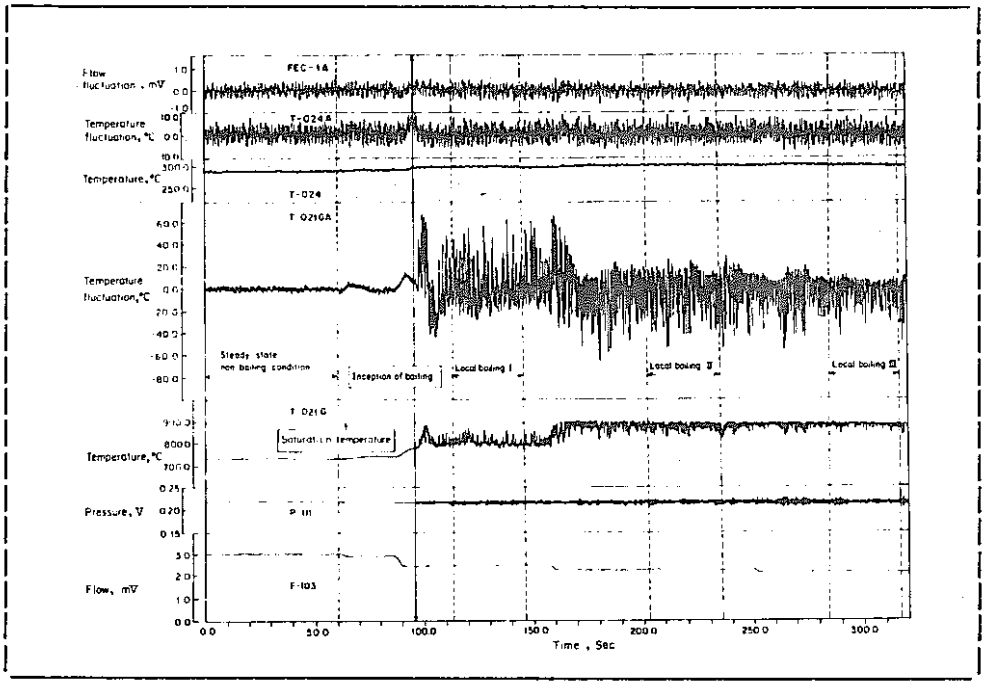


LOCAL BOILING RUN .... (Next slide, please. SLIDE No. 4, i.e. Fig. 3)

This slide shows the progress of the present local boiling run, Run No. 61WLB-101.

The horizontal axis is a relative time. FEC-1A is the flow fluctuation signal measured by the eddy-current flow-meter. T-024 and T-024A are the subassembly outlet temperature and its fluctuation, respectively. T-021G and T-021GA are the other pair-signals from the thermocouple whose location is 34 mm downstream from the blockage. In this study, T-021GA can be treated as the source term of the boiling information. P-111 is the subassembly outlet pressure. Inception of the local boiling was identified by this pressure signal. F-103 is the subassembly inlet flow velocity.

The flow velocity was initially adjusted to the constant value of 1.5 m/sec, and the heat flux of each pin was maintained to be 61 W/cm$^2$. After attaining the steady-state condition, the flow rate was reduced stepwise.

The local boiling was initiated at the second flow reduction step. Three steady-state local boiling tests were conducted through under different flow velocity conditions. We call them "Local Boiling I", "II" and "III". During the Local Boiling II and III tests, T-021G was at the saturation temperature. On the other hand, the subassembly outlet temperature T-024 increased only by 3 to 5 degrees at each flow reduction step at the level far below the saturation temperature.

At the instances of the second and the third flow reductions, conspicuous increases were found in both the temperature T-021G and its fluctuation T-021GA. However, little changes were found in the subassembly outlet temperature fluctuation T-024A except at the second flow reduction. The flow fluctuation FEC-1A did not show any visiable changes not only during the flow reductions but also at the onset of the local boiling.

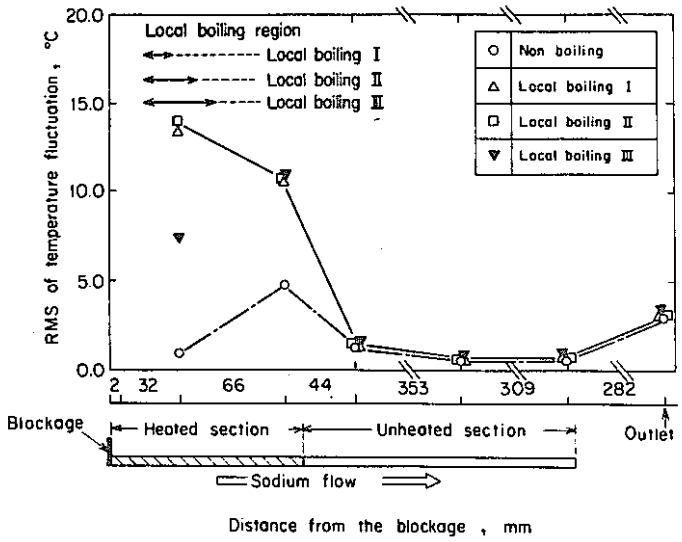


RMS ANALYSIS ..... (Next slide, please. SLIDE No. 5, i.e. Fig. 4)

This slide shows the comparison of the RMS values of temperature fluctuations observed at several axial locations behind the blockage during every tests. The local boiling regions at every boiling tests are noted here.

We can summarize the results of the RMS analysis as follows:

First; at the position immediately behind the blockage, the RMS values of temperature fluctuations under local boiling conditions were about 15 times as large as that under non-boiling condition. Second; at the downstream unheated positions, little changes were found in the RMS values of temperature fluctuations during whole local boiling tests. Third; the RMS values of the subassembly outlet temperature fluctuations were about 5 times as large as those observed near the upper end of the pin bundle.

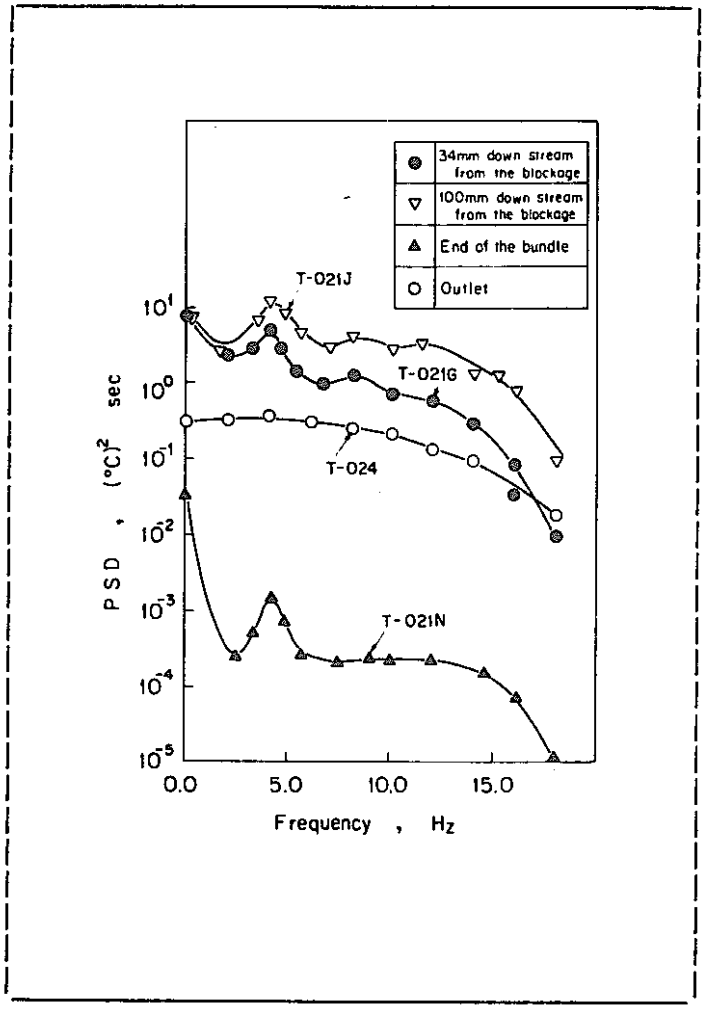


PSD ANALYSIS ..... (Next slide, please. SLIDE No. 6, i.e. Fig. 6)

This slide shows the Power Spectral Densities of the same temperature fluctuations. Only the results of Local Boiling III test are drawn here.

You can easily find that the temperature fluctuations within the pin bundle have spectral peaks at the frequency of around 4 Hz. The peak frequency is identical with the repetitive cycle of the bubble expansion and contraction under the oscillatory boiling. On the other hand, the subassembly outlet temperature fluctuation has no spectral peak.

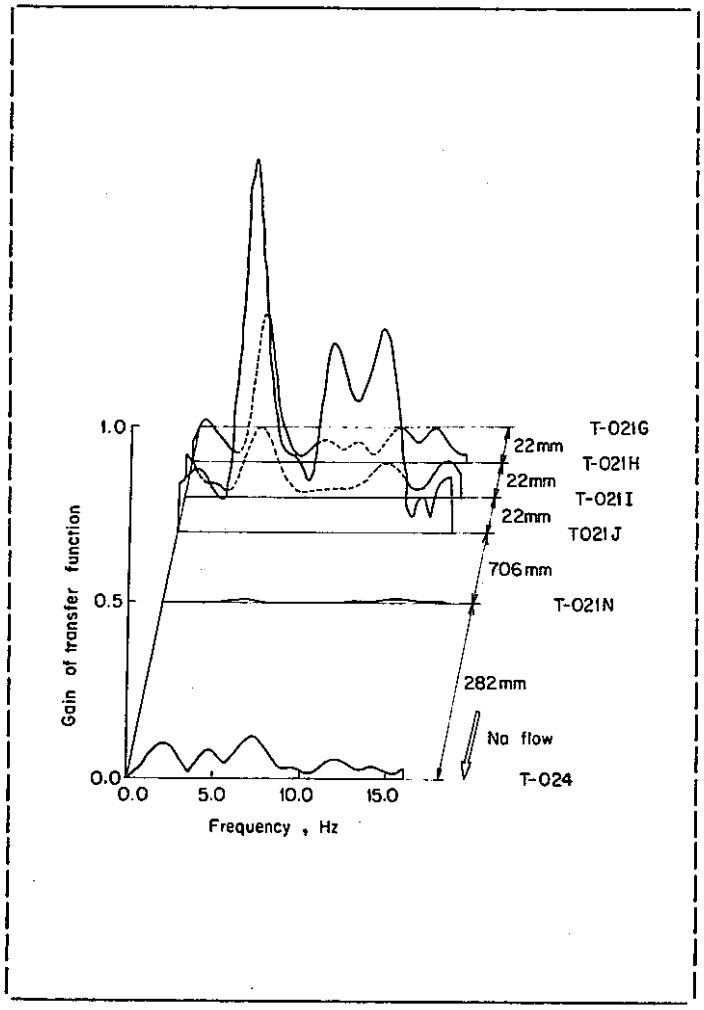


TRANSFER FUNCTION ..... (Next slide, please. SLIDE No. 7, i.e. Fig. 8)

This slide shows the Transfer Functions between several pairs of temperature fluctuations observed at Local Boiling III test, where one of the pair is a source term and is always fixed to that measured at immediately behind the blockage T-021GA, and another is selected from those measured at various downstream locations.

We can identify the peaks around 4 Hz only when we select the pair from those measured at the neighboring region less than 66 mm (T-021JA) downstream from the blockage. Otherwise, the peak was not found at that frequency point.

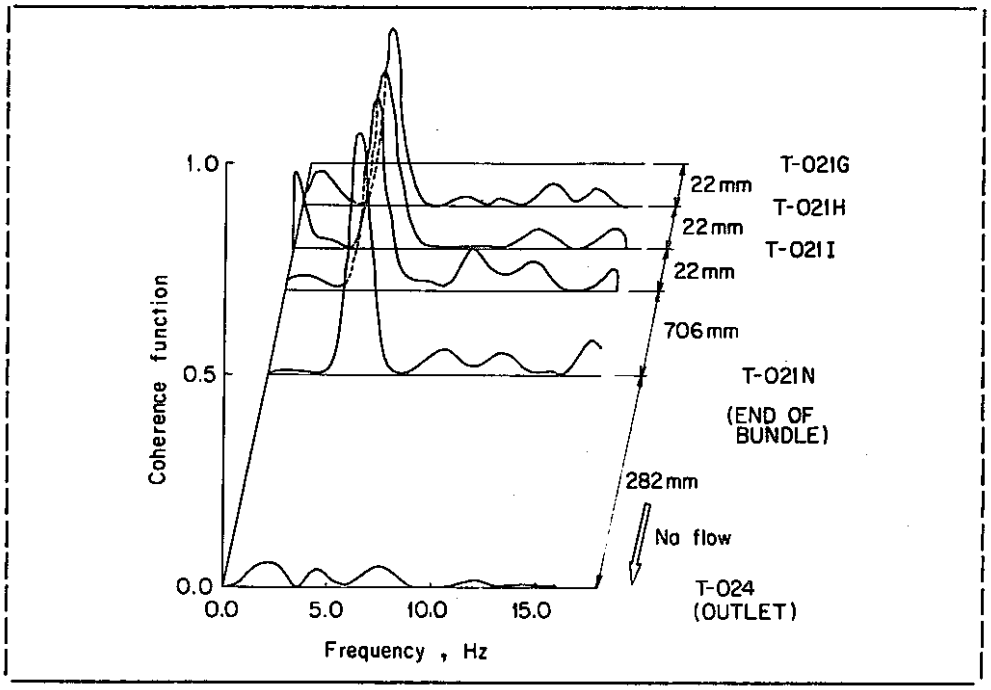


COHERENCE FUNCTION .... (Next slide, please. SLIDE No. 8, i.e. Fig. 9)

This slide shows the Coherence Functions between the same pairs of temperature fluctuations. In this analysis, we can find the large peaks within the whole bundle section. However, it was hardly found at the subassembly outlet.

TRANSFER CHARACTERISTICS OF THE TEMPERATURE FLUCTUATION

From these analysis, we can now make clear the followings:

First; the different space dependencies of the transfer functions and the coherence functions both calculated with the same pairs of the temperature fluctuations can be ascribed to the strong attenuation of the fluctuation levels at the unheated downstream region. Yet, the information of the local boiling is surely transferred to the upper end of the pin bundle, even if it is fairly small.

Second; the subassembly outlet temperature fluctuation is never correlated to that at the boiling position. We can consider that the subassembly outlet temperature fluctuation is generated mainly by the turbulent mixing of the coolant flow, during it moves from the upper end of the pin bundle to the subassembly outlet.

## The whiteness test method( I )

**Step I**

$$\varepsilon_n = \underline{X}_n - \sum_{i=1}^{M} \hat{a}_i X_{n-i}$$

$\varepsilon_n$: residual random Process

$\underline{X}_n$: fluctuation to be diagnosed

**Step 2**

$$\Psi_{\varepsilon\varepsilon}(n, \tau) = \frac{1}{L} \sum_{j=1}^{N_0} \varepsilon_{n-j}^{*} \varepsilon_{n+j-\tau}$$

$$\tau = 1, 2, \cdots\cdots, \tau_{max}$$

$\tau_{max}$: maximum lag number of the autocovariance function

ANOMALY DETECTION METHOD ..... (Next slide, please. SLIDE No. 9)

We have tried the boiling detection under this difficult situation. Now, I would like to show the principle of an anomaly detection method which uses the Auto-Regressive Model. We call it "Whiteness Test Method".

First of all, we prepare the reference auto-regressive model using the data observed under normal condition. In this process, we can specify the AR model coefficient $A_i$ and the regression order M. Then, we are ready for the anomaly detection.

In the first step, we update the residual random time series data set of the inputted fluctuation signal one by another. The oldest one is omitted from the data set, and a newly calculated one is added to the data set. This data set can inform us a scale of the model fitting error. Of course, the model is preparatively so defined that the fitting error is minimized at the normal condition.

Next, we update the auto-covariance function using the updated data set. However, when we use the usual data handling method for this calculation, it takes a very long computation time and a large computer memory size. So, we rearranged the handling method into two steps. The second and the third steps show these processings.

## The whiteness test method(2)

**Step 3**

$$\phi_{\varepsilon\varepsilon}(n+N_0, \tau) = \phi_{\varepsilon\varepsilon}(n, \tau) + \Psi_{\varepsilon\varepsilon}(n, \tau) - \Psi_{\varepsilon\varepsilon}(n-L, \tau)$$

**Step 4**

$$I(n+N_0, M, L, \tau_{max}) = \sum_{\tau=1}^{\tau_{max}} |\phi_{\varepsilon\varepsilon}(n+N_0, \tau)|^2$$

**Step 5**

$I^{\ell}_{mt} \leq I(n+N_0, M, L, \tau_{max}) \leq I^{u}_{mt}$ : Normal

Otherwise : Anomaly

$I^{\ell}_{mt}$, $I^{u}_{mt}$ : alarm levels

..... (Next slide, please. SLIDE No. 10)

In the fourth step, we take the summation of the square of updated auto-covariance function. We call the result "AR Index".

The last step is a limit level checking of the updated AR Index. When the index lies within the range between lower and upper alarm levels, our Whiteness Test Method algorithm judges that the status is normal, and otherwise anomaly.

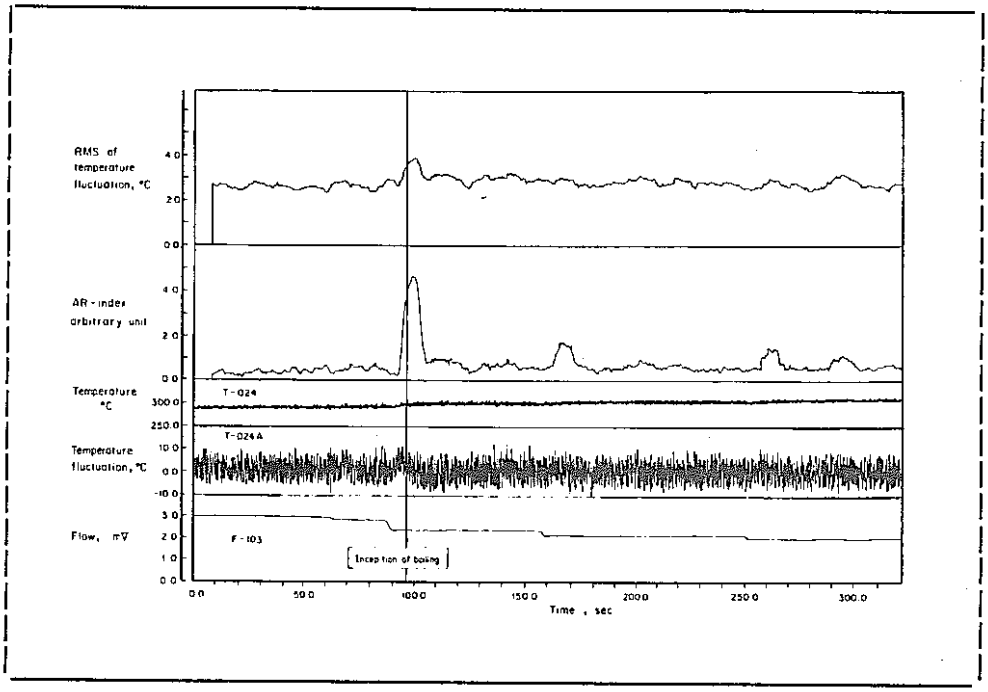


ANOMALY DETECTION ... (Next slide, please. SLIDE No. 11, i.e. Fig. 10)

This slide shows the first example, where the RMS Method and the present Whiteness Test Method are applied to the subassembly outlet temperature fluctuation.

Concerning the RMS values of the temperature fluctuation, little changes were found during the run. In the history of the AR Index of temperature fluctuation, you can find remarkable increases immediate after every flow reductions.

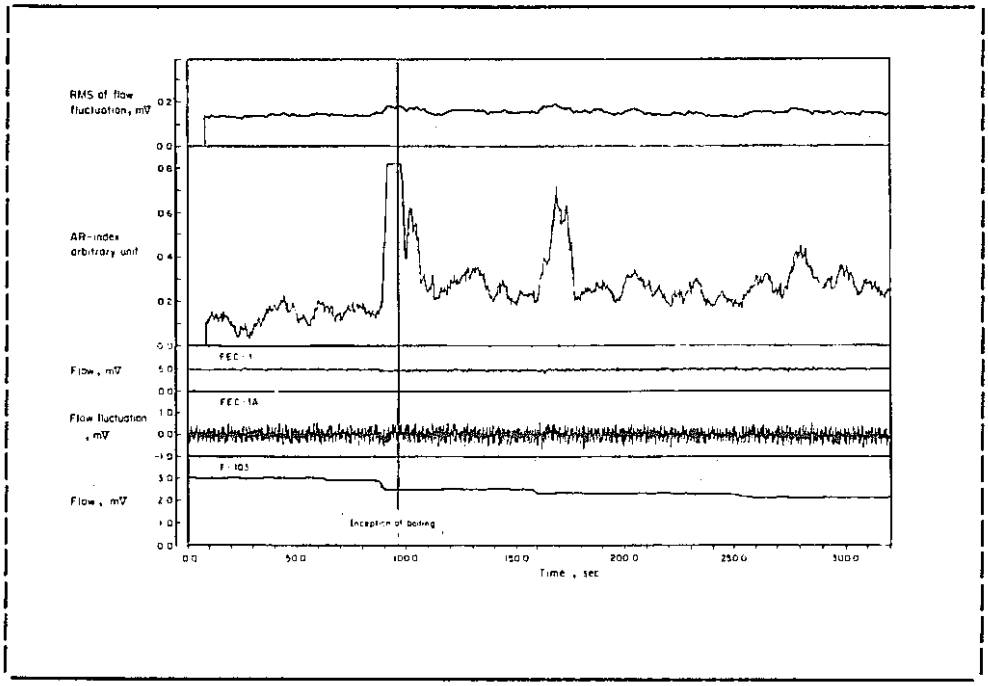


..... (Next slide, please. SLIDE No. 12, i.e. Fig. 11)

This is the second example, where the two methods are applied to the flow fluctuation. We can see the similar tendency.

The mean levels of the AR Indices at three sustained steady-state local boiling tests increased fairly from the reference level at the non-boiling condition. On the other hand, the amount of the increase in the RMS level was less than 20 %. This level will be insufficient to identify the local boiling.

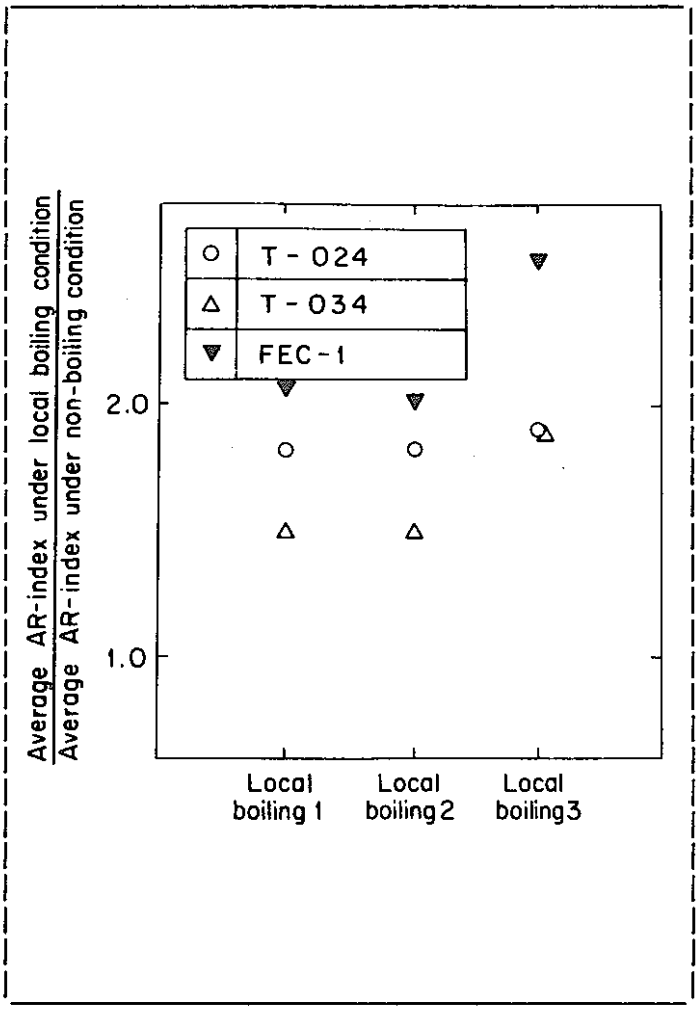


SENSITIVITY ..... (Next slide, please. SLIDE No. 13, i.e. Fig. 12)

This slide shows the ratio of the AR Index levels under steady-state local boiling tests with respect to the non-boiling condition. For the subassembly outlet temperature fluctuation, the ratio was from 1.5 to 1.8, and for the flow fluctuation, it was from 2.0 to 2.5. We can expect from this figure that the ratio will increase with boiling intensity.

We can say that the local boiling may be detected when the boiling region is large enough to change the turbulent mixing at the subassembly outlet, or, in other words, the boiling detection will be possible when the local boiling transits to the oscillatory pattern as is usually observed prior to the occurrence of pin failure.

CONCLUSIONS PNC-FS-018s

(1) THE STRONG CORRELATION WAS FOUND FOR THE TEMPERATURE FLUCTUATIONS OBSERVED AT THE BOILING POSITION AND THE END OF THE BUNDLE, WHILE THE CORRELATION HAS NOT BEEN CLARIFIED WITH REGARD TO THE FLUCTUATION AT THE SUBASSEMBLY OUTLET.

(2) IT WILL BE PROMISING TO DETECT LOCAL BOILING ACCIDENT WHEN THE BOILING INTENSITY BECOMES FAIRLY LARGE.

(3) THE WHITENESS TEST METHOD (WTM) OF FLUCTUATION SIGNAL WAS A SENSITIVE AND RELIABLE METHOD FOR DETECTING A LOCAL BOILING ACCIDENT WITHIN A SUBASSEMBLY.

CONCLUSIONS ..... (Next slide, please. SLIDE No. 14)

I would like to summarize the present work.

First; the coherent correlation was found for the temperature fluctuations observed within the whole pin bundle region, while it was not identified at the subassembly outlet.

Second; it will be promising to detect the local boiling when the boiling intensity becomes large. In order to assure the integrity of the fuel pins, superior cooling performance by the two-phase flow is needed. The oscillatory boiling will satisfy this condition.

Third; the Whiteness Test Method of fluctuation signal was a sensitive and reliable method for detecting a local boiling accident within a fuel subassembly.

That is all. Thank you.

Liquid Metal Boiling Working Group

9th Meeting
June 4 - 6, 1980
Rome, Italy

# LOCAL TEMPERATURE RISE AND BOILING BEHAVIOR BEHIND A CENTRAL BLOCKAGE IN A WIRE-WRAPPED PIN BUNDLE

K. Yamaguchi, M. Uotani, K. Haga and M. Hori

O-arai Engineering Center, Power Reactor
and Nuclear Fuel Development Corporation, Japan

## ABSTRACT

The succeeding series of central-type blockage experiments were completed by the present one with 61-pin bundle test section. The interpretations of the present test results and those of our previous bundle configurations were summarized in the present paper.

Concerning the single-phase flow, an empirical formula was derived to estimate the temperature rises behind various central-type blockages: $\tau U_B/d_h = 35.3(D_B/p)^{0.85}$, where $\tau U_B/d_h$ is the dimensionless residence time and $D_B/p$ is the Ring Parameter newly introduced here. This formula was validated to be effective within the region up to x4 mockup scale ($3.0 \leq d_h \leq 16.1$ mm) and was also supported by the data of KfK and ORNL. It was guessed that the apparent peaking factor of temperature rises in the wake region that would be observed in case of bare bundle was about 1.5 and that the effect of three-dimensional distortion due to spacer wires was from 0.9 to 1.2. The estimation of peak temperature rise by the present formula and two kinds of constants led the conclusion that the central-type blockage will not cause local boiling without being detected by an in-core flow-meter.

In case of sodium boiling two-phase flow, existence of a large boiling window could be identified through the experimental knowledge on oscillatory boiling and dry-out mechanism: the stable oscillatory behavior of a single bubble (or a cluster of bubbles) was never terminated untill the saturated region being widely built up enough to yeild the one-sided expansion of bubbly region and following clad melting. The oscillation improved the mass exchange between localized bubbly region and surrounding subcooled free stream region in compared with that under non-oscillatory conditions, and often relieved clads from melting.

## INTRODUCTION

In the current safety research of an LMFBR, the formation of local flow blockage has been treated as one of the possible initiator of fuel failure propagation in a subassembly. In the present paper, we deal with the early two stages in the event tree in question:

(1) the estimation method of temperature field behind the blockage, which results in the conditions of the onset of sodium boiling;
(2) the critical conditions of the occurrence of local clad melting followed by local dry-out of pin surfaces.

## EXPERIMENTAL EQUIPMENT AND OPERATING PROCEDURES

### Test Section

A series of experiments were carried out with the Sodium Boiling and Fuel Failure Propagation Tesst Facility SIENA in FBR Safety Section of OEC/PNC.

Figure 1 shows a sketch of the locally blocked 61-pin bundle wire-spacer type test section. In order to simulate an LMFBR fuel subassembly, a total of 61-pin bundle was installed in a hexagonal tube of 64.1 mm inside flat-to-flat distance. The bundle consisted of central 37 heater pins and surrounding 24 dummy pins. The diameter of each pin was 6.5 mm and the pin pitch was 7.9 mm. As concerns the heater pin, the axial heated length was 450 mm and the heat flux was uniform. A spacer wire of 1.3 mm diameter was wrapped around each pin with helical pitch of 265 mm. At nearly middle position of the heated section, a centrally located blockage of 5 mm thickness stainless steel was attached. The blockage covered 36 % of the total flow area.

The pin surface and sodium temperatures were measured by many chromel-alumel thermocouples. All thermocouples were calibrated prior to experiments by checking their outputs at various isothermal conditions. The inlet sodium flow rate was measured by an electromagnetic flow-meter. The output signals from the thermocouples and flow-meter were recorded on a digital data acquisition system.

### Operating Procedure

In the first stage where temperature rises were measured under steady-state single-phase conditions, the sodium flow rate and the power level were adjusted to the aimed ones within the following ranges:

| | | |
|---|---|---|
| Inlet flow velocity | 0.50 - 4.07 | m/s |
| Heat flux | 4.58 - 94.33 | $W/cm^2$ |

In the second stage where coolability was examined under quasi-steady-state conditions, the flow rate was initially maintained at the constant value and the heat flux of each pin was adjusted to be aimed one. After steady-state condition was attained, three local boiling steps were conducted by reducing the flow rate. The conditions of boiling experiment were:

| | | |
|---|---|---|
| Inlet flow velocity | 1.46 - 1.08 | m/s |
| Heat flux | 61.0 | $W/cm^2$ |

No dry-out test was conducted with the present 61-pin bundle because of the early failure of heater pins.

## SINGLE-PHASE TEST RESULTS AND DISCUSSIONS

### Temperature Distributions

Figure 2 shows a typical two-dimensional isotherms of sodium temperature rises behind the blockage. The horizontal and vertical axes represent the subchannel No. and the distance from the blockage, respectively. Here, the three-dimensional distortion effect of spiral wires on the isotherms was eliminated as small as possible by picking up those data which were measured rotationally with wire angle. The dotted points in each subchannel mean the location where the axial temperature distribution curve takes its minimum values. The broken line is, therefore, the envelope of recirculating sodium flow, i.e. the wake region. The shape and size of the wake were not particular to each run but were much the same with many other results, even if the flow velocity was very slow. The isotherms disagreed with recirculating flow patterns and the maximum temperature position appeared again at immediate vicinity of the blockage center[1].

### Dimensionless Residence Time

Based on the familiar definition of residence time,

$$\tau = \frac{d_h}{4} c_p\gamma \frac{T_{wk}-T_c}{q'}, \qquad \cdots\cdots\cdots\cdots\cdots\cdots\cdots\cdots \quad (1)$$

we calculated $\tau$ for various core flow velocities $U_B$. The tendency of $\tau$ against $U_B$ should be in inverse proportionality, since mean recirculation pass was surely kept constant and the mean recirculation velocity was considered to be proportional to $U_B$. However, this was not always the case due to the molecular heat conduction for very slowly recirculating sodium behind rather large blockage.

From the insight of the isotherms, we first assumed that the asymptotic value of $\tau U_B$ ($\propto T_{wk}-T_c$) at high velocity data may be determined cheifly by the heat and mass exchanges through small gaps of only a limited number of pins whose radial locations are just inside of the contour line of blockage. The localized heat and mass exchanges can be considered to extend to a short distance characterized by subchannel diameter $d_h$ rather than whole blockage size $D_B$. Based on the present assumption, we used not $\tau U_B/D_B$ but $\tau U_B/d_h$ for the dimensionless residence time and examined the analogy of temperature fields observed behind various sizes of blockages. As a natural product of our assumption, we introduced a new dimensionless variable named Ring Parameter. The definition is $D_B/p$ (characteristic length of blockage/pin pitch). The Ring Parameter is correctly proportional to the number of pins around the contour line of blockage when central-type blockages are concerned.

In Fig. 3, the dimensionless residence times are plotted against the Ring Parameter. Almost all data available converged into one line, and was expressed by the empirical formula:

$$\tau U_B/d_h = \frac{c_p\gamma}{4} \frac{U_o}{q'(1-F)} (T_{wk}-T_c) = 35.3(D_B/p)^{0.85}. \qquad \cdots\cdots\cdots \quad (2)$$

The result supported the varidity of our treatment. It will be deduced from this result that the interface area between wake and free stream, where geometrical configuration of triangularly arranged pins plays an important rule for the sodium cross flow, will sheild the long-distance heat and mass transfer. In such a case, major parts of the heat and mass transfer, i.e. the energy balance within the wake, is controlled by the Ring Parameter as formulated in Eq.(2). The power 0.85 on the Ring Parameter can be regarded as the blockage-size dependency of the ratio: (the effective area of heat and mass

exchanges) : (the wake volume).

The utilization of the empirical formula was restricted to asmall pin-gap bundle and to small fraction range of blocked flow area. The available data indicates that the formula is effective for the bundles whose subchannel diameters lie within the range $3.0 \leq d_h \leq 16.1$ mm. Similarly, for the fraction of blocked flow area, the restriction becomes $0 \leq F \leq 0.6$ of 169-pin bundle. For very large blockage and large pin-gap configurations, the surrounding pressure field makes the recirculating flow being in abnormally coupled with the core flow[2]. This forces our premises into being invalidated.

Extrapolation to Reactor Conditions

The peaking factors, $C_{B,max}=(T_{B,max}-T_c)/(T_{wk}-T_c)$ and $C_w=(T_w-T_c)/(T_B-T_c)$, were obtained, where $T_B$ means an apparent local temperature in the wake that will be observed in case of bare bundle and $T_w$ is the real local temperature under wire-wrapped bundle configuration. From many temperature data measured rotationally at different positions on the same axial location, we estimated that the peaking factor $C_w$ lay from 0.9 to 1.2. The bare bundle peaking factor $C_{B,max}$ was 1.5 to 1.6.

These values were directly multiplied to the estimated wake temperature from Eq.(2). The resultant local temperature rises for the conditions of Japanese prototype reactor MONJU are shown in Fig. 4. In the case of central-type blockage, the local temperature rise first increases with the fraction of the blocked area, and after attaining a 320 °C peak temperature rise at F = 0.3, decreases gradually. The latter tendency, which was similar to that evaluated by Basmer et al. for SNR-300[3], is ascribed to the increase of core flow velocity $U_B$. It is seen that the central-type blockage will not cause local boiling without being detected by an in-core flow-meter, since the flow-meter can sense the global flow reduction of greater than 10 %. One of the critical conditions of the incipient boiling was the overlapping of the formation of 30 % blockage and the operation under 125 % mismatching of power-to-flow ratio.

## BOILING TEST RESULTS AND DISCUSSIONS

Oscillatory Boiling Behavior

Figure 5 shows typical signals observed during the initial non-boiling step of local boiling experiment (Run No. 61WLB-101). The flow velocity was maintained at the constant value of 1.46 m/sec and the heat flux of each pin was adjusted to be 61 W/cm$^2$. The inlet sodium temperature was 503 °C and the cover gas pressure was 1.01 bar.

In this experiment, three steady-state local boiling steps were conducted under different conditions by reducing the flow velocity stepwise. After the first flow reduction, where the flow velocity was changed to 1.24 m/sec level, the maximum temperature observed within the wake region reached saturation level. Little amounts of initial boiling superheat were identified. During the first step of steady-state local boiling, small vapor bubbles were formed irregularly according to the fluctuation of sodium temperature.

Further reduction of flow velocity caused oscillatory boiling. Figure 6 shows typical signals of inlet velocity, temperatures, pressure and void fraction during the second step of local boiling experiment, where the mean flow velocity was changed to 1.08 m/sec level. During this step, small amount of vapor bubble always survived the oscillation. This conclusion was derived from the attentive interpretation of the present experimental data. The same conclusion has been obtained in the experiments of KfK[4], ECN[5] and PNC[6]

(our previous experiments with 37-pin bundle central-type blockage test section). This finding conflicts with the analytical model of oscillatory boiling in which the isothermal compression process of a single bubble is assumed[7]. In other words, total amount of energy transported from bubble to surrounding liquid must be less than the total internal energy of the oscillated bubble: a certain part is originated by the continuous heat input and the other part is worked by the contraction of bubble volume. However, the model brought us contradict answer.

To evaluate more practically the bubble oscillation frequency observed in the present 61-pin and previous 37-pin test bundles, an analytical model has been developed.

The oscillatory behaviors of both liquid and bubble were first formulated by the one dimensional momentum equation of liquid column. Dynamic behavior of liquid column was then expressed by the ordinaly differential equation. In this derivation, linear perturbation method was applied. The bubble behavior was coupled with the displacement of liquid column under the following assumptions:

(1) bubble is represented by a single sphere;
(2) in the process of bubble expansion, vapor pressure is presented by Gast's model (linear temperature profile is assumed within the wake);
(3) in the process of bubble contraction, vapor pressure is presented by polytropic change (i.e. $P_b V^n$=const.).

The experimentally estimated value of mean bubble volume was inputted to the code. The polytropic index was also fixed through the interpretation of measured data. The proper value was 0.1 to 0.2 (for the isothermal and constant pressur compression process menthioned above, "n" equals to 0).

Figure 7 shows the comparison of oscillation frequencies, one was observed in the experiment and another was evaluated from the present code. The horizontal axis means the temperature gradient within the wake. For the derivation of this value, maximum and minimun values of measured temperatures within the wake were used. Concerning the 37-pin bundle results, calculated frequency agreed well with the measured one. However, discrepancy appeared between calculated frequency and measured one in the case of 61-pin bundle.

The tendency of the calculated frequency being higher than the actual one was preparatively examined and its major cause was ascribed to the over-estimation of the used value of temperature gradient. Due to many trouble encountered in the present experiment with 61-pin bundle, we could not obtain enough data to check the reasons of the discrepancy in detail.

Restricting ourselves within rough estimations, we summarized the phenomena of oscillatory boiling and its termination as follows:

(1) oscillatory boiling is stably succeeded when there exists a large difference between the temperatures measured at the wake center and the core flow region;
(2) the oscillation is gradually damped in keeping with the build up of high temperature region around the wake, and at last it will be stabilized (when the coolability is assured).

Dry-out Behavior

Prior to the present 61-pin bundle experiment, dry-out test was conducted with the 37-pin bundle test section (Run No. 37(19)WLB-114). The flow velocity was initially maintained at the constant value of 1.70 m/sec and the heat flux was adjusted to be 167 W/cm$^2$. The inlet sodium temperature was 461 °C and the cover gas pressure was 1.05 bar.

In this test, the heat flux was increased stepwise with the other conditions being held almost constant. Figure 8 shows the signals observed during the instance of permanent dryout. Horizontal axis means the relative time defined such that the switching off of heater power can be identified by t = 0 sec.

After the stable oscillatory boiling being succeeded for a long period, the amplitude of osillatory signals became to show damping tendency during the time interval -2 sec to -1 sec in Fig. 8. It was obvious from the experimental data and the analytical estimation curves drawn in Fig. 7 that the gradual growth of radial and axial high temperature region forced the oscillation being stabilized. The main driving force of this behavior was the reduction of the amount of condenced vapor.

As was shown in Fig. 8, pin surface and sodium temperatures measured at the locations both 22 mm downstream of blockage showed steep increases due to the occurrence of dry-out. The sudden one-sided expansion of voiding region was accompanied. The voiding region was, however, limited locally: concerning radial direction, it was extended within about three quarters of blockage diameter, and for axial, it was about three times as long as blockage diameter. The global flow reduction and flow instability were never observed during this dry-out phase. At about 1.5 sec later after the occurence of local dry-out, heater power was cut by detecting local clad melting.

The theoretical excess temperature at the instance of dry-out, which was equal to the temperature rise exceeding saturation temperature and was calculated from simple heat balance equation, was nearly 140 °C. The excess temperature was correlated to the subcooled temperature measured at the axial end of wake region at the instance of boiling inception. Many available data were also refered. The margin to the boiling crisis was found to depend on the subcooled temperature, i.e. a decreasing function of power to flow ratio $q'/U_o$. It was thus concluded to be sufficiently large for the actual fuel subassembly in compared with our too high $q'/U_o$ conditions.

## CONCLUSION

The succeeding series of central-type blockage experiments were completed The results were summarized as follows:

(1) Single-phase flow

a) The empirical formular was derived to estimate the local temperatur rises behind various central-type blockage.

b) The central-type blocakge will not cause local boiling without being detected by the in-core flow-meter.

(2) Two-phase flow

a) Existance of a large boiling window could be identified.

b) Stable oscillatory boiling improved the coolability of localized bubbly region. Due to this effect, the critical condition of clad melting was expected to be fairly shifted toward that of integral boiling.

These results will be generalized to arbitral type blockages after performing the interpretation of the data that will be derived from our final experiment with 91-pin bundle edge-type blockage test section.

## ACKNOWLEDGEMENTS

The authors are indebted to Mr. T. Isozaki and Mr. T. Komaba for their

technical contributions to the present experimental work.

## NOMENCLATURE

$c_p$ : Specific heat of sodium
$D_B$ : Characteristic length of blockage
$d_h$ : Equivalent diameter of subchannel
$F$ : Fraction of blocked flow area
$P_b$ : Bubble pressure
$p$ : Pin pitch
$q'$ : Heat flux
$T_c$ : Average temperature in core flow
$T_{wk}$ : Average temperature in the wake
$U_o$ : Inlet flow velocity
$U_B$ : Flow velocity at unblocked area
$V$ : Bubble volume
$\tau$ : Coolant residence time
$\gamma$ : Specific gravity of sodium

## REFERENCES

[1] M. Uotani et al.: "Local Flow Blockage Experiments in 37-pin Sodium Cooled Bundles with Grid Spacers", 8th LMBWG Meeting, Mol (1978)
[2] M. H. Fontana et al.: "Thermal-hydraulic Effects of Partial Blockages in Simulated LMFBR Fuel Assemblies with Application to the CRBR", ORNL-TM-4779 (1975)
[3] P. Basmer et al.: "Experiments on Local Blockages", 6th LMBWG Meeting, Riseley (1975)
[4] F. Huber, W. Peppler: "Form and Development of Boiling behind a 49 % Central Blockage in a 169 Pin Bundle", 7th LMBWG Meeting, (1977)
[5] B. Dorr, J. E. deVries: "The ECN/KfK Local Boiling Experiments in Petten", 8th LMBWG Meeting, Mol (1978)
[6] M. Uotani et al.: "Local Boiling Experiments in a Wire-Wrapped 37-pin Bundle with a Central Blockage", Preprint 1979 Annual Meeting of the Atomic Energy Society of Japan (1979)

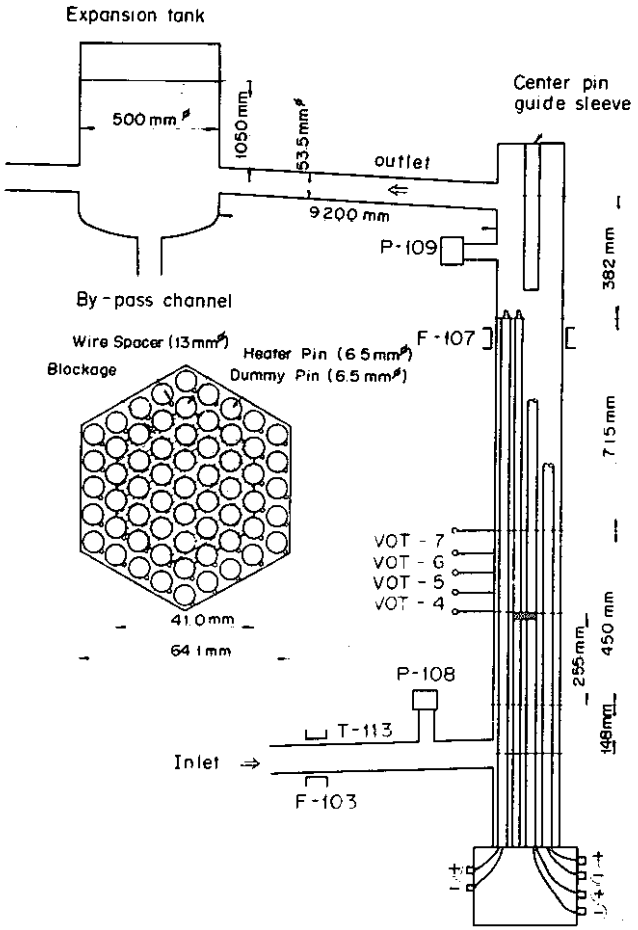


Fig. 1 Locally blocked 61-pin bundle test section (PNC-FS-1179)

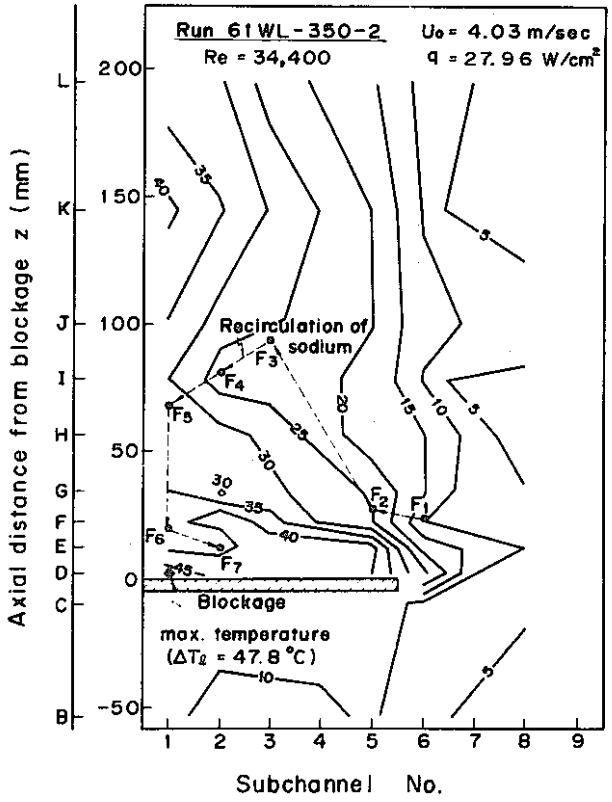


Fig. 2 Isotherms of sodium behind the blockage (PNC-FS-1086)

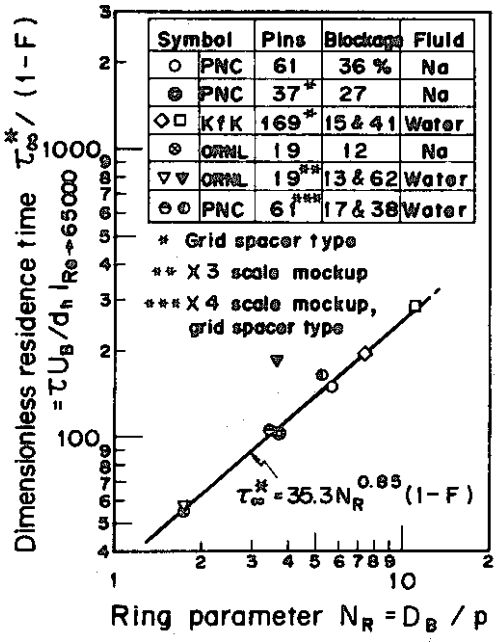


Fig. 3 Correlation between dimensionless residence time and Ring Parameter (PNC-FS-1103)

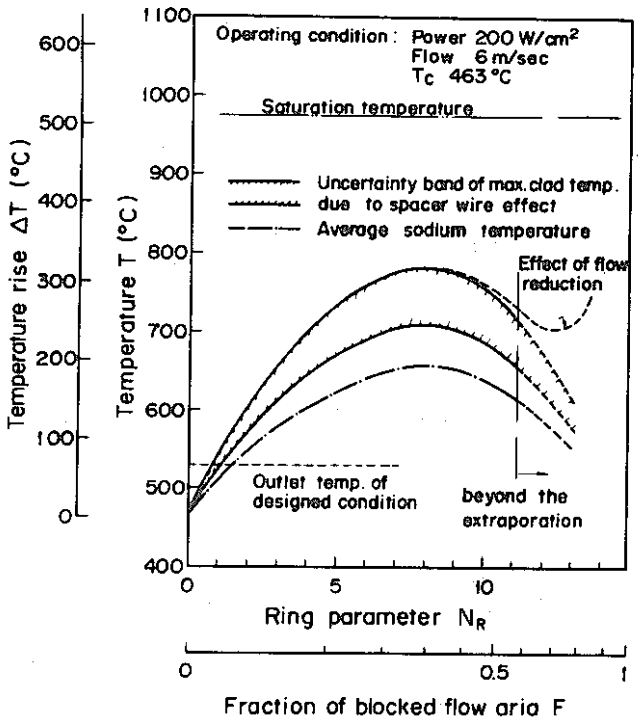


Fig. 4 Estimation of temperature rises behind various blockages, — MONJU condition (PNC-FS-1107)

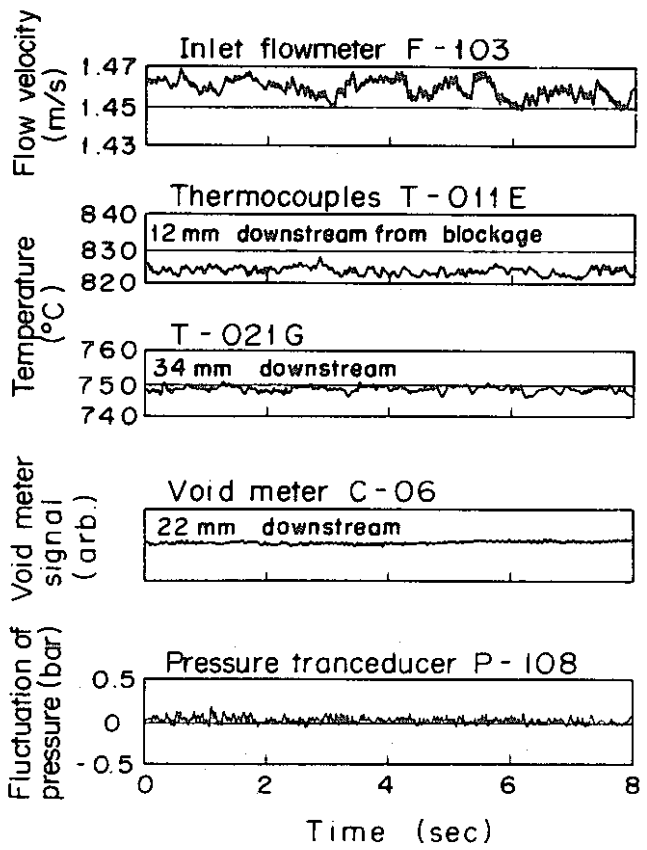


Fig. 5 Signals under non-boiling condition, -- Run No. 61WLB-101 (PNC-FS-1180)

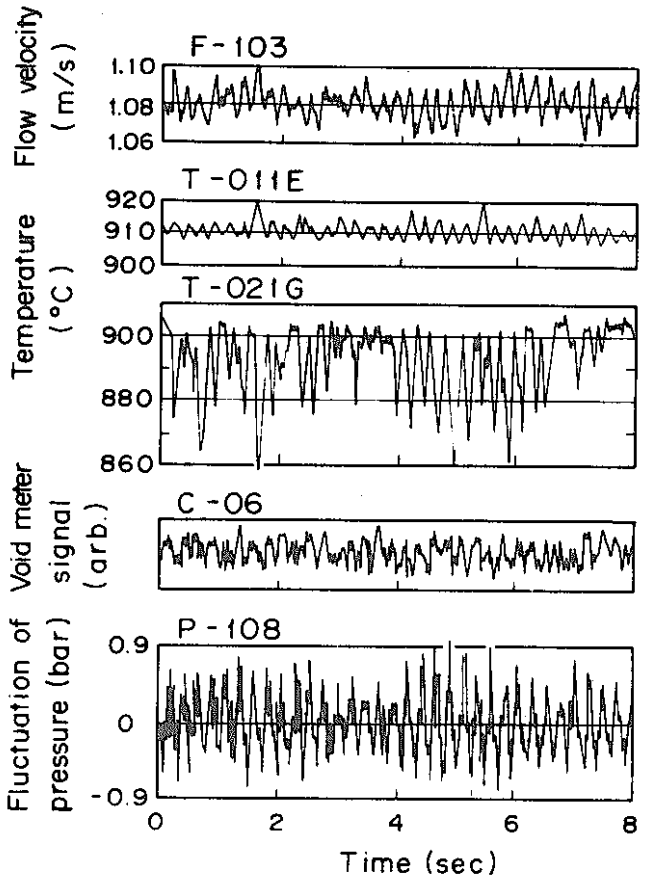


Fig. 6 Signals under oscillatory boiling condition, -- Run No. 61WLB-101 (PNC-FS-1181)

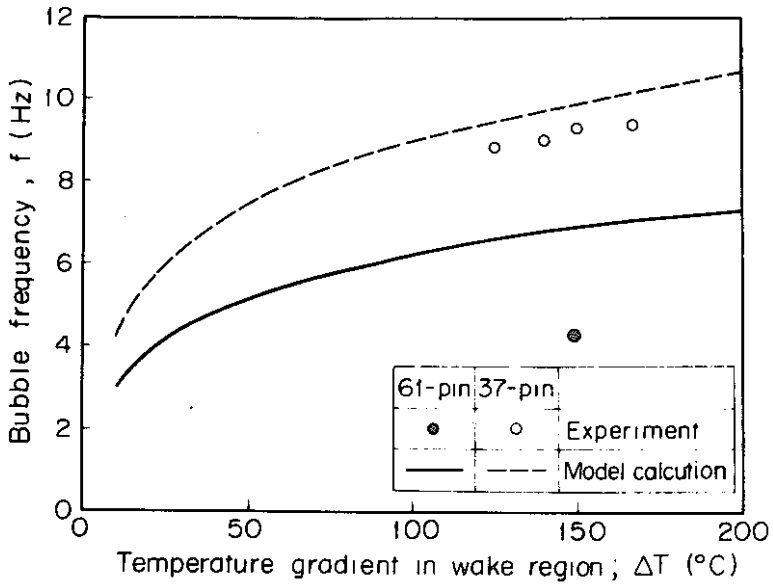


Fig. 7 Effect of temperature gradient in the wake region on the oscillation frefuency
(PNC-FS-1188)

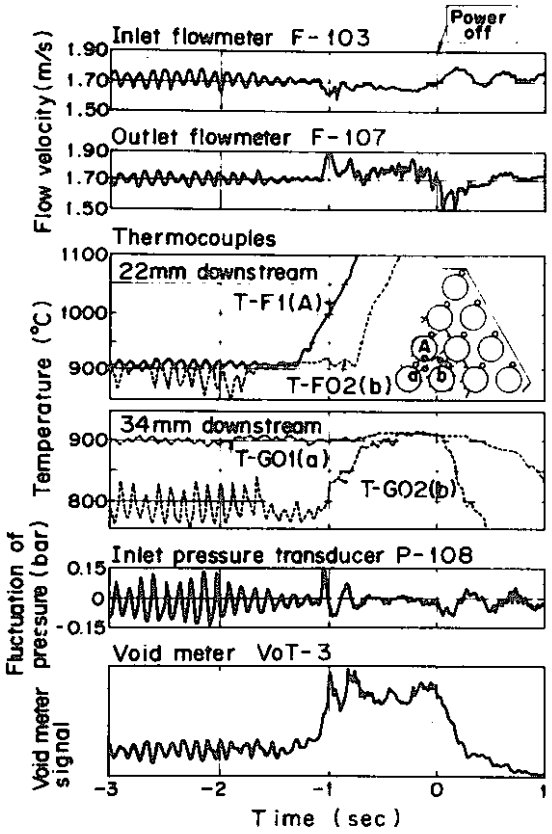


Fig. 8 Signals at the occurrence of permanent dry-out, -- Run No. 37(19)WLB-114
(PNC-FS-1109)

# APPENDIX: SCOPE OF PRESENTATION

Liquid Metal Boiling Working Group

9th Meeting
June 4 - 6, 1980
Rome, Italy

## LOCAL TEMPERATURE RISE AND BOILING BEHAVIOR BEHIND A CENTRAL BLOCKAGE IN A WIRE-WRAPPED PIN BUNDLE

K. Yamaguchi, M. Uotani, K. Haga and M. Hori

O-arai Engineering Center, Power Reactor
and Nuclear Fuel Development Corporation, Japan

## INTRODUCTION

Thank you, chairman. Next, I would like to present our recent progress on the Local Flow Blockage Experiments.

9TH LIQUID METAL BOILING WORKING GROUP MEETING (PNC-FS-022s)
ROME, ITALY, JUNE 4-6, 1980

# LOCAL TEMPERATURE RISE AND BOILING BEHAVIOR BEHIND A CENTRAL BLOCKAGE IN A WIRE-WRAPPED PIN BUNDLE

K.YAMAGUCHI, M.UOTANI, K.HAGA AND M.HORI
FBR SAFETY SECTION, OEC/PNC, JAPAN

OBJECTS

(1) ESTIMATE THE TEMPERATURE FIELD BEHIND A BLOCKAGE
.... ONSET OF SODIUM BOILING

(2) EXAMINE THE CRITICAL CONDITIONS OF LOCAL CLAD MELTING
.... FLOW PATTERN, BURN-OUT MECHANISM,
BURN-OUT REGION, ETC.

OBJECTS ..... (First slide, please. SLIDE No. 1)

We have two objects for our Local Flow Blockage Experiments. The first one is to find the estimation method of temperature fields behind arbitral sizes of blockages. Whether or not the flow blockage leads to sodium boiling is a matter of argument. The second one is to find the critical conditions of the occurrence of local cladding melting. And, what we want to clarify further is the accident scenario of the fuel failure propagation.

For these studies, we have conducted four series of central-type blockage experiments until last year. The first series used a 7-pin bundle grid type subassembly, the second and the third series used 37-pin bundle grid and wire-wrapped ones, and the last series used the 61-pin bundle wire-wrapped one. We have no future plan to conduct further experiments with respect to central-type flow blockages.

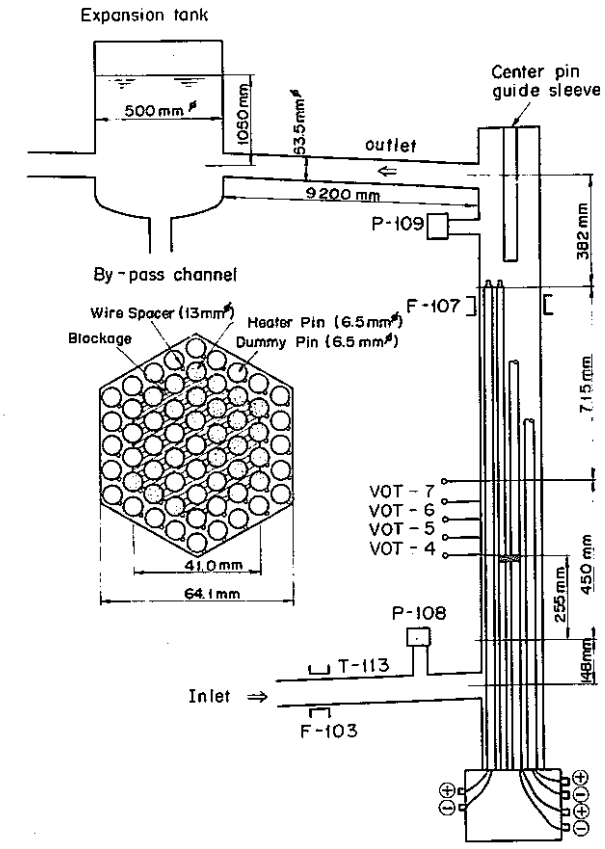


Fig Locally blocked 61-pin test section (PNC-FS-1179)

TEST SECTION ..... (Next slide, please. SLIDE No. 2, i.e. Fig. 1)

This is the 61-pin bundle test section we have used in the last series experiments. It was mounted in the out-of-pile test facility, SIENA. I want to omit the explanation of it, because it is the same one I have mentioned in my last presentation.

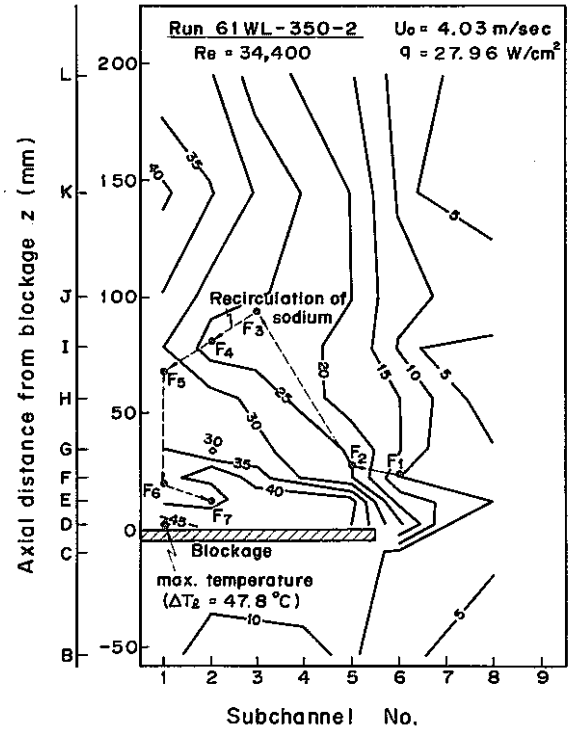


Fig. 8-3 Isotherms of sodium behind blockage
(PNC - FS - 1086)

ISOTHERMS ..... (Next slide, please. SLIDE No. 3, i.e. Fig. 2)

First of all, I would like to present the single-phase test results.

This slide shows the typical two-dimensional isotherms of sodium temperature observed in the 61-pin bundle. The horizontal axis is a subchannel No. counted from the bundle center, and the vertical axis is a distance from the blockage. A total of about 60 points temperature rise data were used to draw these isotherms.

I think, you feel that the global pattern of the isotherms is quite different from those measured previously by the KfK members. We have examined the cause of the difference in detail and reached the following conclusion.

It is mainly ascribed to the geometrical difference around the edge of the blockage.

In our test section, there exists no obstract in the unblocked region except for the wires. This permits the sodium to flow fairly freely toward the arbitral direction around the blockage. On the other hand, the grid spacer in the unblocked region of KfK's test section forces the sodium to flow almost regularly toward the vertical direction. Only a small difference in the sodium flow pattern in this region makes, I believe, a large difference in the recirculation flow pattern and the isotherms of sodium behind the blockage.

By the way, the present isotherms indicate us that a large amount of heat is transported from the wake to the core flow through the narrow region at the edge of the blockage. This fact plays an important role in our following discussions, because our method of estimating the temperature rise within the wake based on the analogy of the thermo-hydraulic field within this restricted region. The other part of the isotherms show rather gentle slope, and the point where the sodium temperature takes its maximum value appeared again near the surface of the blockage center.

In order to calculate the residence time of the recirculating sodium flow, we must, at first, specify the outline of the wake region. It was made by finding the minimum temperature point in the axial temperature profile along the individual subchannel flow passage. These points are dotted in this figure. Thus, the broken line drawn from point $F_1$ to point $F_7$ means the envelope of the recirculating flows. Within our experimental conditions, this shape was not changed without regards to the core flow velocities and heat flux.

The wake length estimated by the usual definition was 1.8 times as large as the characteristic length of the blockage.

RESIDENCE TIME (PNC-FS-023s)

$$\tau = \frac{D_H}{4} c_p \gamma \frac{T_{WK}-T_C}{q'}$$

RELATION

$$\tau U_B = \frac{D_H}{4} c_p \gamma \frac{U_B}{q'} (T_{WK}-T_C) = \underline{\text{CONST.}}$$

.... FOR A GIVEN GEOMETRY OF BUNDLE, BLOCKAGE, ETC.

- MEAN RECIRCULATION PASS IS KEPT CONSTANT
- MEAN RECIRCULATION FLOW VELOCITY IS DIRECTLY PROPORTIONAL TO CORE FLOW VELOCITY
- MOLECULAR HEAT CONDUCTION CAN BE NEGLECTED

RESIDENCE TIME ..... (Next slide, please. SLIDE No. 4)

Once we have specified the wake region, we can roughly calculate the mixed mean sodium temperature within the wake, $T_{wk}$, under the assumption of uniform sodium flow profile. The residence time tau is, then, derived from this equation.

The calculated residence time became to be inversely proportional to the core flow velocity $U_B$ when the velocity was sufficiently high. You can easily understand that this conclusion is a natural result when following facts are satisfied:

First; the mean recirculation pass is kept constant. Second; the mean recirculation flow velocity is directly proportional to the core flow velocity. Third; the molecular heat conduction can be neglected. The first and the third items were verified in the present tests, and the second one was confirmed by the water mockup tests in PNC.

Now, let us notice on a question "How the asymptotic value tau*$U_B$ changes for different blockages and bundle configurations?".

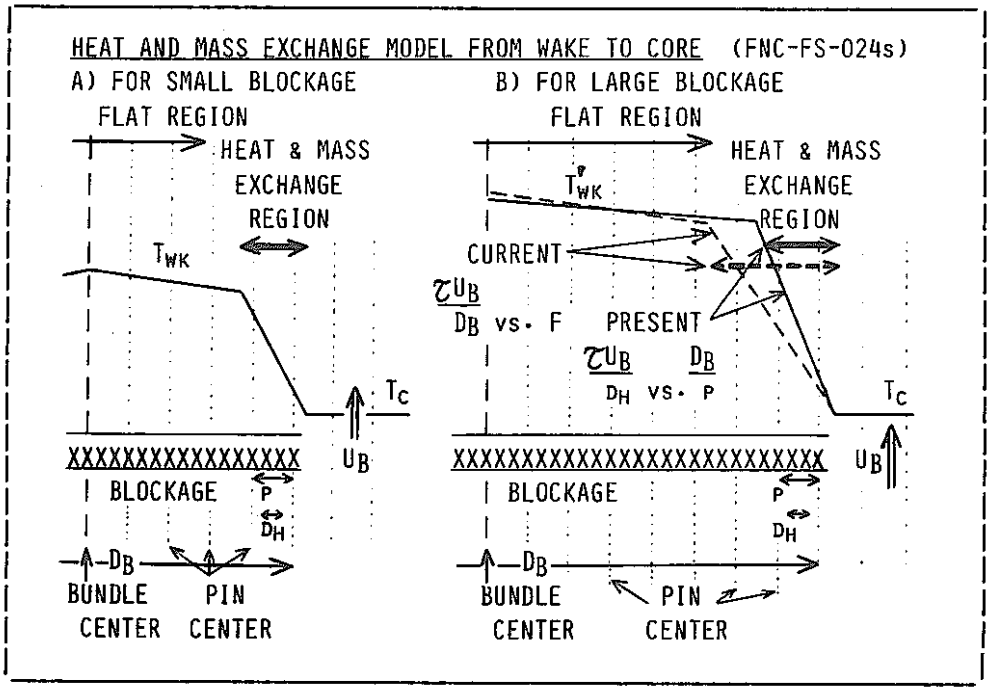


HEAT & MASS EXCHANGE MODEL ..... (Next slide, please. SLIDE No. 5)

This slide shows two models which treat the temperature fields under different situations.

Please suppose that the left illustration is a measured radial temperature profile at a certain plane behind a small blockage. And, for a short time, let us assume that the effect of the wrapper tube on the temperature field is negligible.

The current model stands on the global analogy, in other words, it assumes that the temperature field behind a large blockage will be an expanded on by the scale factor between two geometrical configurations. This idea will yield the broken curve drawn in the right illustration. The current definition of the dimensionless residence time $\tau U_B/D_B$ is certainly consistent with this idea, because the asymptotic value of $\tau U_B$ is normalized by the characteristic length of the blockage $D_B$.

If we are based on the assumption that the effect of the wrapper tube is important for the wake formation, then the dimensionless residence time should be correlated by the functional form of the blockage ratio F. However, this idea will not bring us successful result, as you will see later.

The second model is what we want to propose today. It stands on the assumption that the wake temperature depends only on the heat and mass exchanges within the narrow region illustrated by the solid arrows.

If it is true, we will better normalizing the asymptotic value of tau*$U_B$ by the subchannel hydraulic diameter $d_h$. In other words, we have considered the analogy of the thermo-hydraulics only within the narrow region characterized by the pin pitch and the pin diameter. For us, the complex temperature profile in the residual parts do not have any matter in this step. Because, it is more or less integrated to yield the whole sodium enthalpy within the wake.

In our model, we consider that the pins within the narrow region play as the shielding obstracts for the sodium cross flow. Therefore, the dimensionless residence time should be correlated, in our case, by the geometrical conditions of the pins participated in the noticed shielding phenomenon. This idea brought us a new parameter $D_B/p$, where p is a pin pitch. We named it "Ring Parameter". The value of the Ring Parameter is proportional to the total number of the pins or pin gaps at the edge of the blockage. So, we are ready to examine by this Ring Parameter the shielding effect of the pins.

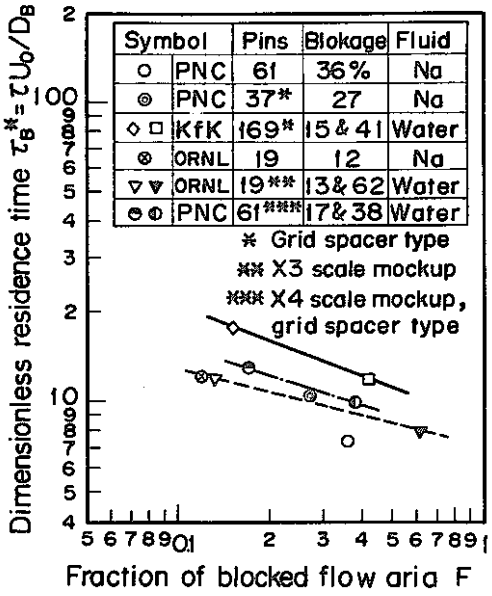


Fig.20-3 Rundom plot of all results for the dimensionless residence times (PNC-FS-1104)

CURRENT MODEL ..... (Next slide, please. SLIDE No. 6)

Before showing our results, I would like to remember the pending problem in the foregoing discussions.

In this figure, the familiar dimensionless residence time tau*$U_B/D_B$ are plotted against blockage ratio F. Here is our last one with the 61-pin bundle. These are the data measured in the water mockup experiments in PNC. The difference of the experimental configurations between them lies only in the mockup scale. So, the difference between these data evidently implies us the insufficiency of the current approach, especially when we want to know the effects of pin diameter and pin pitch.

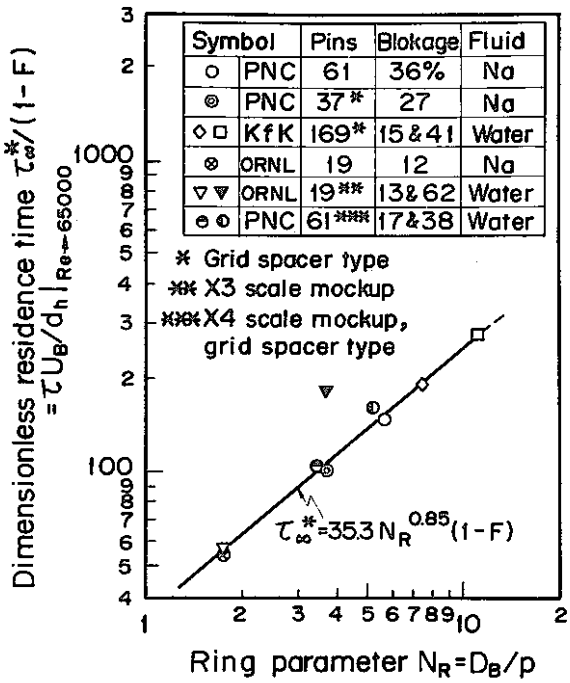


Fig.20-2 Correlation of residence time inside of the wake behind the central blockage in 169-pin bundle (PNC-FS-1103)

PRESENT MODEL ..... (Next slide, please. SLIDE No. 7, i.e. Fig. 3)

This slide shows the results of our approach. Symbols are equal to that in the previous figure. The vertical axis is the residence time normalized by the hydraulic diameter of the subchannel. The horizontal axis is the Ring Parameter. Almost all data available converged into a solid line.

We must emphasize, at least, two problems from this result. First; our premise, on the thermo-hydraulic analogy will not hold for a very large blockage case, say, for more than 60 % blockage. Second; the analogy may not be effective for a large scale mockup configuration, for instance, more than 4 times as large as the usual pins in a reactor. It can be seen from this figure, where the slight divergence from the solid line is identified on this point.

Now, we can find the empirical formula for estimating the mean temperature rises within the wake. It is shown here.

ESTIMATION OF LOCAL PEAKING FACTOR (PNC-FS-025s)

ASSUMPTION

THE PEAKING FACTOR OF TEMPERATURE FIELD OBSERVED IN 61-PIN BUNDLE IS EQUAL TO THAT IN 169-PIN BUNDLE

APPROACHES

(1) BARE BUNDLE PEAKING FACTOR:

$$C_{B,MAX} = (T_{B,MAX}-T_C)/(T_{WK}-T_C) \quad \cdots\cdots 1.5 \text{ -- } 1.6$$

(2) SPACER WIRE EFFECT:

$$C_W = (T_W-T_C)/(T_B-T_C) \quad \cdots\cdots 0.9 \text{ -- } 1.2$$

RESULT

$$(T_{MAX}-T_C) = \frac{C_W * C_{B,MAX} * 35.3(D_B/P)^{0.85}}{\frac{C_P\gamma}{4} * \frac{U_0}{Q'(1-F)}}$$

PEAKING FACTOR ..... (Next slide, please. SLIDE No. 8)

What we want to know next is the peaking factor for estimating the maximum temeprature rise under wire wrapped bundle configuration.

For this purpose, we took the following steps. First of all, we assumed that the peaking factor of the temperature field observed in our 61-pin bundle is equal to that in the full bundle. Then, two kinds of peaking factors were estimated.

The first one means the apparent peaking factor of the temperature profile that will be observed in the case of bare bundle. And, the second one is that relating to the three-dimensional distortion of the temperature field caused by the swirl flow in the wire-wrapped bundle.

These values were from 1.5 to 1.6 and from 0.9 to 1.2, respectively. Using these two peaking factors, we can now evaluate the maximum temperature rise within the wake.

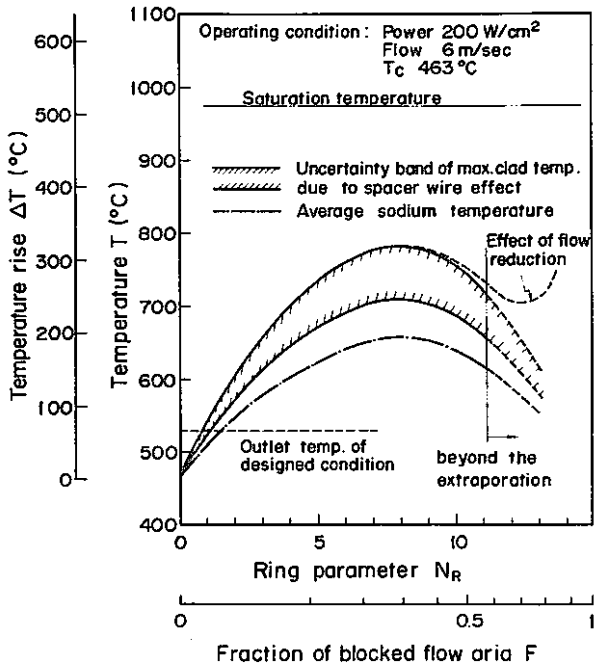


Fig. 23-1 Estimations of maximum clad surface temperature and mixed mean sodium temperature in the wake
(PNC-FS-1107)

EXTRAPOLATION ..... (Next slide, please. SLIDE No. 9, i.e. Fig. 4)

This slide shows the estimated temperature rises behind various sizes of central-type blockages. The design parameters of the Japanese prototype reactor were used.

The local temperature rise first increases with blockage size, and after attaining a 320 °C peak temperature rise at the 30 % blockage ratio, then decreases gradually due to the increased core flow velocity. This tendency is quite similar to that evaluated by Mr. Basmer for the SNR-300 condition. However, our formula yielded higher values of bare bundle maximum temperature rises than his predictions by about 30 %. Up to now, the reason of the difference is not made clear.

We can say that the central-type blockage will not cause local boiling without beeing detected by an in-core flow-meter. One of the critical condition of the boiling onset is the overlapped case of the 30 % blockage formation and 25 % over-mismatch of power-to-flow ratio.

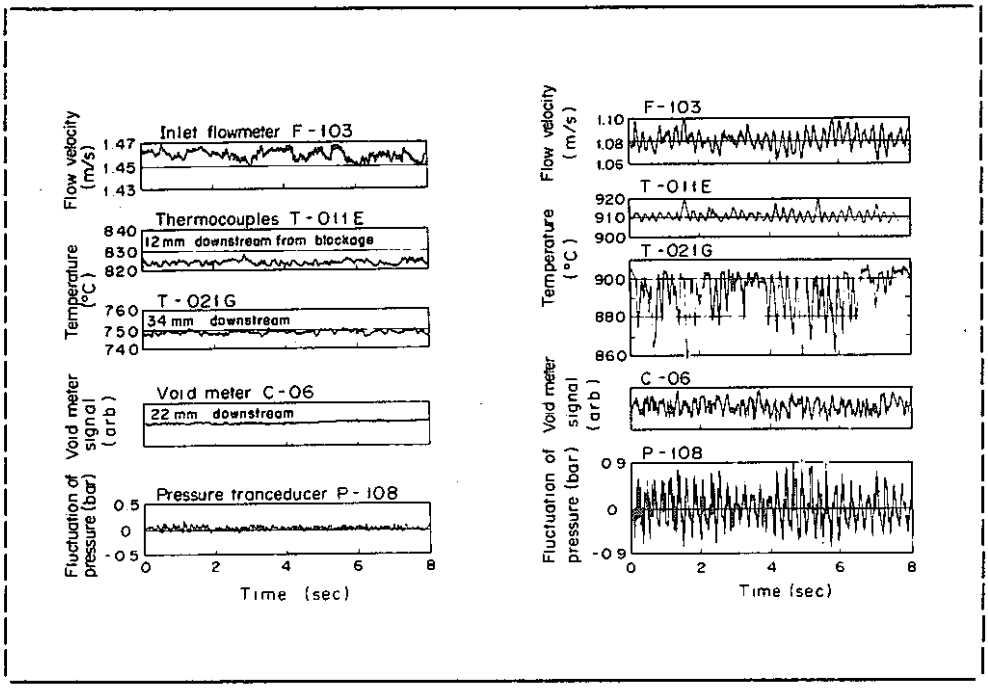


OSCILLATORY BOILING

..... (Next slide, please. SLIDE No. 10, i.e. Figs. 5 and 6)

Next, I would like to show the results of the Local Boiling Tests.

This run is the same one I have shown in my last presentation. The left figure shows signals under non-boiling condition. The initial flow velocity was 1.46 m/sec.

Three steps of local boiling tests were conducted by reducing the flow rate. In the first step, small vapor bubbles were formed irregularly according to the fluctuation of sodium temperature. Further reduction of the flow rate caused the oscillatory boiling. The right figure shows this situation. the mean flow velocity was 1.08 m/sec. During this step, a certain part of the vapor bubble always survived without complete collapsing. To this finding, we could not get any support from the analytical prediction, such as the isothermal compression model submitted by Gast and Fauske.

BUBBLE OSCILLATION MODEL (PNC-FS-026s)

- SINGLE SHERICAL BUBBLE
- ONE DIMENSIONAL MOMENTUM EQ. OF LIQUID COLUMN
- LINEAR TEMPERATURE FIELD
- VAPOR PRESSURE
  EXPANSION ..... GAST'S MODEL
  CONTRACTION .... POLYTROPIC CHANGE

(POLYTROPIC INDEX AND MEAN VAPOR VOLUME
ARE OBTAINED FROM EXPERIMENT

ANALYSIS ..... (Next slide, please. SLIDE No. 11)

In order to account for the oscillation frequency more precisely, we devised an analytical code. The one dimensional momentum equation of liquid column was formulated based on the single spherical bubble model. Dynamic behavior of the liquid column was then expressed by the ordinal differential equation. The linear perturbation method was applied in this process and the linear temperature profile was assumed within the wake region.

Concerning the change of the vapor pressure, the Gast's model was applied to the expanding bubble, and the polytropic change, for the contracting bubble. The polytropic index was found experimentally. The proper value was from 0.1 to 0.2.

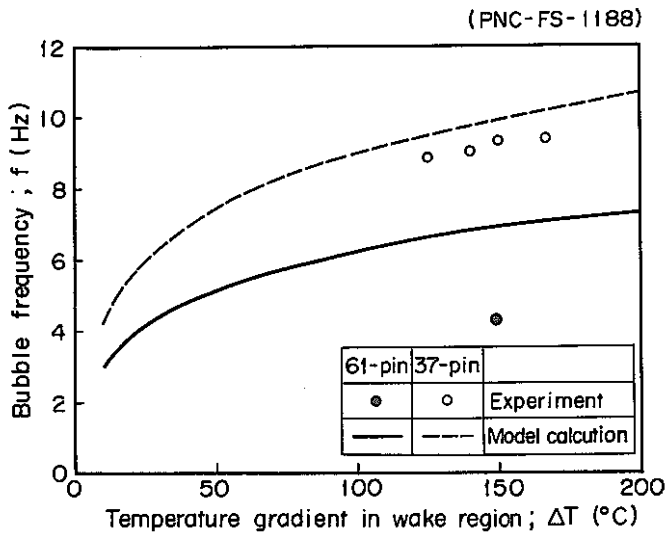


Fig. Effect of temperature gradient in wake region on bubble frequency

COMPARISON ..... (Next slide, please. SLIDE No. 12, i.e. Fig. 7)

This figure shows the comparison between observed oscillation frequencies and those estimated by the present code. The horizontal axis is the temperature gradient within the wake region. The estimated frequencies agreed well with those observed during the 37-pin bundle experiments. However, discrepancy appeared in the case of 61-pin bundle experiment.

The tendency that the calculated frequency is always higher than the actually observed ones was preparatively examined, and its major reason was ascribed to the over-estimation of the used value of temperature gradient.

Due to many trouble encountered in the last experiment with the 61-pin bundle, we could not obtain enough data to check the reasons of the discrepancy in detail.

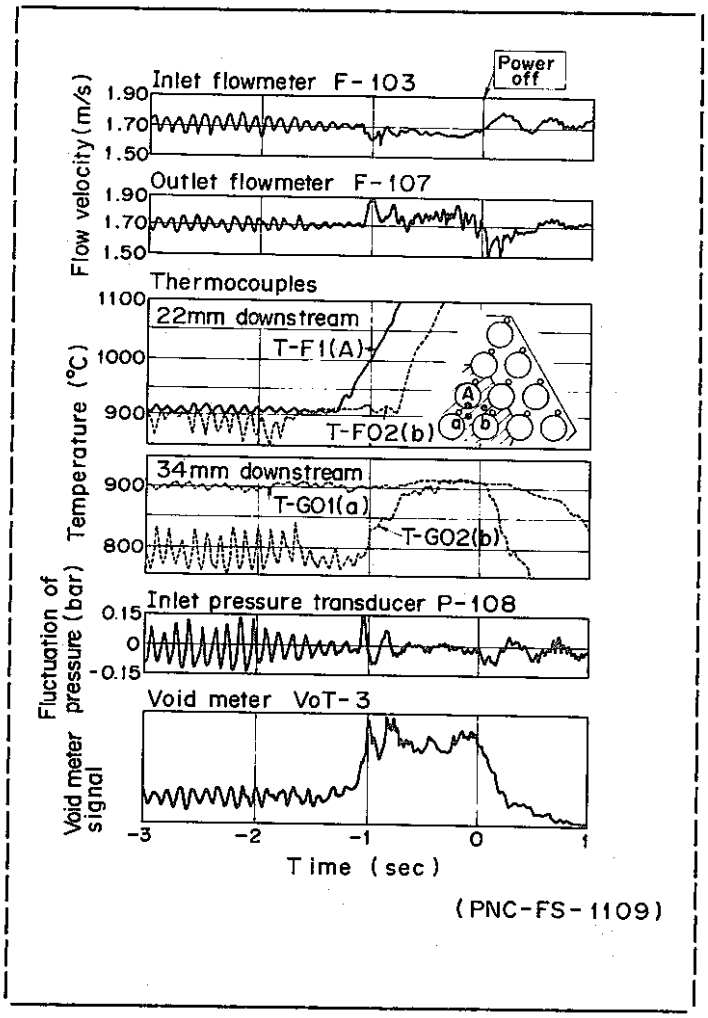


DRYOUT DATA ..... (Next slide, please. SLIDE No. 13, i.e. Fig. 8)

Dryout test was conducted with the 37-pin wire-wrapped bundle, Run No. 37(19)WLB-114. In this test, only the heat flux was increased stepwise under constant flow rate condition.

This slide shows the signals at the instance of permanent dryout. After the sustained oscillatory boiling, the amplitude of the oscillation became to show damping tendency during the time from -2 to -1 seconds. It was obvious that the gradual growth of radial and axial high temperature region forced the oscillation to be stabilized.

The pin and the sodium temperatures at the 22 mm downstream plane from the blockage showed steep increases. The sudden one-sided expansion of the voided region was followed. The reached volume of the voided region was about three quarters of the blockage size in radial direction and about three times as long as the blockage size in axial direction. The global flow reduction due to the expanded void was never observed during the dryout.

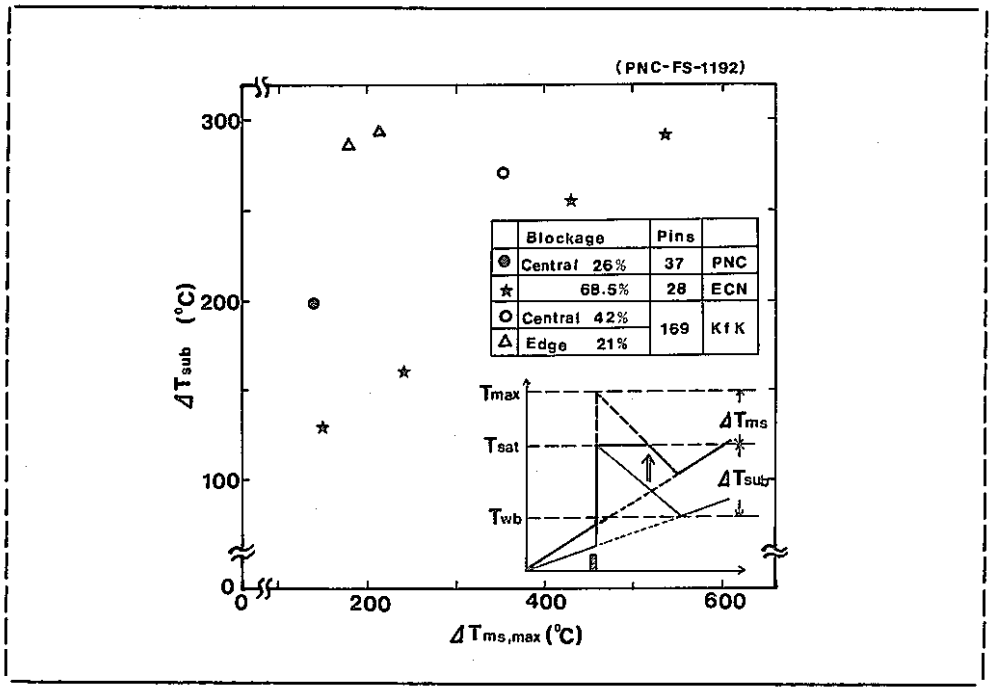


CORRELATION ..... (Next slide, please. SLIDE No. 14)

The theoretical excess temperature at the occurrence of dryout was about 140 °C. We have tried to correlate the excess temperature by the incipient boiling subcooled temperature measured at the upper end of the heated section. Many available data are referred. However, these data were not converged due to the differeces in the flow patterns at the instance of dryout.

We can confirm that the coolability is extremely improved by the oscillatory boiling. The margin to the cladding melting seemed to depend on the initial subcooled temperature. In other words, it will be a decreasing function of power-to-flow ratio $q'/U_o$.

In our dryout run, the value of power-to-flow ratio was fairly large. Consequently, we can conclude that the margin will be sufficiently large for the reactor conditions in compared with our too high power-to-flow ratio experiment.

CONCLUSIONS (PNC-FS-028s)

(1) SINGLE-PHASE FLOW:

- THE EMPIRICAL FORMULA WAS DERIVED TO ESTIMATE LOCAL TEMPERATURE RISES BEHIND VARIOUS CENTRAL-TYPE BLOCKAGES
- CENTRAL-TYPE BLOCKAGES WILL NOT CAUSE LOCAL BOILING WITHOUT BEING DETECTED BY AN IN-CORE FLOW-METER

(2) TWO-PHASE FLOW:

- EXISTANCE OF A LARGE BOILING WINDOW WAS IDENTIFIED
- THE OSCILLATORY BOILING, WHICH IMPROVED THE COOLABILITY OF LOCALIZED BUBBLY REGION, OFTEN RELIEVED CLADS FROM MELTING.

CONCLUSIONS ..... (Next slide, please. SLIDE No. 15)

Now, I would like to summarize the present work.

For single-phase flow, we have derived the empirical formula to estimate the local temperature rises behind various central-type blockages, and we have concluded that the central-type blockage will not cause undetected local boiling.

For two-phase flow, we have identified the existance of a large boiling window, where the coolability is assured. We have recognized that the oscillatory boiling improves the coolability of localized bubbly region.

That is all. Thank you.

Liquid Metal Boiling Working Group

9th Meeting
June 4 - 6, 1980
Rome, Italy

# DECAY HEAT REMOVAL UNDER BOILING CONDITION IN A PIN-BUNDLE GEOMETRY

K. Haga, M. Uotani, K. Yamaguchi and M. Hori

O-arai Engineering Center, Power Reactor
and Nuclear Fuel Development Corporation, Japan

## ABSTRACT

Decay heat removal capability under boiling condition was investigated using an electrically heated 37-pin bundle test section. The flow was driven by natural circulation force of the out-of-pile sodium loop SIENA in O-arai Engineering Center, PNC. As the heater power was increased, the two-phase flow regime changed from bubbly flow to slug flow and then to annular or annular mist flow. In 15 runs, dry-out was not observed in the average exit quality region of less than 0.5. The results indicated the existance of a large "boiling window" for low flow rate and low power conditions.

## INTRODUCTION

In the analysis of Loss of Pipe Integrity (LOPI) and Loss of Shutdown Heat Removal System (LSHRS) accidents in a LMFBR, the reacter power is assumed to be less than 10 % of its normal operating condition. In the events where the core flow rate is degraded, sodium boiling can result. From the point of reactor safety, it is important to check the capability of heat removal by sodium boiling, because if permanent dry-out occurs, fuel pin melting will follow.

Some experiments have been made to investigate the dry-out phenomena under low flow rate conditions. Garrison et al.[1] conducted a series of natural convection sodium boiling experiments using a single-channel mockup heated by a radiant furnace. In their experiments, stable boiling was observed for a coolant power densities between 160 and 200 W/cm$^3$, and film dry-out appeared between 200 and 210 W/cm$^3$. These results were similar to those estimated by Hinkle[2] from his single-channel low pressure water boiling experiments under natural convection.

It is well known that, under transient conditions, voiding dynamics in a multi-channel bundle is differnt from that in a single-channel test section, because two-dimensional effects tend to ameliorate the course of the transient by delaying the onset of flow reversal and dry-out[3],[4]. To investigate the two-dimensional effects under dacay heat level sodium boiling, experiments in bundle geometries were conducted by Kaiser et al.[5],[6]. In their seven-pin bundle test section, dry-out appeared when the inlet valve was completely closed at the heat flux of 8.3 W/cm$^2$[5]. In their 37-pin bundle

test section, permanent dry-out was observed at the heat flux of 11.7 W/cm$^2$ (linear heat rate of 22 W/cm) and the estimated local quality of 0.8[6]. The complete inlet valve closure represents an unrealistically severe condition being considered in the present study. Furthermore, the 37-pin bundle experiments were conducted without heating the central 6 pins because of a blockage plate attached to the central subchannels.

The present report deals with a series of out-of-pile experiments which were conducted with an electrically heated 37-pin bundle test section. The sodium flow was driven by natural circulation and boiling was accomplished by increasing heater power. After stable boiling was established, the heat input was further increased stepwise. Three runs were terminated by the occurence of dry-out.

## TEST FACILITY

The experiments were carried out in the Sodium Boiling and Fuel Failure Propagation Test Loop SIENA in O-arai Engineering Center, PNC. Figure 1 shows a schematic of the SIENA loop. The sodium from the test section flowed into the expansion tank, separator, cooler, pump and returned to the test section.

The test secton is shown in Figure 2. The bundle consisted of 37 electrically heated pins. Tantalum was used as the heating element in the pins. The electrical resistance of tantalum is sensitively changed by the temperature such that the maximum heat flux under boiling condition was higher than the mean axial heat flux by 10 to 20 %. Each pin of 6.5 mm diameter was wrapped by a 1.3 mm diameter spacer wire with a 264.8 mm helical pitch. The diameters and the pin pitch of 7.9 mm were the same configuration with those in the MONJU fuel subassemblies. The bundle had a 450 mm heated length and a 750 mm simulated FP gas plenum at its downstream position. The 37 pins were installed in a hexagonal inconel tube of 10 mm thickness so that the gap between the peripheral pins and the inner duct wall was 1.45 mm. Thermal insulator on the outer wall of the hexagonal tube minimized heat losses through duct wall.

Chromel-Alumel thermocouples of 0.3 mm diameters were located at 10 cross-sections to measure pin surface and subchannel temperatures. They were embedded in the outer surface of pin sheath, and the probes for subchannel temperature measurment were projected from the pin surface. Subchannel thermocouples were also located in several spacer wires. The test section inlet and outlet temperatures and hexagonal tube temperatures were monitored by additional thermocouples. Two types of void-meter were used to detect voids. A total of 14 resistive void-meters were attached within the test section. In addition, a total of 10 Chen-type void-meters located in the spacer wires were used to detect local voids. The sodium velocities at the inlet and outlet of the test section were measured by electromagnetic flow-meters. Pressure transducers (Kaman type KP-1911, frequency response range: 0 to 8300 Hz) were also provided at the inlet and outlet of the test section to measure the pressure changes during boiling experiments.

## OPERATING PROCEDURES AND TEST CONDITIONS

Prior to the boiling experiments, the linearity of inlet flow-meter was checked in the low velocity range of 0.05 to 0.2 m/sec. The result showed acceptable accuracy (within $\pm$ 7 %) for the purpose of the present experiment.

The amount of the natural circulation sodium flow was controlled by an opening of inlet valve in the main loop. The oxygen concentration was kept under 10 ppm by the purification unit. After cover gas pressure, inlet temperature and valve openings were set, the heater power was increased stepwise until boiling was initiated. After stable boiling was observed, as indicated by temperature, void, flow rate and pressure signals, the heater power was increased further to higher levels. Argon gas was injected from the inlet tube of the test section in two runs (quality range of 0.014 to 0.017) to investigate the effect of noncondensable gas on the boiling phenomena.

One heater pin was failed in the early stage of test program and two additinal pins were failed in the final stage. The majority of the runs were conducted using residual 36 heater pins.

The experimental conditions are summarized as follows:

| | |
|---|---|
| Sodium system pressure | 1.21 - 1.48 bar |
| Inlet temperature | 324 - 486 °C |
| Flow velocity at boiling inception | 0.03 - 0.18 m/sec |
| Heat flux (maximum) | 6.9 - 51.4 W/cm$^2$ |

## TEST RESULTS

Figures 3-1 and 3-2 show pin surface temperatures (those measured at 6 different axial locations are gathered in Fig. 3-1 and those measured at 6 different radial locations near the end of heated section are in Fig. 3-2), inlet pressure and inlet flow-meter signals during the dry-out test (Run No. 37LHF-123).

When the thermocouples located at G-section (11.3 mm upstream from the end of heated section) showed the onset of boiling, the reading of inlet velocity was 0.18 m/sec and that of maximum heat flux was 42.2 W/cm$^2$. After the onset of boiling, sodium flow was accelerated gradually due to natural circulation to yeild the termination of boiling. The boiling duration time of this step was about 30 sec.

Then, the heat flux was raised to 45.5 W/cm$^2$ level and the continuous boiling was observed in the central subchannels of G-section and F-section (33.4 mm upsteam from the end of heated section). The signal of void-meter C-07 indicated that the flow regime was bubbly flow.

When the heat flux was raised further more to 52.0 W/cm$^2$ level, oscillatory boiling appeared. It was proved by the succeeding power increases that the amplitude and period of inlet flow oscillation were increased with heat flux. At the heat flux of 56.6 W/cm$^2$, as can be seen in Fig. 3-2, saturation temperature region near the end of heated section was extended radially toward the peripheral pins and duct wall. During this step, formation and collapse of vapor slugs caused the violent oscillations of inlet flow and pin surface tempertures measured at the outer subchannels. The pressure pulses measured at the inlet of the test section (P-108) corresponded to the collapses of large vapor slugs.

At the heat flux of 62.4 W/cm$^2$, the two-phase region expanded upstream and reached B-section (257.4 mm upstream from the end of heated section). The oscillation of inlet flow was stabilized at a constant value of 0.09 m/sec. Figure 4 compares the signals of two types void-meters: the resistive void-meter VOT-** and the Chen-type one C-**. The void-meters VOT-9 and C-8 were located at the same axial position. At the latter half of this experimental step, the void-meter signals became to take certain plateau levels, i.e. the conditions of almost whole cross-section beeing filled by sodium vapor. Therefore, it was considered that the flow regime was altered from slug to

annular or annular mist flow.

After the heat flux was raised to 63.4 W/cm$^2$ the signal measured by the thermocouple T-204G showed a steep increase due to the occurrence of dry-out, and the pin power was cut by the pin protection limit (1000 °C) switch. During this run, inlet sodium temperature was maintained at 370 °C.

Figure 5 shows the typical signals of tmperature, pressure and inlet flow in the next dry-out test (Run No. 37LHF-124). This run was conducted under the conditions of three pins being unheated and flow resistance in the main circulation loop being increased by the further closing of the inlet valve. The inlet sodium temperature was 372 °C.

Boiling was detected at the heat flux of 11.0 W/cm$^2$ and the inlet velocity of 0.05 m/sec. In such a low flow condition, radial temperature profile becomes almost flat except the immediate vicinity of duct wall. This profile caused almost simultanious boiling initiation within the whole cross-section at the end of heated section.

After the occurrence of regular flow oscillation, it was decayed to a constant value. This tendency between heat flux and inlet flow rate was similar to that observed in the previous run. The saturation temperature region reached B-section at the heat flux of 29.9 W/cm$^2$. Although the signal measured by the thermocouple T-204G showed a temporary dry-out, the peak temperature was not high enough to terminate the test.

At the further increase of heat flux to 42.8 W/cm$^2$ level, the inlet flow velocity attained a new level of 0.05 m/sec and the heater power was cut by detecting the temperature overshoot of the thermocouple T-204G.

Figure 6 shows resistive void-meter signal during this run. Liquid slugs were no longer detected at the heat flux range of greater than 29.9 W/cm$^2$ as was the case in the previous run.

Figure 7 shows the map of heat flux versus initial single-phase flow velocity. Dry-outs were measured in three of the 15 runs conducted. Within the tested conditions, noncondesable gas did not affect the dry-out heat flux.

## DISCUSSIONS

As is seen from the signals of flow-meters and void-meters, the flow pattern was changed with heat flux from bubbly flow to slug flow and then to annular or annular mist flow. The change of two-phase flow pattern was essentially the same with that observed in the forced circulation experiment with single-pin test section[7]. It was in the annular or annular mist flow regime that dry-out appeared. It is natural for us to consider that the dry-out in this flow regime is caused by the disappearence of liquid film on the pin surface under high quality conditions.

From the heat balance of the test section, the average exit quality at the end of the heated section was calculated from heat flux and flow velocity tested. In this calculation, the time averaged inlet flow velocity was used in the steps where the inlet flow velocity showed oscillations.

Figure 8 shows a comparison between the average exit qualities estimated for every step of the present dry-out tests with the dry-out qualities derived in the 19-pin bundle tests of ORNL. The horizontal line means the local dry-out quality derived in the 37-pin bundle tests of KfK. Except high velocity region (> 0.4 m/sec), the dry-out quality in every case was more than 0.5.

Many empirical equations of the critical conditions beyond which the dryout will appear have been proposed for water two-phase flow. In these equations, mass flow rate, heat flux, quality, pressure etc. are included as

the effective parameters. However, few equations cover the low pressure and low flow rate conditions. Biasi et al.[8] obtained the equation using their experimental results. The covered experimental conditions (mass flow rate: 100 to 6000 $Kg/m^2sec$, presssure: 2.7 to 140 $Kg/cm^2$ and pipe inner diameter: 3 to 3.75 mm) were relatively close to those of the present sodium experiments. The calculated dry-out quality from their equation is 0.95 for one of the present cases. Except the verification of the applicability of their equation to the sodium flow conditions, one of the major causes of the difference between calculated value and the actual data of the present sodium experiments may lie in the non-uniform radial distribution of local qualities in the tested pin bundle.

These results shows the existance of a large "boiling window" under low power condition. This conclusion is also expected to stand in a reactor subassembly (unless the inlet flow of a subassembly is completely stopped). Consequently, the decay heat may be removed by sodium boiling when the small amount of inlet flow rate is assured by natural circulation.

## CONCLUSIONS

Experimental study was carried out to investigate natural circulation boiling in a 37-pin electrically heated LMFBR fuel subassembly mockup. The observed flow regime changed from bubbly flow to slug flow and then to annular or annular mist flow in the average exit quality range of less than 0.5. The result indicated the existance of a large "boiling window" at low power conditions in a pin-bundle geometry.

Further study will be required to identify the decay heat dry-out criteria and natural circulation.

## ACKNOWLEDGMENTS

The authors wish to acknowledge the technical contributions of Mr. T. Isozaki, Mr. T. Komaba and Mr. K. Sahashi at all stages of the present experiments.

## REFERENCES

[1] P. W. Garrison et al., International Meeting on Fast Reactor Safety Technology, Seattle, 1686-1695 (1979)
[2] W. D. Hinkle, HNL-Sub-4450-1 (MIT-EL 76-005) (1976)
[3] Y. Kikuchi et al., J. Nucl. Sci. Technol., 15-2, 100-108 (1978)
[4] J. L. Wantland et al., International Meeting on Fast Reactor Safety Technology, Seattle, 1678-1685 (1976)
[5] A. Kaiser et al., CONF 761005-517-7 (1976)
[6] A. Kaiser et al., ENS/ANS Topical Meeting on Nuclear Power Reactor Safety, Brussel (1978)
[7] Y. Kikuchi et al., J. Nucl. Sci. Technol., 12-2, 83-91 (1975)
[8] L. Biasi et al., Energia Nuclear 14, 9 (1967)

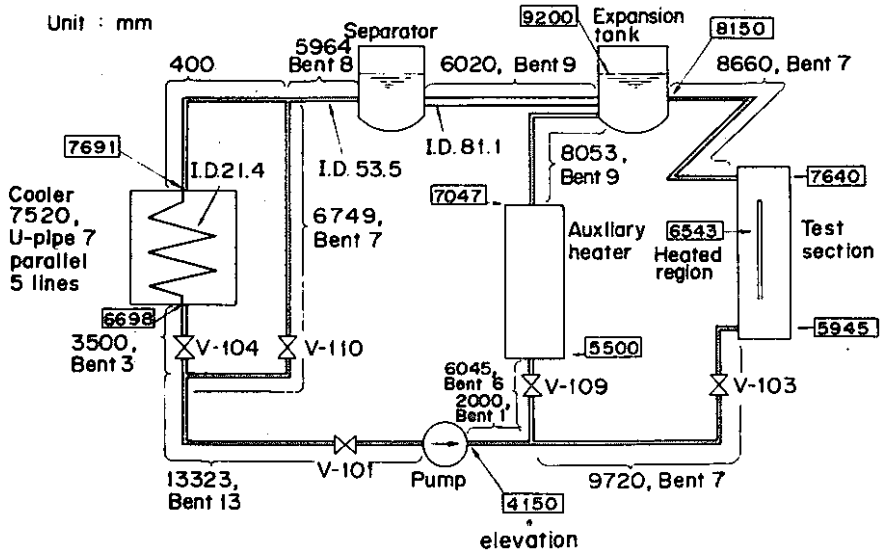


Fig. 1 Geometries of main line and elevations from floor (PNC-FS-960)

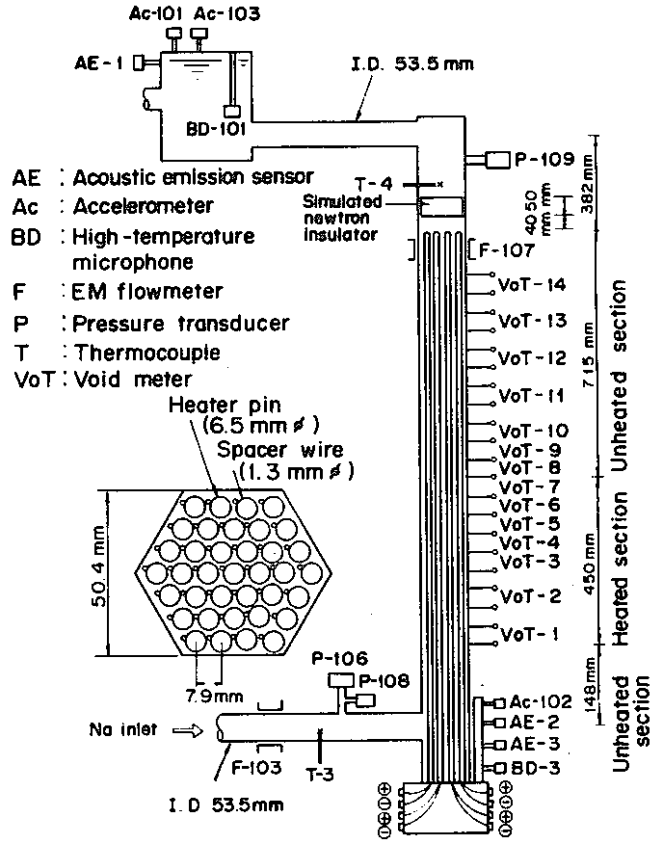


Fig. 2 Wire-wrapped 37-pin bundle test section, 37F T.S. (PNC-FS-962)

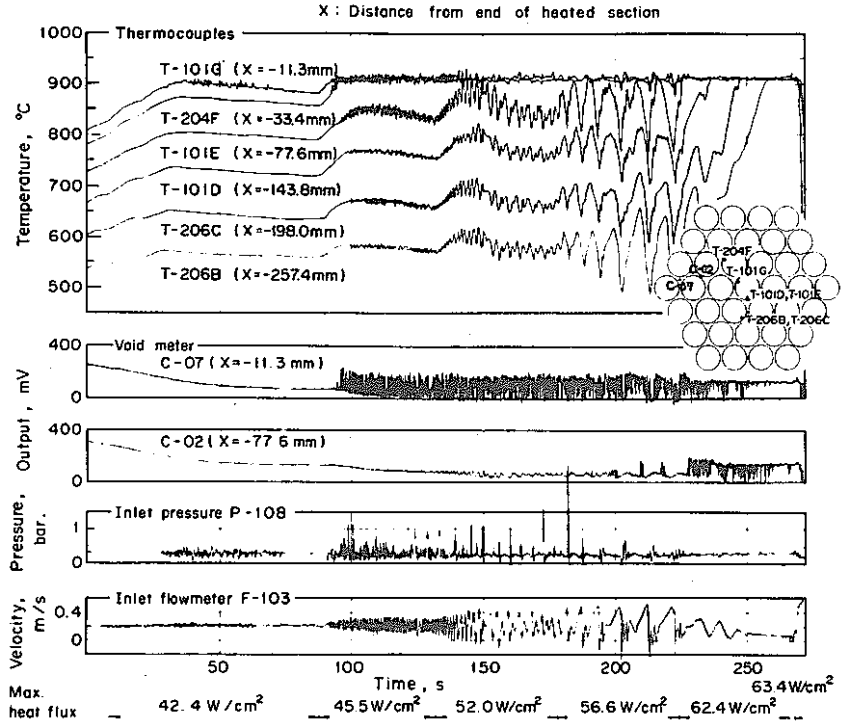


Fig. 3-1 Signals of sodium temperatures, inlet and outlet flow velocities during the dry-out test, Run No. 37LHF-123 (PNC-FS-1112)

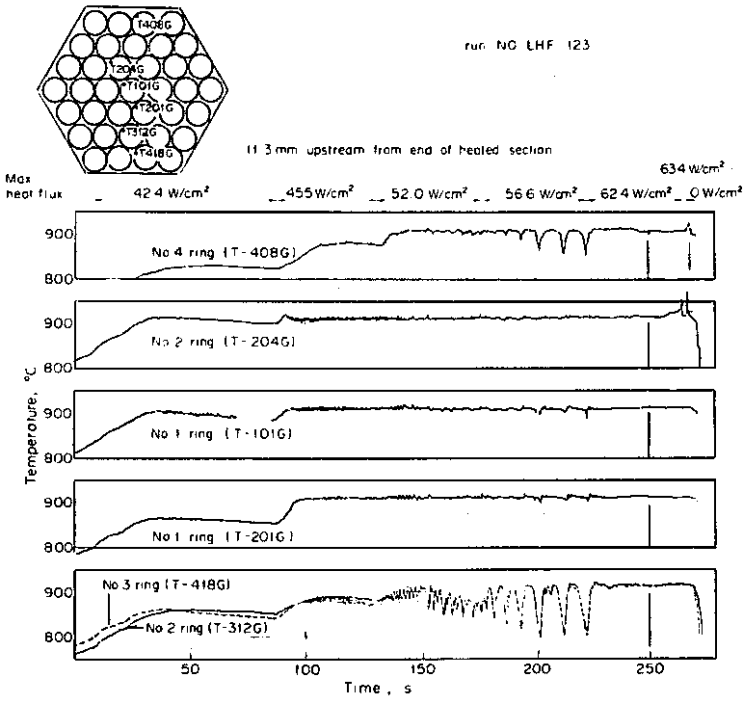


Fig. 3-2 Signals of pin surface temperatures measured at G-section during the dry-out test, Run No. 37LHF-123 (PNC-FS-978)

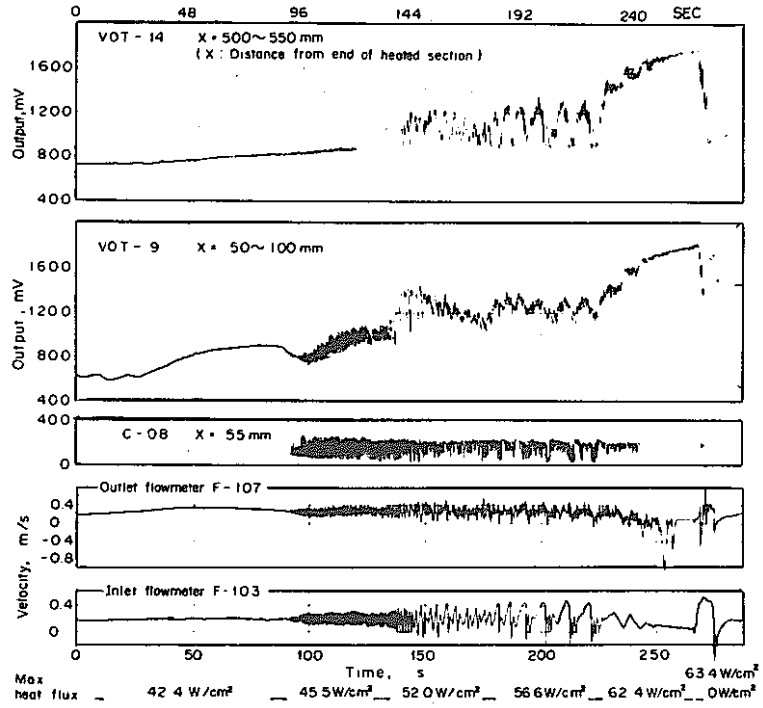


Fig. 4 Signals of two types void-meters: the resistive void-meter VOT-** and the Chen-type void-meter C-**, during the dry-out test, Run No. 37LHF-123 (PNC-FS-977)

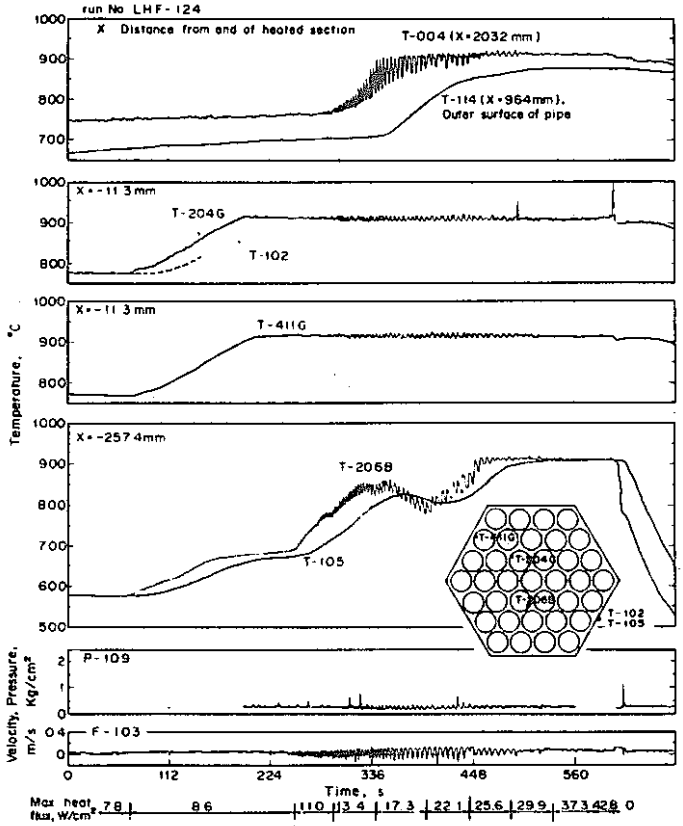


Fig. 5 Signals of temperatures, pressure and inlet flow velocity during the dry-out test, Run No. 37LHF-124 (PNC-FS-989)

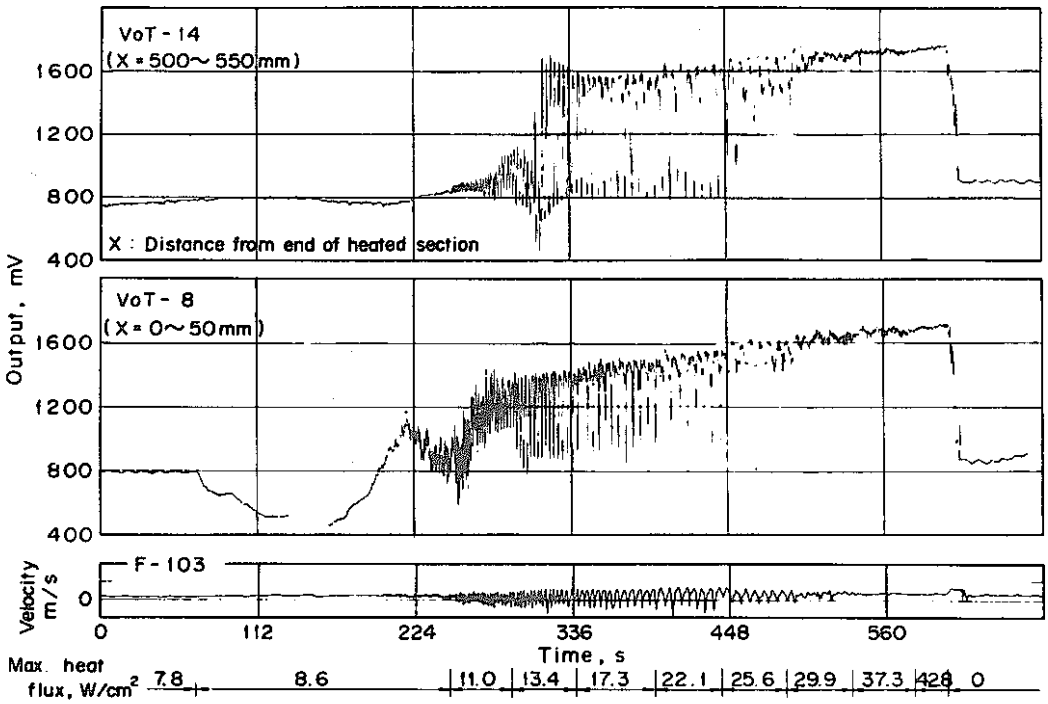


Fig. 6 Signals of resistive void-meters and inlet flow velocity during the dry-out test, Run No. 37LHF-124 (PNC-FS-990)

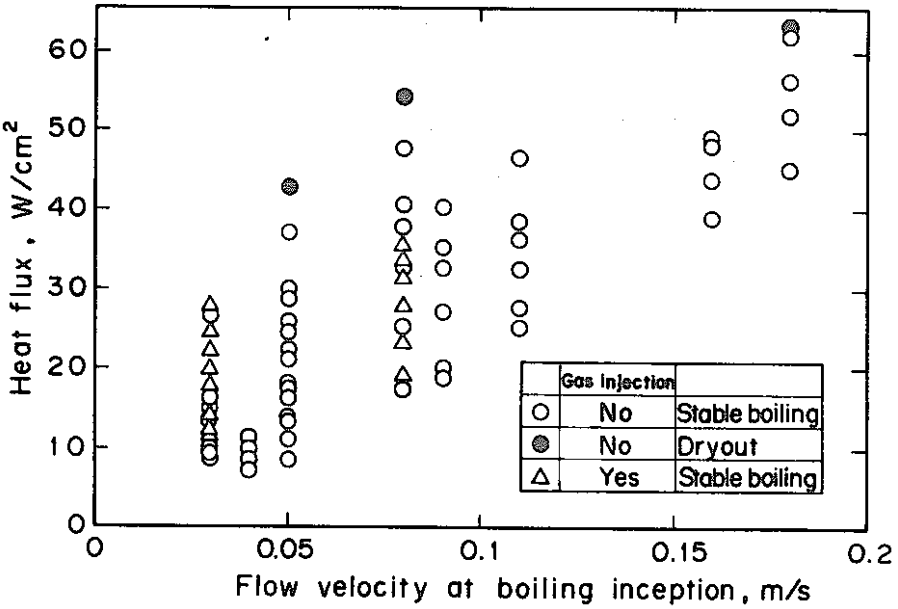


Fig. 7 Experimental conditions of heat fluxes versus initial value of inlet flow velocities (PNC-FS-992)

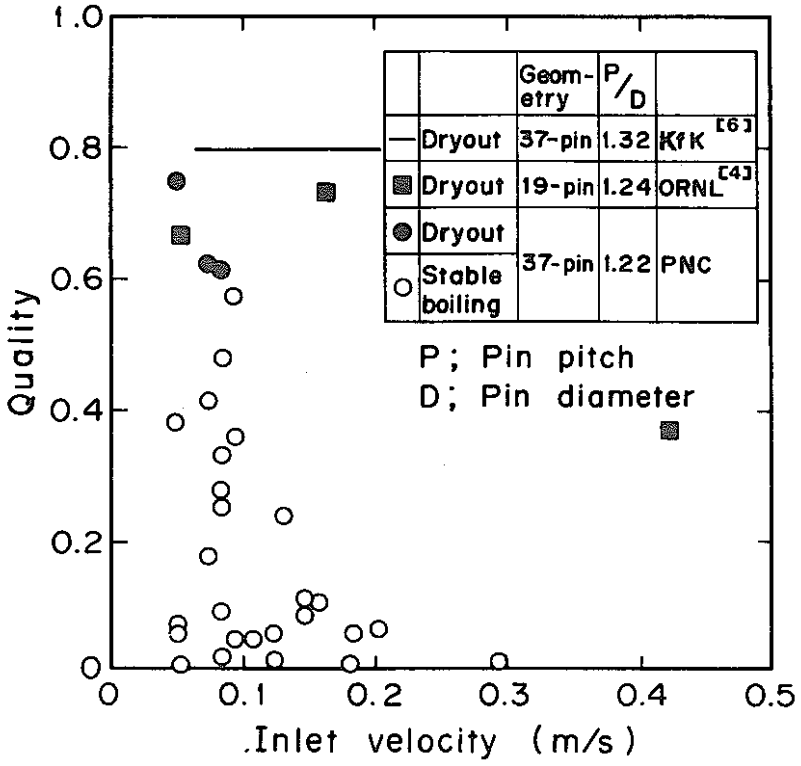


Fig. 8 Comparison between the qualities of the present dry-out tests with available data of dry-out qualities in pin bundles (PNC-FS-1113)

## APPENDIX: SCOPE OF PRESENTATION

Liquid Metal Boiling Working Group

9th Meeting
June 4 - 6, 1980
Rome, Italy

# DECAY HEAT REMOVAL UNDER BOILING CONDITION IN A PIN-BUNDLE GEOMETRY

K. Haga, M. Uotani, K. Yamaguchi and M. Hori

O-arai Engineering Center, Power Reacter
and Nuclear Fuel Development Corporation, Japan

## INTRODUCTION

Thank you, chairman. I would like to introduce our fresh work on the Decay Heat Sodium Boiling Experiment.

9TH LIQUID METAL BOILING WORKING GROUP MEETING (PNC-FS-019s)
ROME, ITALY, JUNE 4-6, 1980

DECAY HEAT REMOVAL UNDER BOILING CONDITION IN A PIN-BUNDLE GEOMETRY

K.HAGA, M.UOTANI, K.YAMAGUCHI AND M.HORI
FBR SAFETY SECTION, OEC/PNC, JAPAN

OBJECTS

(1) TO OBSERVE THE BOILING BEHAVIOR UNDER DECAY HEAT AND LOW FLOW CONDITIONS
(2) TO EXAMINE THE SELFSUSTAINING SAFETY ASPECTS OF NATURAL CIRCULATION FLOW
(3) TO IDENTIFY THE DRY-OUT MECHANISM AND DRY-OUT CRITERIA UNDER DECAY HEAT AND LOW FLOW CONDITIONS

OBJECTS ..... (First slide, please. SLIDE No. 1)

In the case of Loss of Piping Integrity accident or Loss of Shutdown Heat Removal System accident in LMFBRs, the low heat flux sodium boiling may occur following the flow reduction. The most important object of our study is to evaluate the heat removal capability of the fuel subassembly by sodium boiling under the decay heat condition. The examination of the possibility of self-sustaining natural circulation cooling is also included in our objects.

For these purposes, we have conducted two series of experiments. The first series of low heat flux boiling tests was conducted from September in 1978 to Febrary in 1979. And then, we have completed the second series only a month ago. Today, I would like to present you the results of the first one, only.

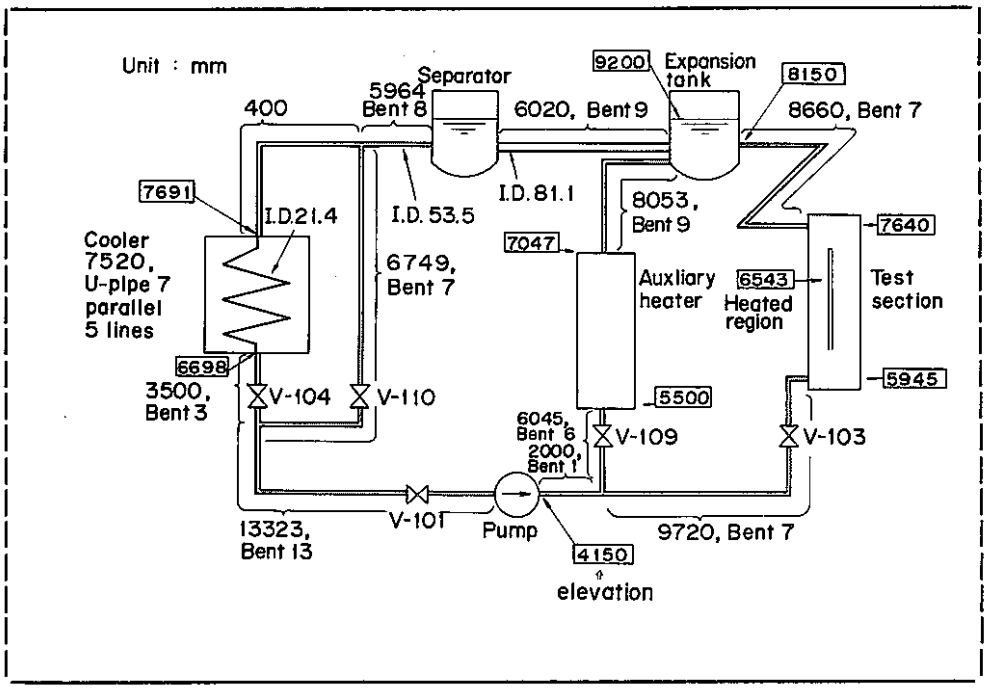


TEST FACILITY ..... (Next slide, please. SLIDE No. 2, i.e. Fig. 1)

We have a mother loop named SIENA in O-arai Engineering Center of PNC. This slide shows its schematic view. Various testing objectives have been met by changing only the test section.

First of all, I would like to explain the function of the mother loop.

The mixture of sodium and its vapor coming from the test section flows into the expansion tank and the separator tank, where only the vapor is separated from the mixture and then flows into the vapor-trap units. On the other hand, the hot sodium goes through the cooler and returns to the test section. Although there is an electro-magnetic pump to drive the sodium, all runs of the present tests were conducted under natural circulation conditions. The bypass line was not used during these tests.

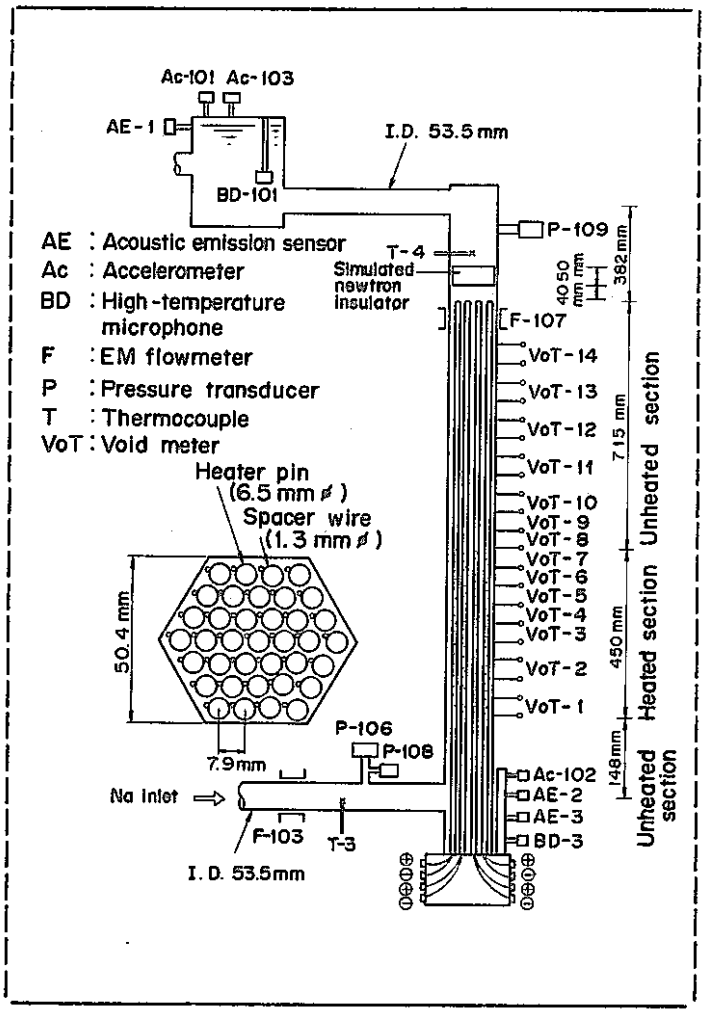


TEST SECTION ..... (Next slide, please. SLIDE No. 3, i.e. Fig. 2)

This slide shows the test section used in the present tests. An electrically heated 37-pin bundle is installed in a hexagonal wrapper tube made of inconel. The diameter of the heater pin is 6.5 mm. The pin pitch is maintained to be 7.9 mm by the spiral turns of the spacer wire whose diameter is 1.3 mm. The axial length of the heated section is 450 mm and the heat flux profile is almost uniform.

We took great care of the thermal insulation of wrapper tube to assure the heat balance at the test section under steady-state conditions. Since our aim was directed toward investigating the steady-state heat removal capability, the transient heat loss through the wrapper tube was not simulated.

The pin surface and the sodium temperatures were measured mainly by the 0.3 mm diameter thermocouples which were equipped at 10 different axial planes. A total of about 100 thermocouples were used.

The sensors denoted by the capitals F and P are the electro-magnetic flow-meter and the pressure transducer, respectively. The sensors denoted by the symbol VoT are the resistance-type void-meters, while those denoted by the capital C are the Chen-type void-meters. The former void-meter is used to measure the average void fraction, while the latter void-meter senses the presence of local void.

EXPERIMENTAL PROCEDURES (PNC-FS-020s)

- THE FLOW IS DRIVEN BY NATURAL CIRCULATION OF THE TEST FACILITY "SIENA", WITH THE INLET VALVE BEING THROTTLED
- THE HEATER POWER IS INCREASED STEPWISE UNTIL THE DRY-OUT IS DETECTED

EXPERIMENTAL CONDITIONS

| | | | |
|---|---|---|---|
| • SYSTEM PRESSURE | : | 1·21 - 1·48 | BAR |
| • INLET SODIUM TEMPERATURE | : | 324 - 486 | °C |
| • INLET FLOW VELOCITY | : | 0·03 - 0·18 | M/SEC |
| • HEAT FLUX (MAXIMUM) | : | 6·9 - 51·4 | $W/CM^2$ |

EXPERIMENTAL PROCEDURE ..... (Next slide, please. SLIDE No. 4)

This slide shows the experimental procedures and the conditions.

The sodium flow was driven by the natural circulation of our test facility. The flow rate of each run was roughly controlled, beforehand, by adjusting the throttling of the inlet valve. Then, the heater power was increased stepwise to change the test conditions.

Before going into the boiling steps, we waited for a long period enough to attain the steady-state conditions. Sodium boiling was started by raising the heater power further more. Some of the boiling tests were continued until the heater power was turned-off by the detection of the permanent dryout. The judgement of the permanent dryout was made whether or not any observed temperatures were exceeding 1,000 °C level.

The matrix of the experimental conditions are listed here. We sometimes could not realize the violent boiling under sufficient low flow conditions due to the difficulty of the valve setting. All dryout runs fell short of our expectations and were realized at the heat flux beyond the decay heat level. Consequently, I have no intension to say that the dryout is not caused under decay heat flux condition.

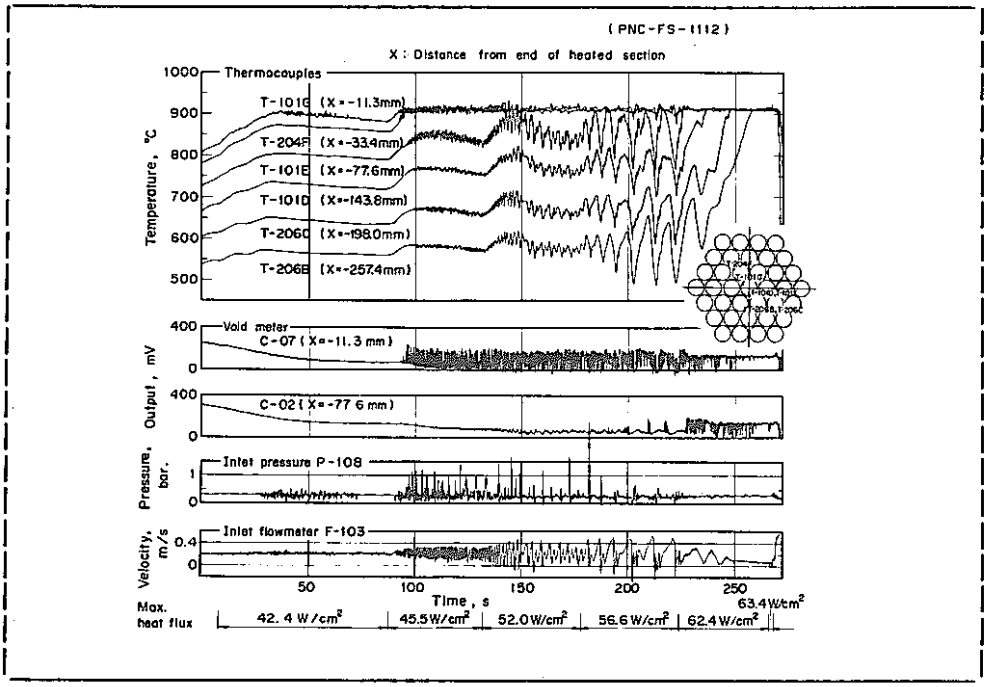


DRYOUT RUN 37LHF-123

..... (Next slide, please. SLIDE No. 5, i.e. Fig. 3-1)

Now, I would like to show you the results. This figure shows typical signals of inlet velocity, inlet pressure, Chen-type void-meter, and pin surface temperatures measured at 6 different planes during the dryout run, Run No. 37LHF-123.

Here, you can see that the temperature measured at G-plane, that is the nearest plane to the upper end of the heated section, indicates the onset of sodium boiling. At that instance, the inlet flow velocity was 0.18 m/sec, and the heat flux was already far beyond the decay heat level and was 45.5 W/cm$^2$. After the onset of boiling, sodium flow was accelerated gradually with the growth of natural circulation and forced the boiling being terminated at about 30 sec later.

Then, we raised the power. After that, we can observe the continuous boiling at the upper two measurement planes. You can easily notice the transition of the boiling patterns observed during the following several steps. Obviously, the flow regime was initially a bubble flow and then changed to a oscillatory slug flow.

During the step before last, two-phase region expanded and reached a middle plane of the heated section. At the end of this step, an annular or annular-mist flow regime was attained. You can easily confirm it from the void-meter signals. The oscillation of the inlet flow has disappeared.

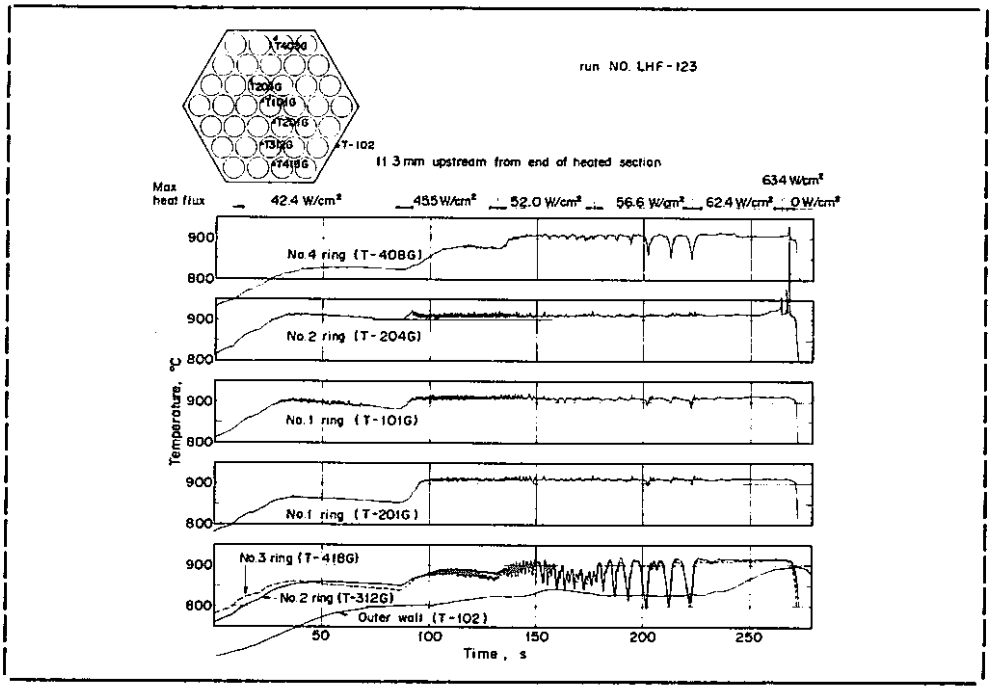


..... (Next slide, please. SLIDE No. 6, i.e. Fig. 3-2)

We have tried the last power-up.

We would like to concentrate our attantion on the temperature histories all observed near the upper end of the heated section. Radial locations of the thermocouples are illustrated here.

A few seconds after the last power-up, the signal measured at this position, T-204G, shows a steep increase due to the occurrence of local dryout. We can also find a similar, but a little smaller peak in the history of temperature "T-408G". This thermocouple is embedded in the outermost ring pin. No other signals show such an over-shoots. So, we can guess that the dryout region was limited within the localized part of the pin bundle.

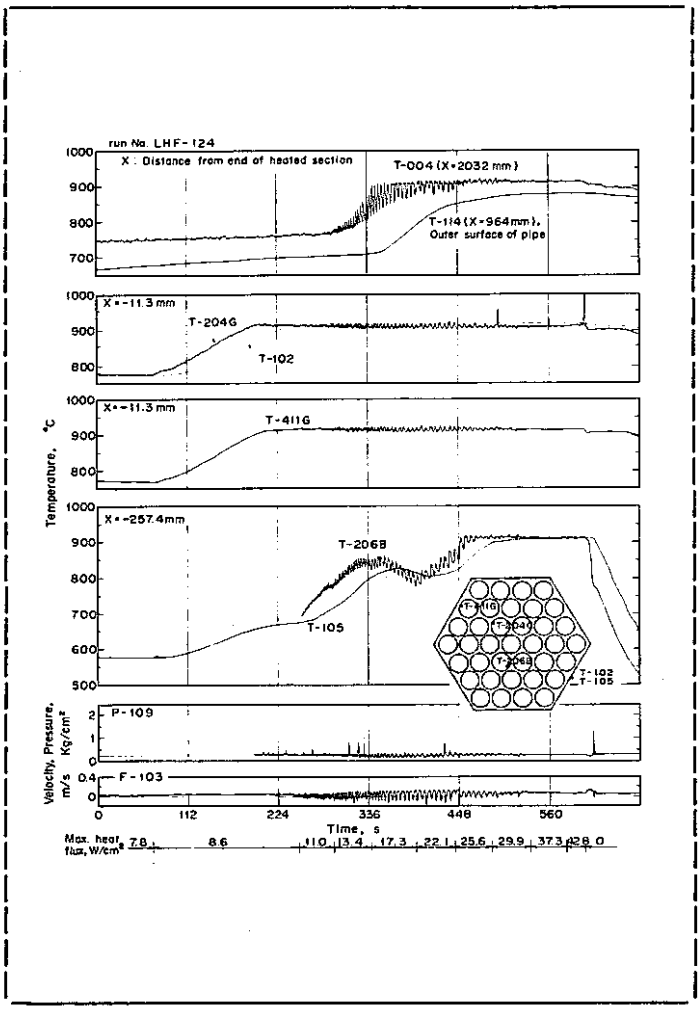


DRYOUT RUN 37LHF-124 ... (Next slide, please. SLIDE No. 7 i.e. Fig. 5)

We will show the next dryout run, Run No. 37LHF-124. Typical signals of inlet velocity, outlet pressure, and temperatures measured at various locations are drawn here.

Since we had throttled the inlet valve further more, we could now attain a low flow condition of 0.05 m/sec at the instance of boiling inception, and a low-heat-flux boiling at a power level of 11.0 W/cm$^2$.

A different penomenon appeared when we raised the heat flux from 25.6 to 29.9 W/cm$^2$. Now, the inlet flow was stabilized. The annular or annular-mist flow regime was just attained. The voided region extended one-half of the heated length. Then, the temperature "T-204G" showed a small over-shoot. This is a typical feature of the temporary dryout. The thermocouple in question is the same one that showed permanent dryout in the previous run. At the last step of this run, the same thermocouple catched the permanent dryout again.

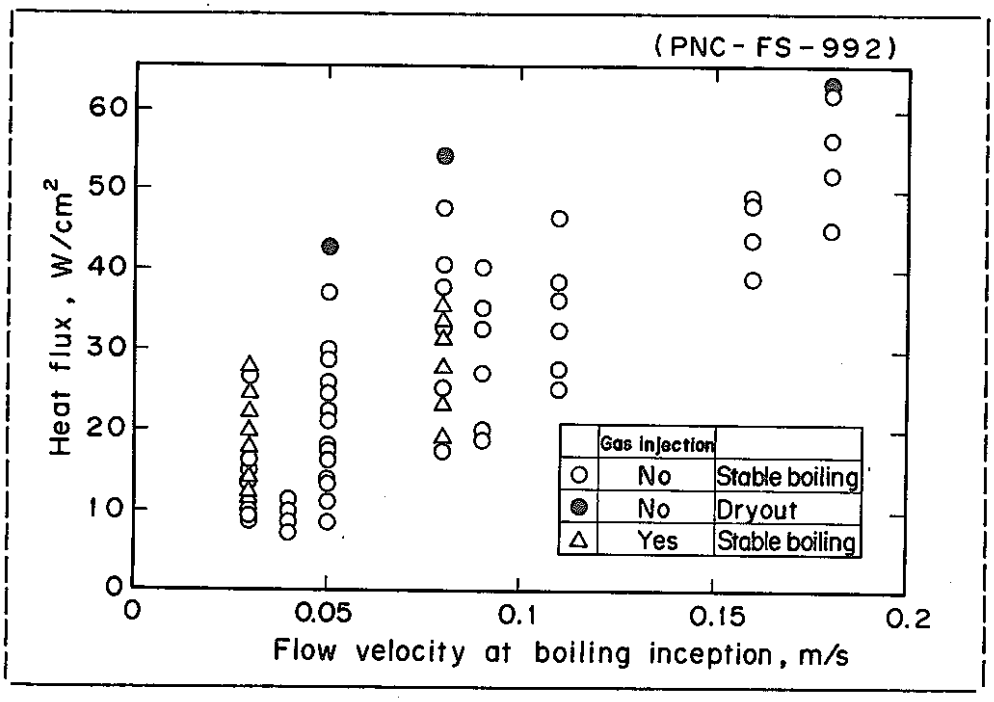


DRYOUT CRITERIA ..... (Next slide, please. SLIDE No. 8 i.e. Fig. 7)

Now, let us consider the critical condition of the occurrence of dryout. We want to know the safety zone on the operational map whose vertical and horizontal axes are heat flux and flow velocity. Here is an attempt. The tested heat flux is plotted versus flow velocity at boiling inception.

The reason of using the initial velocity, instead of the actually measured ones at each boiling step, is as follows:

We, at first, considered that the steady-state condition was not attained during each power increase step due to the natural circulation of long time constant. Second, we aimed at obtaining an initial conclusion whether or not a certain initial condition would result in cladding melting in the coming transient of natural circulation. At this stage, we considered that no further power increase step was required to cause dryout.

We have conducted 15 boiling runs and have got 3 dryout data. Each step of them are plotted in this figure. Circles mean that the coolability is assured by sodium boiling. Temporary dryout data were not classified, because, even in such cases, clad integrity was assured. Triangles show the steps during which argon gas is injected from the inlet of the test section. Within the tested conditions, noncondensable gas did not affect the dryout phenomena.

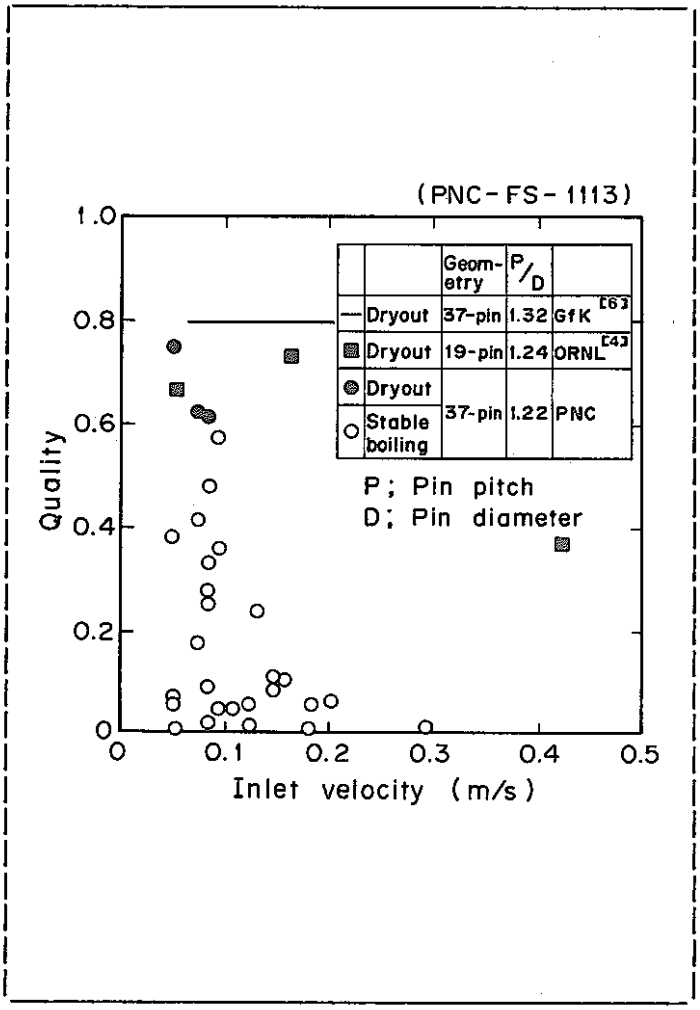


..... (Next slide, please. SLIDE No. 9 i.e. Fig. 8)

As you can remind, it was under the annular or annular-mist flow regime that dryout appeared. It is natural for us to consider that dryout under this flow regime is caused by the disappearance of liquid film from the pin surface. Of course, local quality should be extremely high.

It has been said that the high quality dryout does not depend on the heat flux but strongly related to the quality. From this viewpoint, we calculated the average exit quality at the upper end of heated section. Simple heat balance equation was used.

This slide shows the results. The blank circle means the coolable situation and the dot means the dryout condition. Available data of ORNL and KfK for pin bundle geometries are also shown. Except for the high velocity data, dryout quality in every case was more than 0.5.

In order to evaluate a local quality, we tried to use an empirical equation proposed by Biasi et al. for usual working fluid. The calculated answer was 0.95.

The solid line drawn in this figure is the local quality data estimated in KfK. In compared with its value 0.8, our rough estimation yielded fairly higher value. However, when we consider the perfect evaporation of liquid film on the pin surface, the value around 1.0 will be more realistic.

If we can assume that the local dryout quality takes the value around 1.0, then a question, "How about the radial quality distribution at the instance of local dryout?", must be solved for the full bundle condition. Our present status is that local dryout may appear when the average exit quality reaches the value exceeding 0.5. Of course, it is under the premise of annular or annular-mist flow of 37-pin bundle.

CONCLUSIONS (PNC-FS-021s)

- FLOW REGIME CHANGED FROM BUBBLE FLOW TO SLUG FLOW AND THEN TO ANNULAR OR ANNULAR MIST FLOW
- TRANSIENT RESPONSE OF SODIUM FLOW CAUSED BY NATURAL CIRCULATION FORCE OF THE TEST FACILITY WAS VERY SLOW
- DRY-OUT APPEARED WHEN THE AVERAGE EXIT QUALITY EXCEEDED THE VALUE SLIGHTLY GREATER THAN 0.5
- EXISTANCE OF A LARGE BOILING WINDOW WAS IDENTIFIED

CONCLUSION ..... (Next slide, please. SLIDE No. 10)

I would like to summarize the present work.

First; with the increase of power-to-flow ratio, two-phase flow regime changed from bubble flow to slug flow and then annular or annular-mist flow.

Second; transient response of sodium flow caused by natural circulation force of our test facility was very slow.

Third; dryout appeared when the average exit quality exceeded the value slightly greater than 0.5.

Fourth; existence of a large boiling window was identified.

That is all. Thank you.

## 2. FRANCO-DEBENE-PNC SPECIALISTS MEETINGS ON FBR SUBASSEMBLY FAULTS AND RELATED THERMOHYDRAULICS

# 4 Recent Progress of Transient Sodium Boiling Tests
Edited by K. Yamaguchi

# 5 Recent Progress of Fuel Failure Propagation Tests
Edited by M. Uotani

These documents were provided for the oral presentation at the first Franco-Debene-PNC Review Meeting on FBR Safety, held at OEC/PNC and Headquarters of PNC on May 19 through 23, 1980. The same documents were used at the Karlsruhe and Grenoble meetings for the guidance of PNC's experimental activities.

SCOPE OF PRESENTATION

Franco-Debene-PNC Specialists Meetings on
FBR Subassembly Faults and Related Thermohydraulics

June 9, 1980
Karlsruhe, Federal Republic of Germany

June 11, 1980
Grenoble, France

# RECENT PROGRESS OF TRANSIENT SODIUM BOILING TESTS

Edited by K. Yamaguchi

FBR Safety Section, OEC/PNC

## INTRODUCTION

My name is Katsuhisa Yamaguchi. I belong to the Core Safety Sodium Behavior Experiment Group. I would like to introduce you our recent progress of Sodium Boiling Experiments.

FRANCO-DEBENE-PNC SAFETY MEETING (PNC-FS-001s)
OEC/PNC, MAY 18 - 26, 1980

SODIUM BOILING AND FUEL FAILURE PROPAGATION TESTS

FBR SAFETY SECTION, OEC/PNC, JAPAN

CONTENTS



(2.2P-1)

GLOBAL DISCUSSIONS ..... (Turn on the light of OHP, OHP No. 1)

We have two subjects. The first one is the Transient Sodium Boiling Test. It is further divided into three: LOF without Scram, Decay Heat Sodium Boiling, and CDA Bubble Behavior. The second one is the Fuel Failure Propagation Test. It is divided into four: Pin Contact, Local Flow Blockage, Molten Clad Relocation, and the soft development of Anomaly Detection.

We have a mother loop named SIENA. Each subject has been carried out by changing its test section. A total of four members, two engineers and two technicians, have been in action.

Now, we will show you our future status, too. The LOF experiments were completed a few weeks ago, and this subject will be restarted in the future Clad Relocation test. The Pin Contact Tests were also finished and the results will be summarized in the final report. The basic soft of Anomaly Detection is already devised. Hence, we can treat this subject as beeing included in the Local Flow Blockage Tests. Moreover, the final experiments of Local Flow Blockage are planned to be started at the end of this year. We have no further plan on this subject. Consequently, the newly established three subjects and, perhaps, plus one will be continued in the future.

Next, let us go into individual details. I would like to explain about the first item, Transient Sodium Boiling. You will have the presentation of the second item from Mr. Uotani.

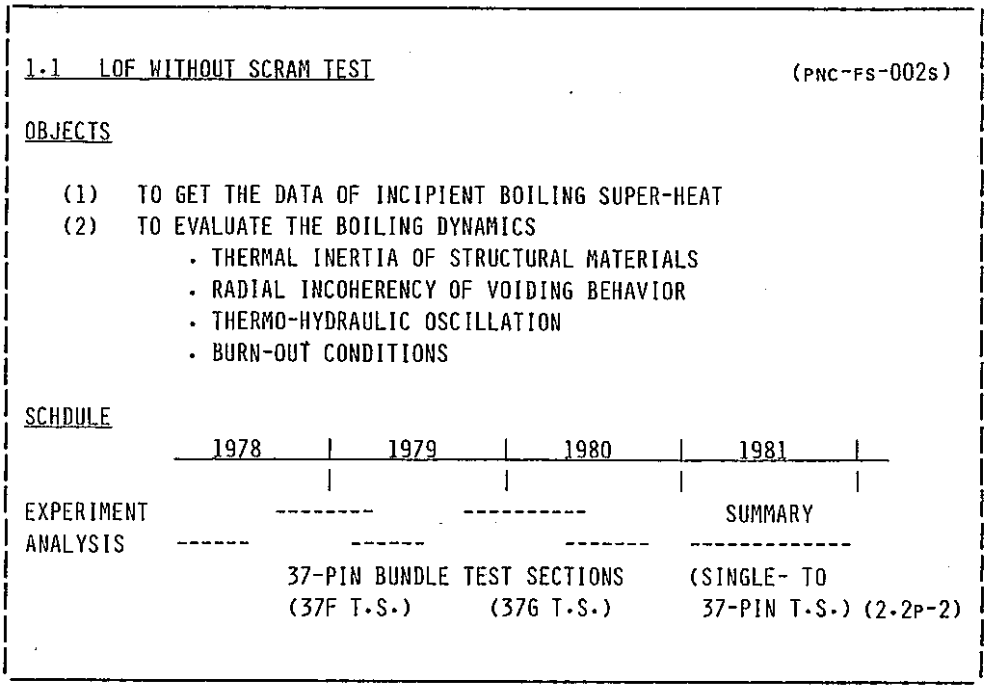


## INDIVIDUAL DISCUSSIONS

1.1 LOF without Scram ..... (Change the OHP sheet, OHP No. 2)

You can see the object of our LOF Test. The First one is to get the I.B. super-heat data as many as possible. The second one is to evaluate the boiling dynamics. Our interests lie in the following four problems: thermal inertia of structural materials, radial incoherency of voiding behavior, thermohydraulic oscillation, and critical conditions of burn-out. The last one is what we want to know ultimately.

The time schedule of LOF Tests is shown below. This program is started seven years ago. All of the experiments were completed. These results will be summarized next year.

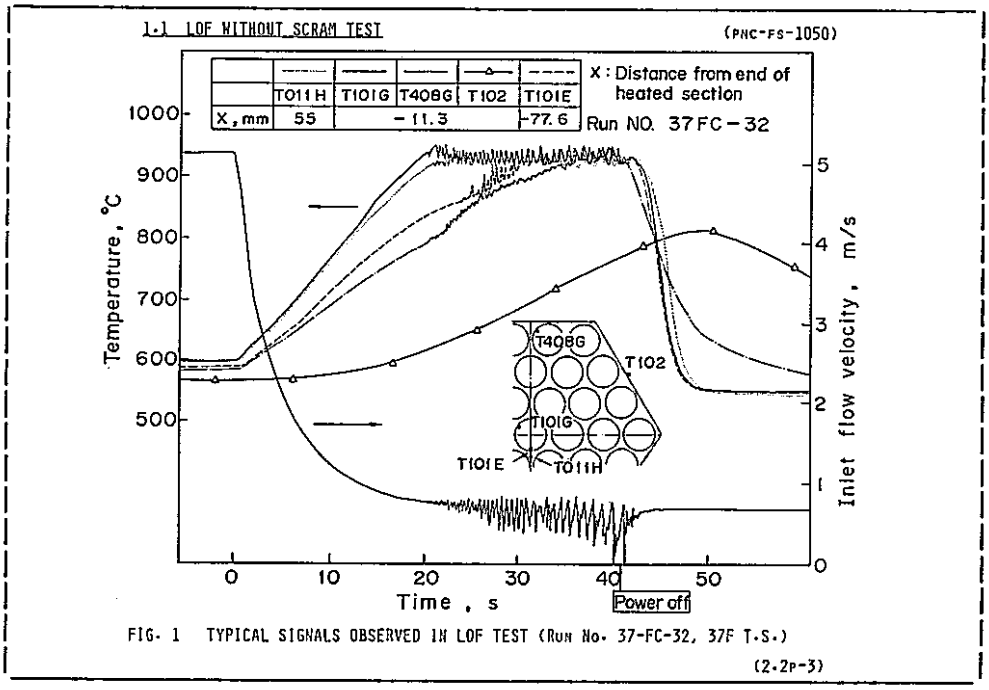


FIG. 1 TYPICAL SIGNALS OBSERVED IN LOF TEST (Run No. 37-FC-32, 37F T.S.)

(2.2P-3)

..... (Change the OHP sheet, OHP No. 3 i.e. Fig. 1)

I would like to show you a typical result obtained by the test before last. Concerning the I.B. super-heat, the observed values were very small. No effects could be identified of the experimental parameters. So, it will be reasonable to consider that the onset of sodium boiling in the bundle is similar to the boiling in usual working fluid.

For the boiling dynamics, the story is summarized as follows: After a few second into boiling, the saturated temperature region expands axially around the central subchannels, although it is not shown in this figure. At the same time, the thermohydraulic oscillation synchronized with repetitive bubble formation and collapse is initiated. For LOF conditions, you can easily understand that the oscillation is not stable but divergent.

During a gradual growth of the oscillation, a cluster of bubbles becomes to form a vapor core at the center of the bubbly region. When the vapor core grows up large enough to obstruct sodium entry during the oscillation, the pin surfaces covered by the vapor core will be soon dryed out. The actual burn-out is followed after a few times' repetetions of dryout and rewetting.

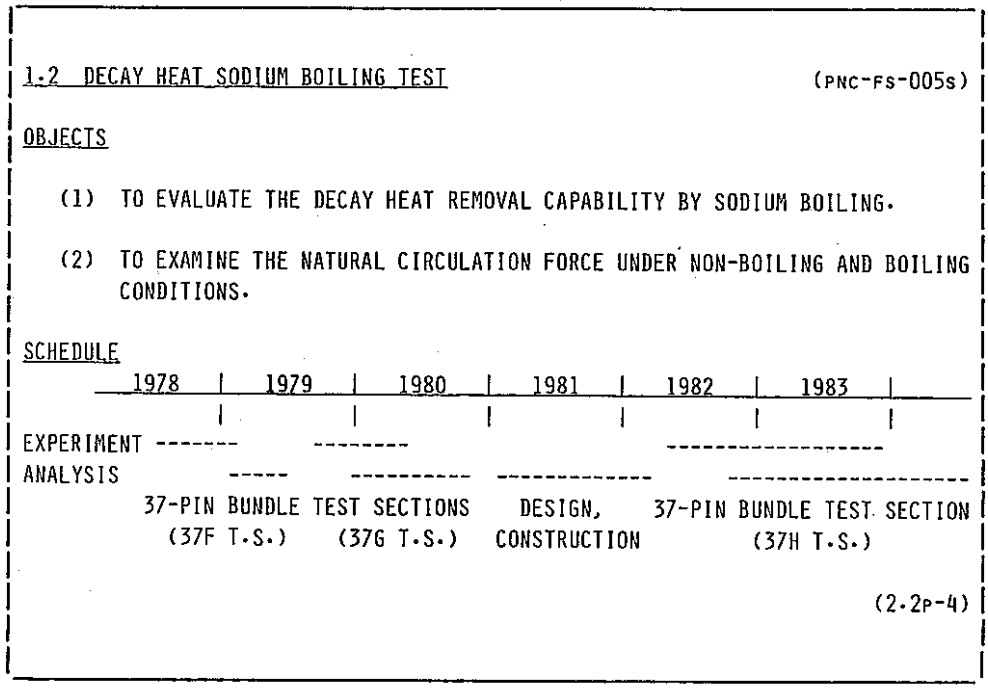


## 1.2 Decay Heat Sodium Boiling Test

..... (Change the OHP sheet, OHP No. 4)

Next is the Decay Heat Sodium Boiling Test. We have two objects. The first one is to evaluate the dryout criteria under low heat flux and low flow conditions. The second one is to examine the selfsustaining safety aspect of natural circulation.

The time schedule is shown below. This program was started two years ago using the same test section with LOF experiments. We are now considering the further advanced program, where not only the reversal flow under LOPI transient but also the natural circulation flow under Loss of Heat Sink transient will be attained.

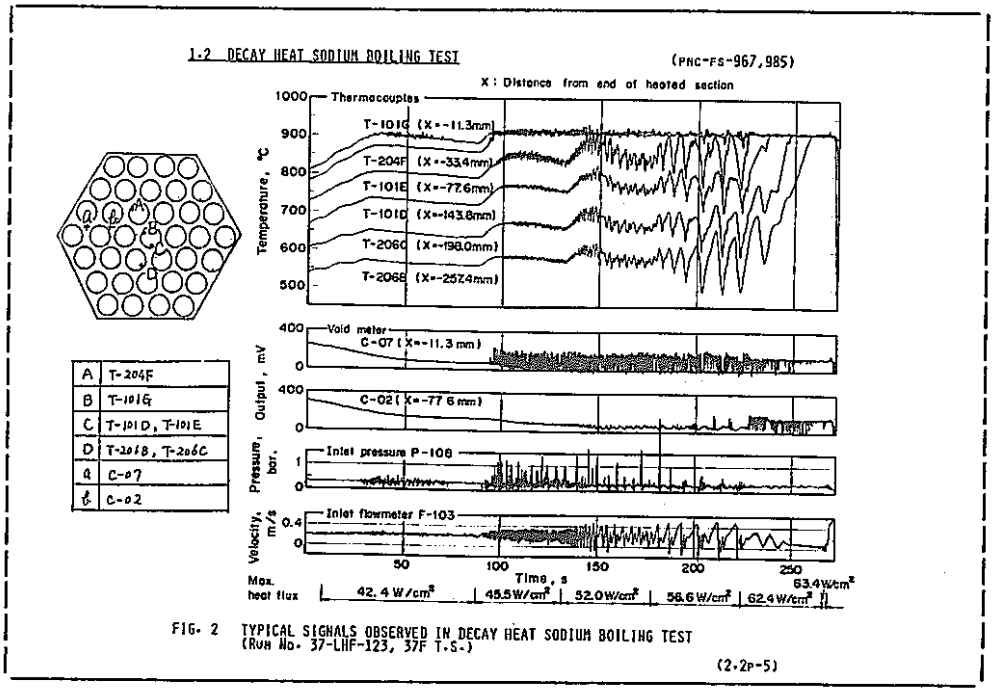


FIG. 2 TYPICAL SIGNALS OBSERVED IN DECAY HEAT SODIUM BOILING TEST
(Run No. 37-LHF-123, 37F T.S.)

(2.2P-5)

..... (Change the OHP sheet, OHP No. 5 i.e. Fig. 2)

This figure shows an example of dryout run carried out last year. The sodium flow was driven by natural circulation of our test facility. Sodium boiling was first started, here, and was restarted by the additional heat up. In the latter half of this run, you can identify the regular oscillation caused by the slug flow and its termination. Prior to the instance of dryout, the flow pattern was changed to annular or annular-mist flow. The estimated average exit quality at dryout was greater than 0.5.

1.2 DECAY HEAT SODIUM BOILING TEST (CONTINUED) (PNC-FS-007s)

RESULTS ..... (376 T.S.)

- FOR VERY LOW FLOW CONDITIONS INCLUDING PERFECT BLOCKING AT THE INLET, THE FLOW REGIME WAS HARDLY CHANGED FROM SLUG FLOW TO ANNULAR FLOW.
- THE SLUG FLOW HAD EXTREMELY HIGHER CAPABILITY OF DECAY HEAT REMOVAL THAN THE ANNULAR FLOW, BECAUSE OF THE REPETITIVE RE-WETTING OF DRYED-OUT PIN SURFACES.
- CONCERNING POST-DRY-OUT HEAT TRANSFER, IRREGULAR RADIAL AND AXIAL MOVEMENTS OF DRY-OUT REGIONS WERE OBSERVED FOR A LONG PERIOD.

(2.2P-6)

..... (Change the OHP sheet, OHP No. 6)

Quite recently, we have got additional 20 points dryout data at the heat flux range from about 4% to 15% of reactor condition. The results are summarized here. The former two suggested us that we should check the reason why the oscillation was terminated in many runs except for very low flow runs. For the decay heat conditions, dryout did not necessarily cause burn-out. In other words, the post-dryout heat transfer was not so bad except when noncondensable gas was injected. This fact implies that the spray cooling by entrained droplets plays an important roule in the post-dryout heat transfer.

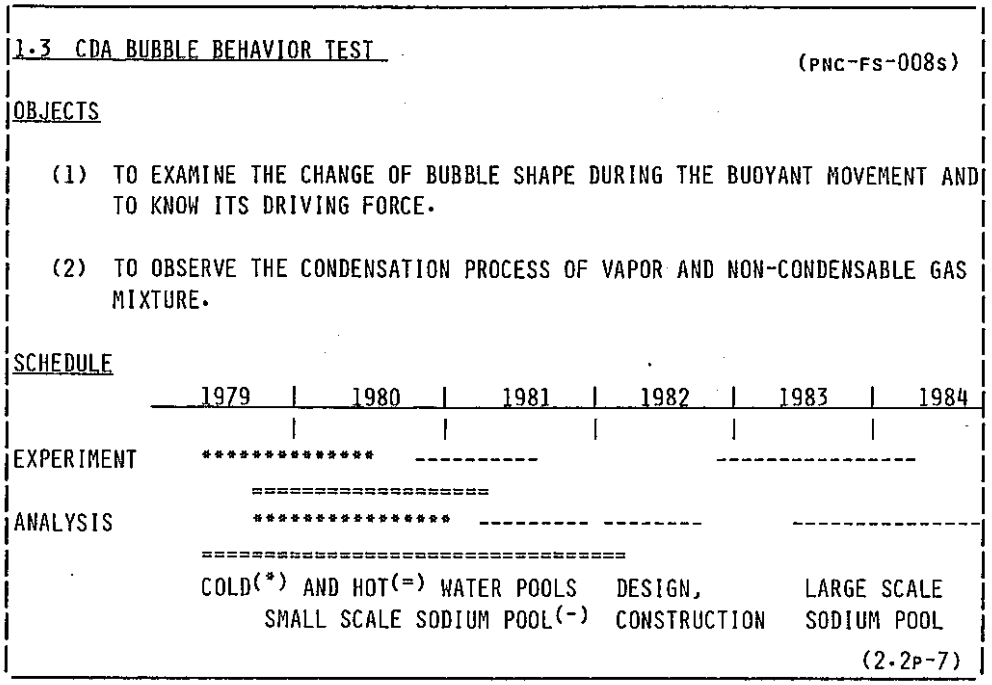


1.3 CDA Bubble Behavior Test .... (Change the OHP sheet, OHP No. 7)

The last is the CDA Bubble Behavior Test. Its object are shown here. We are going to examine two problems: the change of the shape of a large bubble during its buoyant movement, and the condensation of it. This test is similar to the FAST program in USA and the EXCOBULL test in France.

As are shown in the time schedule, this program has been conducted since last year. A small scale in-sodium test vessel is now under construction. Besides in-sodium test, two mockup tests are running in parallel using cold and hot water pools. The results are expected to be used for the back-up of the interpretation of in-sodium test results we will have.

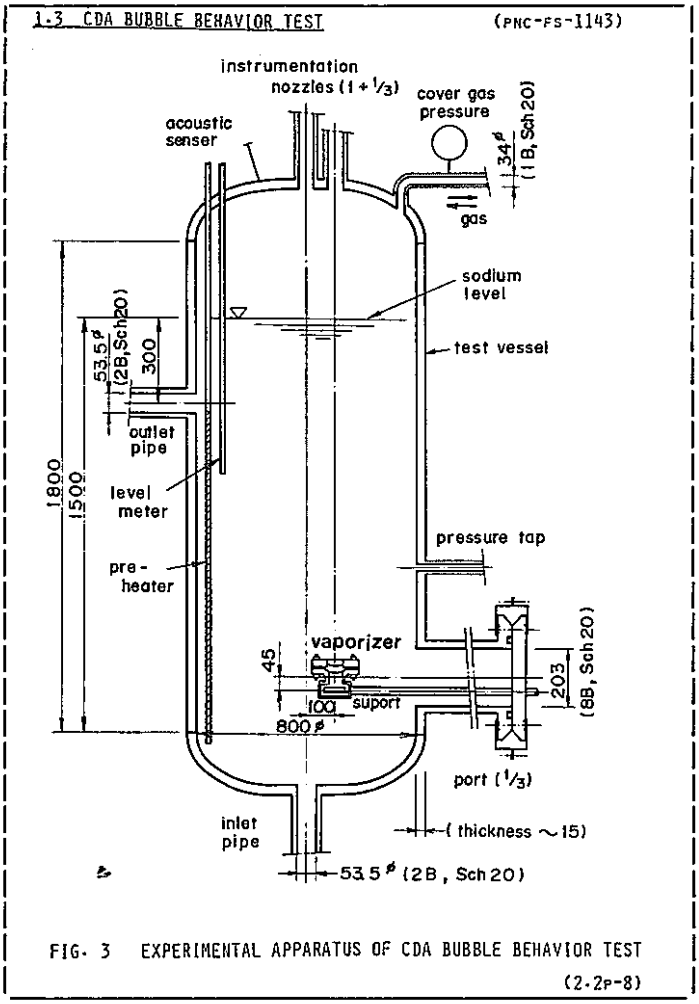


FIG. 3 EXPERIMENTAL APPARATUS OF CDA BUBBLE BEHAVIOR TEST
(2-2P-8)

..... (Change the OHP sheet, OHP No. 8 i.e. Fig. 3)

This is the test vessel. We are planning to make a large bubble of sodium vapor and noncondensable gas mixture by a vaporizer unit. The capability of this method has been preliminarily checked in water.

Two important problems are left unsolved: One is the scale effects of bubble and in-vessel structures. The other is the effect of initial condition of bubble formation. Discussion has been continued to design the next large scale in-sodium test vessel.

END REMARKS ..... (Turn off the light of OHP)

Now, I would like to finish my presentation, thank you.

SCOPE OF PRESENTATION

Franco-Debene-PNC Specialists Meetings on
FBR Subassembly Faults and Related Thermohydraulics

June 9, 1980
Karlsruhe, Federal Republic of Germany

June 11, 1980
Grenoble, France

# RECENT PROGRESS OF FUEL FAILURE PROPAGATION TESTS

Edited by M. Uotani

FBR Safety Section, OEC/PNC

## INTRODUCTION

I would like to present our recent progress of Fuel Failure Propagation Tests.

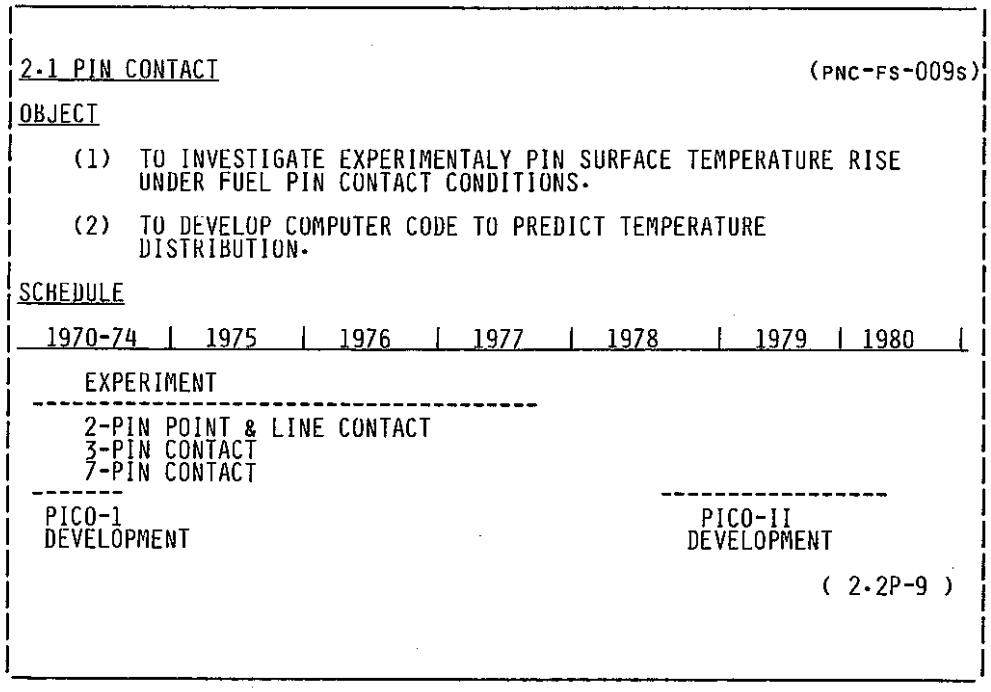


## INDIVIDUAL DISCUSSIONS

2.1 Pin Contact Test ..... (Turn on the light of OHP, OHP No. 1)

The first item is the Pin Contact Tests. Its first object is to estimate experimentally the temperature rise under fuel pin contact conditions. The second object is to develop a computer code to predict temperature distributions.

The time schedule of the Pin Contact experiments is shown below. Four kinds of experiments, such as a 2-pin point contact, a 2-pin line contact, a 3-pin point contact, a 7-pin point contact, were conducted and completed already in 1977.

2.1 PIN CONTACT (CONTINUED) (PNC-FS-010s)

RESULTS

(1) LOCAL TEMPRTATURE RISES IN REACTOR CONDITIONS EXTRAPOLATED BY PICO-I CODE

| 2-PIN POINT | 2-PIN LINE | 3-PIN POINT | 7-PIN POINT |
|---|---|---|---|
| 40°C | 70°C | 100°C | 150°C |

(2) PICO-II IS UNDER DEVELOPMENT, MODIFYING FUEL PIN AND CROSS-FLOW MODEL

( 2.2P-10 )

..... (Change the OHP sheet, OHP No. 2)

Experimental results were extrapolated to the reactor condition by the PICO-I code. The results are summarized here.

Now, updated PICO-II code is under development, modifying fuel pin and cross flow calculation models. This task will be completed in a few months.

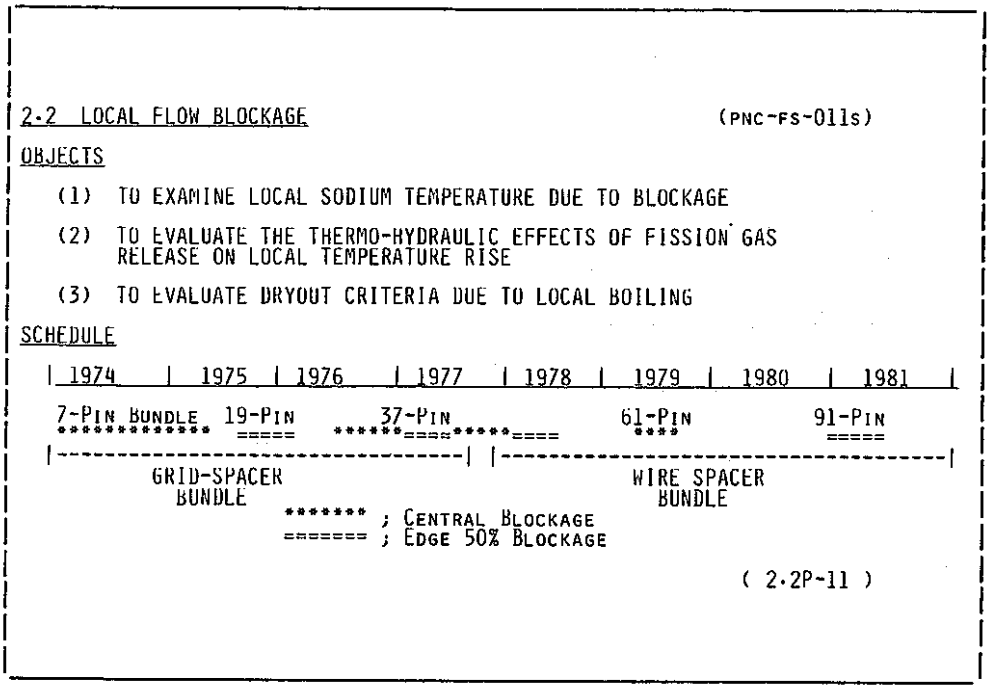


2.2 Local Flow Blockage ..... (Change the OHP sheet, OHP No. 3)

Next item is the Local Flow Blockage Tests. We have following three objects: The first one is to examine local sodium temperature rise caused by the blockage. The second one is to evaluate the thermohydraulic effect of fission gas release on local temperature rise. The last one is to evaluate dryout criteria under local boiling condition.

This program was started in 1974. Last year, we have finished the final central blockage experiment with a 61-pin bundle. The final experiment with a 91-pin bundle with 50% edge blockage will be conducted during a period from the end of this year to the middle of next year.

2.2 LOCAL FLOW BLOCKAGE (CONTINUED) (PNC-FS-012s)

RESULTS

(1) UNIVERSAL EMPIRICAL CORRELATIONS WERE OBTAINED TO EVALUATE LOCAL TEMPERATURE RISE
SODIUM BOILING WOULD NOT OCCURE BEHIND A CENTRAL BLOCKAGE (< 60% ), WHILE EDGE BLOCKAGE CAUSE SODIUM BOILING.

(2) GAS RELEASE INTO WAKE REGION CAUSED SEVERE TEMPERATURE RISE

(3) STABLE OSCILLATORY BOILING WAS OBSERVED, AND THE MARGIN TO BOILING CRISIS WAS CONCLUDED TO BE SUFFICIENTLY LARGE.

( 2.2P-12 )

..... (Change the OHP sheet, OHP No. 4)

The results obtained up to now are shown here.

For single-phase flow, universal empirical correlations were obtained to evaluate the local temperature rise. The detail will be presented at the 9th Liquid Metal Boiling Working Group Meeting which will be held in Italy next month. Extrapolation of the experimental results to a reactor condition leads to the conclusion that sodium boiling would not occur behind a central local blockage, while edge blockage will cause sodium boiling.

For simulant fission gas release, it was found that the gas release into the wake region would cause severe temperature rise, because of the gas accumulation in the wake. Experimental resutls have been analized to evaluate the effects of gas release rate and sodium flow velocity on the gas concentration in the wake region.

For local boiling, continuous oscillatory boiling observed in the wake region behind both central and edge blockages was analized. The measured oscillation frequency agreed well with an analytical prediction. The theoretical excess temperature at the occurrence of dryout was evaluated. Using it, the margin to the boiling crisis was estimated as being sufficiently large.

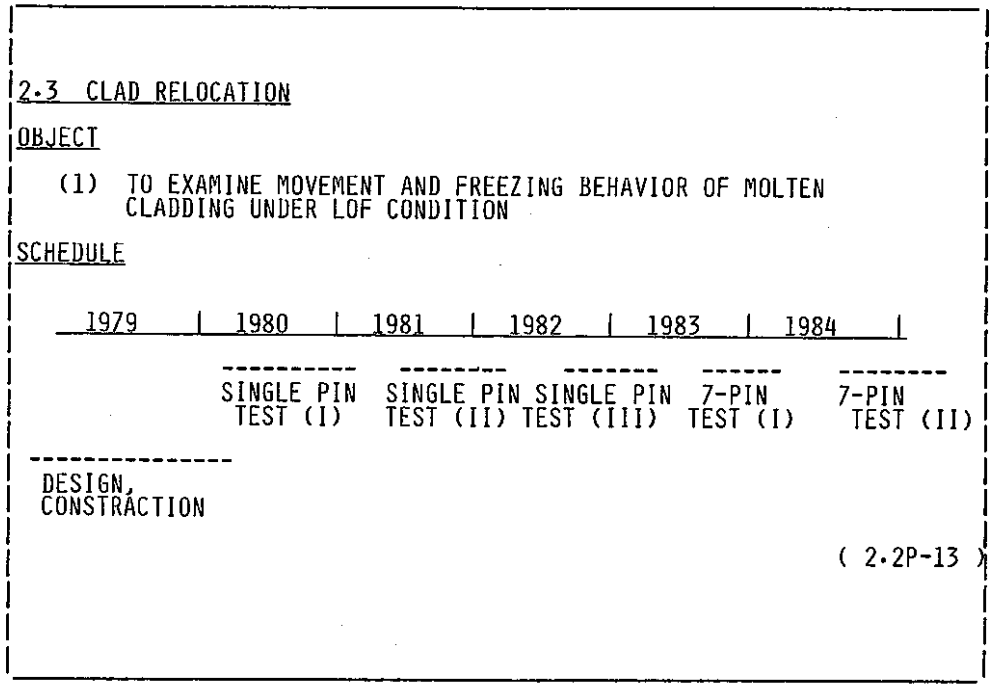


2.3 Clad Relocation ..... (Change the OHP sheet, OHP No. 5)

The third item is the Clad Relocation Test. The object is to examine the movement and freezing behavior of molten cladding under LOF condition, and to provide a physical model to improve computer code.

At present, single-pin test sections are under manufacturing. The first test will be carried out in this financial year. 7-pin bundle tests will be followed in a few years.

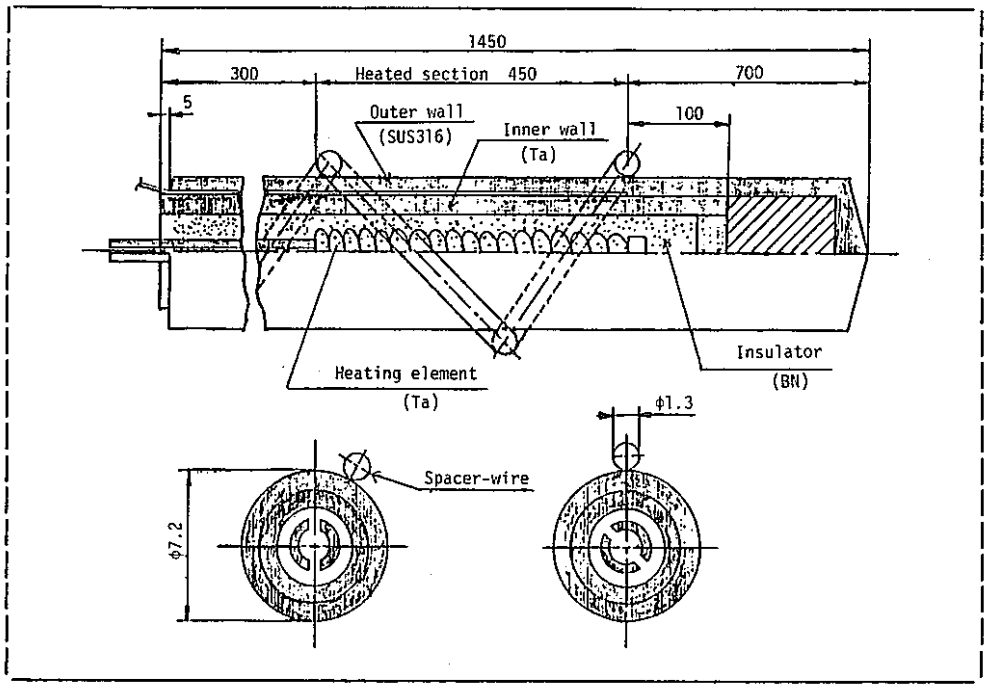


..... (Change the OHP sheet, OHP No. 6)

This is a sketch of the test pin under manufacturing. The outer cladding is made of a stainless steel and the inner one is made of a tantalum. The outer diameter is 7.2 mm. The heating length is 450 mm. The test pin is wrapped with a spacer wire, and is inserted in a hexagonal or circular tube.

Following preliminary tests in air, in-sodium tests will be carried out continuously.

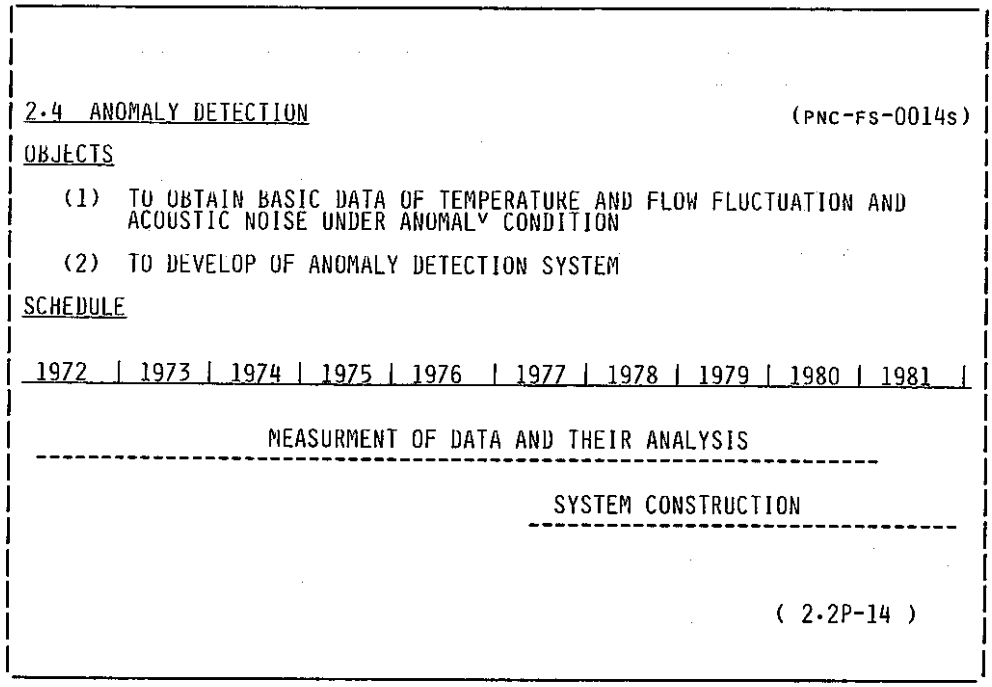


2.4 Anomaly Detection ..... (Change the OHP sheet, OHP No. 7)

The last item is the Anomaly Detection Test. Its first object is to obtain basic data of temperature, flow velocity and acoustic noises under anomaly conditions, such as local cooling disturbance, local boiling, FP gas release. The second object is to develop an anomaly detection system. Development of a new detector is not included in our project.

This program has been progressed in parallel to the sodium boiling and local blockage experiments, as a part of the joint research between PNC and Mitsubishi Electric Company.

A system construction for the Anomaly Detection was started three years ago. This program will be completed at the end of next year.

2.4 ANOMALY DETECTION (CONTINUE) (PNC-FS-015s)

RESULTS

(1) LOCAL FLOW BLOCKAGE CAN NOT BE DETECTED BY TEMPERATURE FLUCTUATION BECAUSE OF FLOW MIXING AT END OF THE BUNDLE

LOCAL BOILING CAN BE DETECTED BY TEMPERATURE AND/OR FLOW FLUCTUATION WHITENESS TEST METHOD IS MORE SUITABLE THAN RMS METHOD

GAS RELEASE DUE TO BURST TYPE ONE PIN FAILURE CAN BE DETECTED BY FLOW FLUCTUATION

BOILING DETECTION BY ACOUSTIC NOISE IS PROMISSING IN THE RANGE OF 5 10 KHZ.

( 2.2P-15 )

..... (Change the OHP sheet, OHP No. 8)

This is the summary of the results.

First; local flow blockage cannot be detected by use of outlet temperature fluctuation, because of the strong flow mixing at the end of the bundle.

Second; local boiling can be detected by use of temperature or flow fluctuation. Especially, the Whiteness Test method is more suitable than the RMS method.

Third; FP gas release due to a burst-type one-pin failure can be detected by use of flow fluctuation.

Fourth; boiling detection by use of acoustic noise is very promising in the frequency range from 5 to 10 kHz.

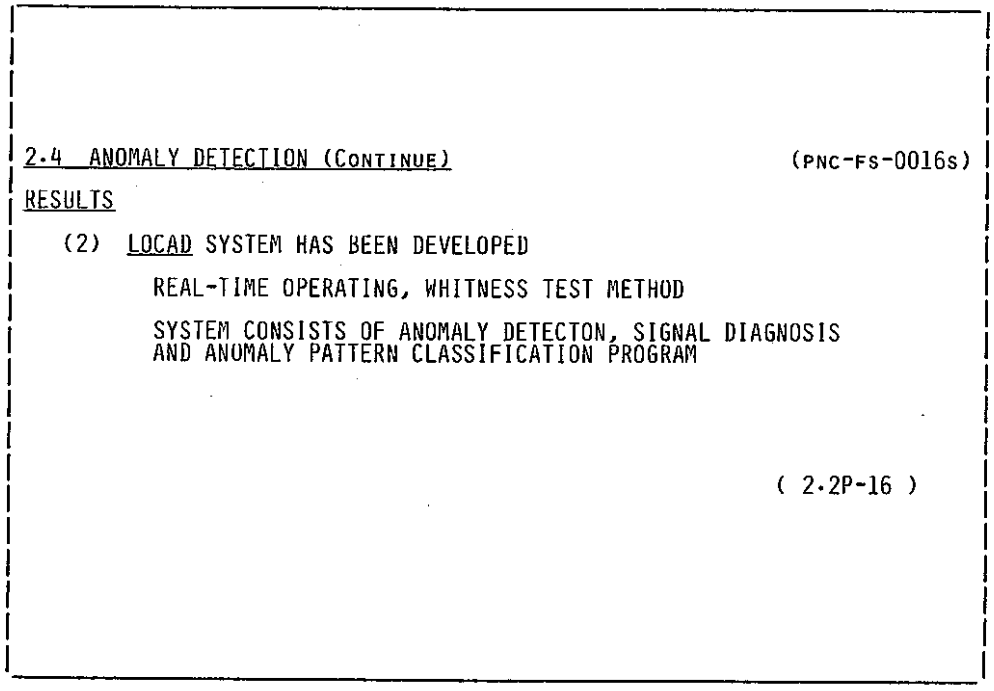


..... (Change the OHP sheet, OHP No. 9)

Anomaly Detection System, named LOCAD, has been developed.

The main specifications of the system are as follows: First; the system can be applied to a real-time monitoring. Second; the system consists of several sub-programs, each of which has a function of anomaly detection, signal diagnosis, and anomaly pattern classification.

END REMARKS ..... (Turn off the light of OHP)

That is all I have to say. Thank you.

## 3. END REMARKS

As are shown in the foregoing chapters, experimental activities of the FBR Safety Section of OEC/PNC over the past years are presented at the 9th Meeting of the LMBWG and at the Franco-Debene-PNC Specialists Meetings on FBR Subassembly Faults and Related Thermohydraulics. A detail report of these meetings is given in the editor's Foreign Trip Report(1). All documents recieved from European side at the Franco-Debene-PNC meetings are recorded as an independent volume(2).

The aim of this report lies in publishing the detailed scope of the presentations by a PNC "N" number report. Legally speaking, the author(s) of the submitted paper ought to write required matters in his (their) paper. However, it is, sometimes, insufficient because of the limitation of pages assigned to the paper and the dead time of the manuscript preparation. The editor considered that supplemental remarks and pointed explanation presented at the meeting should not be lost, to provide future advanced studies.

Contents shown in this report are the past status of June, 1980. Especially, time schedules of the R&Ds were not fixed but changed quite a great amount. Readers can refer the other PNC report(3) to know an updated recent status.

---

(1) K. Yamaguchi, "Foreign Trip Report; 9th Meeting of the Liquid Metal Boiling Working Group, Franco-Debene-PNC Specialists Meetings on FBR Subassembly faults and Related Thermohydraulics, and Visiting to the FBR Safety Research and Development Laboratories," PNC SN960 81-08, June 1981.

(2) Edited by K. Yamaguchi, "Records of Discussion of the Franco-Debene-PNC Specialists Meetings on FBR Subassembly Faults and Related Thermohydraulics," PNC SN960 81-09, June 1981.

(3) Edited by K. Haga, "Activities in the SBL-FPL Loops for LMFBR Safety Studies (II)," PNC N941 81-42, Apr. 1981.